

**An investigation into the expression and function of
uncoupling protein 2 during neonatal sepsis**

Mark Andrew Edginton

A Thesis Submitted to University of London for the Degree of MPhil.

January 2004

**Institute of Child Health
30 Guilford Street
London
WC1N 1EH**

UMI Number: U594050

All rights reserved

INFORMATION TO ALL USERS

The quality of this reproduction is dependent upon the quality of the copy submitted.

In the unlikely event that the author did not send a complete manuscript and there are missing pages, these will be noted. Also, if material had to be removed, a note will indicate the deletion.



UMI U594050

Published by ProQuest LLC 2013. Copyright in the Dissertation held by the Author.
Microform Edition © ProQuest LLC.

All rights reserved. This work is protected against
unauthorized copying under Title 17, United States Code.



ProQuest LLC
789 East Eisenhower Parkway
P.O. Box 1346
Ann Arbor, MI 48106-1346

An investigation into the expression and function of uncoupling protein 2 during neonatal sepsis

Abstract

Uncoupling protein 2 (UCP2) is widely expressed in mammals but its true function has not been established. Present information suggests that like UCP1, UCP2 functions as a proton leak and can uncouple productive mitochondrial respiration. This activity is reported to be functionally dependant on the presence of ubiquinone. The expression of UCP2 is reportedly increased during endotoxaemia, thus it may have a role in immune response.

This study examines the expression of UCP2 protein and its possible function during infection using endotoxaemia in suckling rat pups as a model for neonatal sepsis.

The whole body response to endotoxaemia was investigated using indirect calorimetry. We report that endotoxaemia induces hypometabolism and hypothermia in neonatal rats.

The expression pattern of UCP2 was investigated by developing a protocol for UCP2 western blotting and then using this to analyse appropriate mitochondrial samples from control and endotoxic suckling rats.

UCP2 expression was strongest in mitochondrial preparations from spleen and lung tissue. It was demonstrated that when compared to control samples, UCP2 expression is increased and ubiquinone levels are decreased in mitochondrial preparations from lung tissues of endotoxic rat pups. The increase of UCP2 in endotoxic lung mitochondria could be the result of macrophage infiltration and the decrease in ubiquinone may reflect recruitment of this compound to the plasma membrane. It is possible that the function of uncoupling may be to protect sensitive tissues from damage by free radicals.

The role of UCP2 induced uncoupling in macrophages was investigated by reactive oxygen species (ROS) assays. Using *in vitro* assays of macrophage ROS

generation we demonstrate that known activators of UCP2 such as TTNBP and ubiquinone enriched media can reduce the level of ROS

Our findings support other studies that suggest that UCP2 may be involved in protecting against the detrimental effects of ROS

Contents

Chapter 1. Introduction

1.1.1 Sepsis	p.15
1.1.2 Mitochondria.	p.16
1.1.3 Mitochondrial Proton Leak	p.17
1.1.4 Uncoupling Protein 1	p.18
1.1.5. Other Uncoupling Proteins	p.21
1.1.6. Uncoupling Function of UCP2	p.22
1.1.7. Ubiquinone and UCP function.	p.23
1.1.8. Physiological nature of Uncoupling proteins.	p.25
1.1.9. Studies in UCP2 Knock-out mice ^(-/-) .	p.27
1.1.10. UCP2 uncoupling in macrophages	p.28
1.1.11. Activation of UCP induced uncoupling	p.28

1.2. Discussion	p.31
------------------------	------

1.3 Aims	p.32
-----------------	------

Chapter 2. Whole body energy metabolism of endotoxic suckling rat pups.

2.1 Introduction.	p.34
--------------------------	------

2.2. Methods

2.2.1 Animals	p.35
2.2.2 Endotoxaemia score	p.35
2.2.3 Indirect Calorimetry	p.36
2.2.4 Statistical evaluation	p.36

2.3. Results

2.3.1. Temperature and endotoxaemia	p.37
2.3.2. Oxygen Consumption.	p.38
2.3.3. Correlation between VO ₂ and body temperature	p.39
2.3.4. Endotoxaemia and respiratory quotient.	p.40
2.3.5. Endotoxamia Score	p.41
2.3.6. Carbon dioxide production and energy expenditure	p.42

2.4. Discussion

p.43

Chapter 3. Development of a method for analysis of UCP2 protein levels in tissues.

3.1 Introduction

p.46

3.2. Methods

3.2.1. Animals	p.48
3.2.2. Sample Preparation	p.48
3.2.3. Mitochondria	p.48
3.2.4. Mitochondrial Membranes	p.49

3.2.5. Standard Gel electrophoresis	p.49
3.2.5.1 Silver Staining	p.50
3.2.6 Standard Western Blotting	p.50
3.2.7. Detection	p.51
3.2.7.1 DAB.	p.51
3.2.7.2 Chemiluminescence detection.	p.51
3.2.8. Western blotting adaptations	p.52
3.2.8.1 SCHAD	p.52
3.2.8.2 UCP2	p.52
3.2.8.3. Citrate Synthase	p.52
3.2.9. Dot Blots	p.53

3.3 Results

3.3.1. Gel Composition	p.54
3.3.2. Western Blotting	p.56
3.3.3. Optimising western blotting for SCHAD	p.56
3.3.4. Antibody Concentration (Dot blot)	p.57
3.3.5. Determining Detection limits	p.58
3.3.6. Comparing standard and optimised SCHAD western blotting	p.59
3.3.7. Optimising Western Blotting for UCP2	p.60
3.3.8. Cross reactivity	p.60
3.3.9. Sample Choice	p.64

3.3.10. Controls p.66

3.4. Discussion p.68

Chapter 4. UCP2 western blotting

4.1. Introduction p.70

4.2. Methods

4.2.1. Animals p.71

4.2.2. Mitochondrial Preparation p.71

4.2.3. UCP2 Western Blotting p.71

4.2.4 HPLC analysis of ubiquinone p.72

4.2.5. Citrate synthase Assay p.72

4.2.6. Protein Assay p.73

4.3 Results

4.3.1 Normalisation of data p.75

4.3.2. UCP2 Western Blotting p.77

4.3.3. Ubiquinone p.79

4.4 Discussion p.83

Chapter 5. Reactive Oxygen Species Production in

Macrophages

5.1 Introduction p.87

5.2. Methods

5.2.1. Isolation of monocytes/macrophages from peripheral p.89

whole blood.

5.2.2. Monocyte viability count p.89

5.2.3. Standard curve for 2,7-dichlorofluorescein. p.90

5.2.4. Cuvette assay for reactive oxygen species production. p.90

5.2.5. Non-continuous measurement (methanol added). p.91

5.2.6. Preparation of ubiquinone multi-lamellar liposomes p.91

5.2.7. Microplate Assay. p.92

5.3. Results.

5.3.1 Macrophage ROS Production p.93

5.3.2. Increasing sample size. p.94

5.3.3. Continuous Measurement p.96

5.3.4. Exposure to LPS p.97

5.3.5. TTNPB p.98

5.3.6. Ubiquinone p.99

5.3.7. Microplate Assay p.100

5.3.8. Control Assay p.101

5.3.9. Measuring ROS production	p.102
5.3.10. Incubation with active compounds.	p.103
5.3.11. Attenuating ROS production under stimulated conditions.	p.104
6. Discussion	p.107
Acknowledgements	p.113
Reference list	p.114

List of Figures

Chapter 1.

- Figure 1.1. Appearance of LPS and cytokines in plasma after LPS injection. p.15
- Figure 1.2. Diagram showing the transport of electron through the respiratory chain complexes (I-IV) p.17
- Figure 1.3. Accepted pathway for the stimulation of UCP1 activity by norepinephrine (NE). p.20
- Figure 1.4. Possible mechanism for role of Ubiquinone as an essential co-factor for UCP uncoupling. p.25

Chapter 2.

- Figure 2.1. Sepsis scoring table. p.35
- Figure 2.2. Effect of Endotoxaemia on rectal temperature: p.37
- Figure 2.3. Oxygen Consumption. p.38
- Figure 2.4. Temperature and oxygen consumption. p.39
- Figure 2.5. Respiratory Quotient. p.40
- Figure 2.6. Carbon dioxide production. p.41
- Figure 2.7. Heat production. p.42

Chapter 3.

- Figure 3.1. Electrophoresis of standard proteins on a 10% acrylamide gel. p.54
- Figure 3.2. Electrophoresis of protein standards on a 12 % acrylamide gel. p.55
- Figure 3.3. Results of a Dot blot assay. p.57
- Figure 3.4. Determining the detection limits of SCHAD western blotting. p.58
- Figure 3.5. Before (A) and After (B) SCHAD Western Blot Optimisation: p.59
- Figure 3.6. Cross reactivity of UCP2 antibody. p.61

Figure 3.7. Comparing Santa Cruz and Calbiochem UCP2 Antibody.	p.62
Figure 3.8. Titration of UCP2 Control.	p.63
Figure 3.9. UCP2 western blot sample range.	p.64
Figure 3.10. Optimised UCP2 western blotting.	p.65
Figure 3.11. Western Blotting for Citrate Synthase.	p.67

Chapter 4.

Figure 4.1. Citrate synthase assay trace.	p.73
Figure 4.2. Protein assay trace.	p.73
Figure 4.3. Comparing the level of citrate synthase activity per mg/ml of the total protein content between mitochondria isolated from endotoxic and control rat pups.	p.76
Figure 4.4. UCP2 protein expressed in lung and spleen mitochondria from control and endotoxic rat pups.	p.78
Figure 4.5. Comparing the UQ ₉ /UQ ₁₀ ratio between lung and spleen samples.	p.80
Figure 4.6. Comparing the levels of UQ ₉ and UQ ₁₀ between control and endotoxic mitochondrial preparations from lung and spleen tissue after a 2hr exposure to LPS.	p.81
Figure 4.7. Levels of UQ ₉ and UQ ₁₀ in control and endotoxic mitochondrial preparations from lung and spleen tissue after a 6hr exposure to LPS.	p.82

Chapter 5.

Figure 5.1. The conversion of 2',7'-dichlorofluorescein diacetate to fluorescent 2',7'-Dichlorofluorescein by intracellular ROS.	p.88
Figure 5.2. Standard Curve of DCF.	p.90
Figure 5.3. ROS production from stimulated and control macrophage suspensions.	p.93
Figure 5.4. ROS production from control and stimulated macrophages, prolonged incubation.	p.94
Figure 5.5. Control Assay.	p.96
Figure 5.6. ROS production from stimulated and control macrophages, LPS/PMA exposure.	p.97
Figure 5.7. Effect of TTNPB on LPS induced ROS production.	p.98

Figure 5.8. Attenuation of ROS macrophage ROS production with UQ ₁₀	p.99
Figure.5.9. Absorbance form ^{from} media in the absence of cells.	p.101
Figure 5.10. ROS production in microplate culture	p.102
Figure.5.11. Incubation with enhanced media, difference from control.	p.103
Figure 5.12. Attenuating LPS and PMA induced ROS production.	p.104

Abbreviations

BAT	Brown adipose tissue
BSA	Bovine albumin serum
DCF	2',7'-dichlorofluorescin (Fluorescent)
DCFH	2',7'-dichlorofluorescin
DCFH-DA	2',7'-dichlorofluorescin diacetate
DDT	Dithiothreitol
DMPC	Do-myristylphosphatidylcholine
DMSO	Dimethylsulphoxide
DTNB	Dithio-1,4,-nitrobenzoic acid
<i>E.coli</i>	<i>Escherichia coli</i>
FA	Fatty acids
FAH	Undissociated fatty acids
IL-1,6,	Interleukin 1, Interleukin 6
KOH	Potassium hydroxide
LPS	Lipopolysaccharide
NBT	Nitro-blue-tetrazolium
NE	Norepinephrine
PBS	Phosphate buffered saline
PMA	Phorbol myristate acetate
PMSF	Phenylmethylsulphonylfluoride
ROS	Reactive oxygen species
RQ	Respiratory quotient
SCHAD	Short chain 3-hydroxyl-acyl-coA dehydrogenase
SDS	Sodium dodecyl sulphate
TNF α	Tumour necrosis factor alpha
TTNPB	4-[(E)-2-(5,6,7,8-tetrahydro-5,5,8,8- tetramethyl-2-naphthalenyl)-1-propenyl] benzoic acid
UCP	Uncoupling protein
UQ	Ubiquinone

1. Introduction

1.1.1 Sepsis

Sepsis is part of the systemic inflammatory response to infection and can have broad ranging physiological manifestations in an affected organism¹. Despite medical advances such as improvements in clinical practices and the introduction of a broad range of potent antibiotics, sepsis remains a major clinical problem with a high mortality rate². Investigations into the complex cellular and biochemical events that mediate sepsis are of great importance and are particularly relevant to neonates, who with a reduced immune function are at particular risk when faced by sepsis³.

Neonates that require surgery, parenteral nutrition, mechanical ventilation or those that are born prematurely are at increased risk of sepsis. Systemic inflammatory response syndrome is a sepsis like state in the absence of a detectable infection. Animal models commonly generate a systemic inflammatory response using lipopolysaccharide (LPS). LPS is a product from the cell wall of bacteria that induces a systemic response with a well defined temporal cascade of various proinflammatory cytokines⁴ (Figure 1.1).

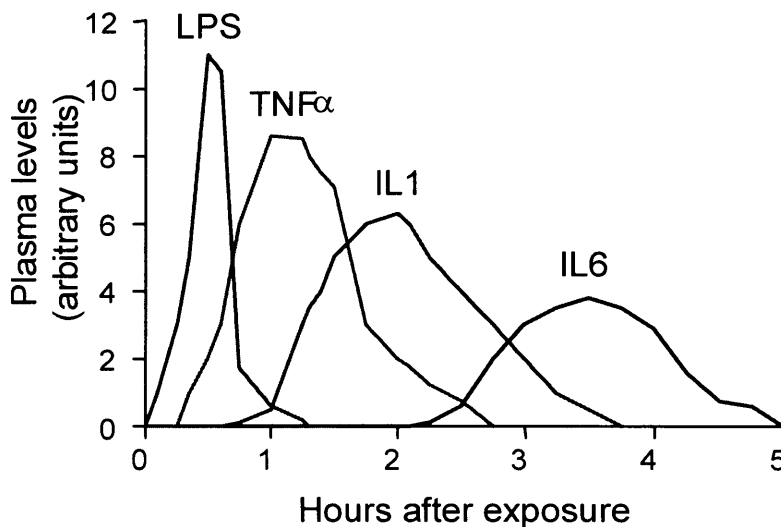


Figure 1.1. Appearance of LPS and cytokines in plasma after LPS injection. Examples of typical temporal cascade of cytokines induced by LPS injection in an animal model of neonatal endotoxaemia TNFα – Tumour Necrosis Factor alpha, IL-1 – Interleukin 1, IL-6 – Interleukin 6. Figure adapted from Anderson⁴

During the early, acute phase of infection proinflammatory cytokines such as tumour necrosis factor alpha (TNF- α) and interleukins IL-1, IL-6 and IL-8 prime neutrophils and macrophages for microbial killing⁵. Microbes can be destroyed by various cytokine induced mechanisms including an oxygen dependent mechanism that produces significant quantities of reactive oxygen species and free radicals that are highly toxic to pathogens. However, excessive free radical production can also damage host tissues.

In later stages of infection elements of the cytokine cascade become responsible for initiating a range of thermoregulatory responses. IL-1, TNF and IL-6 are all pyrogenic and cause an increase in body temperature by raising the set point of the hypothalamic thermoregulatory centre⁶. These cytokines induce the production of prostaglandins in the brain that activates neuronal pathways to increase heat production and decrease heat dissipation in the periphery⁶. However, rat models of endotoxaemia usually display an acute hypothermia that is generally followed by temperature recovery⁷. Compared to adults, neonates have greater difficulties in maintaining physiological body temperature and this hypothermia may increase the risks to neonates during infection. Thus, both hypo and hyper-thermia are amongst the clinical signs of sepsis in neonates¹.

1.1.2. Mitochondria.

Mitochondria are the power houses that drive the majority of ATP production. As mitochondrial respiration is oxygen dependant, they are a major source of reactive oxygen species.
sepsis.

The primary function of mitochondria is to generate ATP via a process known as oxidative phosphorylation. Oxidative reactions that occur in the respiratory chain generate a proton gradient across the inner mitochondrial membrane and this gradient is used by ATP synthase to phosphorylate ADP to ATP⁸.

Mitochondria contain certain enzymes that pass on electrons or protons and can be sources of ROS and in later stages of sepsis can become a direct source of ROS

themselves^{5,9}. This can occur when the level of ROS overcomes the cellular protective scavenging systems and begin to have deleterious effects on mitochondrial oxidation.

1.1.3. Mitochondrial Proton Leak

Not all of the energy from the electrochemical gradient is coupled to ATP synthesis. Some is used up by a proton leak, where protons pumped out of the matrix pass back into the mitochondria through pathways in the inner membrane, circumventing productive ATP synthesis. The proton flux across the inner mitochondrial membrane can be an important area of thermoregulatory control. It is now acknowledged that the inward flow of protons across the inner mitochondrial membrane via a route independent of the F_0F_1 ATP synthase is significant and that this proton leak could act to dissipate fuel-derived energy as heat¹⁰ (Figure.1.2)

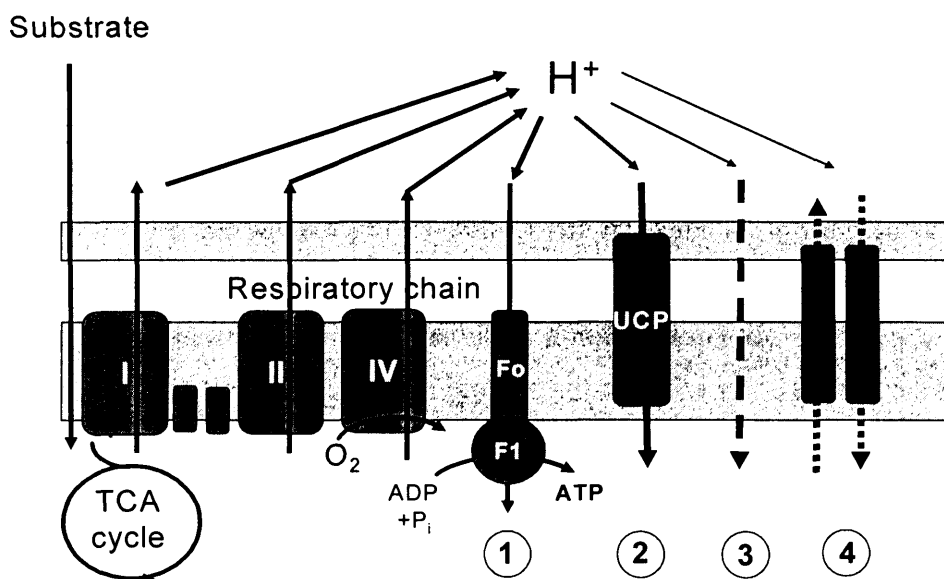


Figure 1.2. Diagram showing the transport of electron through the respiratory chain complexes (I-IV). The process is associated with pumping of protons from the mitochondrial matrix to the intermembrane space, creating an electrochemical gradient ($\Delta\mu H^+$) for ATP synthesis by ATP synthase (F_0F_1) (1). Inward flow of protons independent of F_0F_1 could be via an uncoupling Protein UCP (2) and may drive heat production. Additional routes of F_0F_1 uncoupling could be by direct leakage of protons across the membrane (3), or coupled to ion transport (4)

Studies in rats have shown that the proton leak may contribute up to 25% of the resting oxygen consumption and that the liver is responsible for approximately 20% of the overall standard basal metabolic rate. The liver may therefore be an important organ for thermogenesis.

Uncoupling may have roles in addition to a contribution to basal metabolic rate and adaptive thermogenesis. It is possible that mild uncoupling of respiration could prevent the accumulation of mitochondrial generated oxygen radicals and also play a role in regulating ketogenesis, lipogenesis and amino acid synthesis by controlling the NAD^+/NADH ratio¹¹

The liver's position between the portal and systemic circulation means that it is quickly exposed to substances translocated from the gut. Bacterial translocation across the gut can be an important source of bacterial entry, meaning that the liver can be one of the first organs exposed to the mediators of sepsis.

Impaired oxidative energy metabolism in hepatocytes has been reported in both adult and neonate models of endotoxaemia^{7,12}. Due to little or no cytosolic disturbance being recorded, the metabolic disruption has been allied to an increased level of reactive oxygen species effecting mitochondria directly and inhibiting mitochondrial oxidation. Impaired mitochondrial metabolism has been linked to the decrease in core body temperature displayed by neonatal rat pups during endotoxaemia⁷. It is possible that this could be associated with the inhibition of the proton leak.

1.1.4. Uncoupling Protein 1

The first evidence that proton leaks across the inner membrane could be protein mediated was identified in 1978 and resulted from studies of thermogenesis in Brown Adipose Tissue (BAT)¹³. This tissue is present in most mammals and produces heat in response to specific stimulus such as exposure to cold, birth and at the end of hibernation. It is well developed in large mammals around birth and present throughout the life span of rodents. The topology of its expression is specific so that once

activated, the heat it generates can be moved quickly through large vessels to the thorax, heart, brain and kidneys¹¹.

BAT tissue is composed of brown adipocytes. These cells contain droplets of triacylglycerols and have many specialised mitochondria with highly developed inner membranes. Measurements of oxygen consumption of isolated brown adipocytes confirmed that they had a marked oxidative capacity¹¹.

Studies have shown that the main areas of control for BAT activity are the thermoregulatory centres of the hypothalamus¹⁴. It was discovered that in response to certain stimuli these centres triggered sympathetic nerves that increased oxygen consumption and heat production in BAT, by releasing norepinephrine to the surface of the brown adipocytes. Since norepinephrine activates lipolysis, it was proposed that this heat production was related to the increased oxidation of fatty acids.

Observations that the respiration of mitochondria isolated from BAT was loosely coupled to ADP phosphorylation and that uncoupling was activated by fatty acids and inhibited by purine nucleotides indicated that a controllable uncoupler existed in the inner mitochondria membrane¹⁵. Photo-affinity labeling experiments identified a 32 kDa protein as the binding site for these purine nucleotides and led to this protein being presented as the putative uncoupling protein, UCP¹³. Sequencing and cloning experiments that reproduced this protein's proton translocating ability in liposomes¹⁶ gave rise to general acceptance that this protein was responsible for regulated uncoupling of BAT mitochondria. However, final proof that UCP was in fact the molecular key to adaptive thermogenesis did not come until 1997 when null mutant mice were shown to be unable to maintain their body temperature in a cold environment¹⁷. The BAT uncoupling protein was known simply as UCP until studies indicated the presence of other UCPs (see section 1.1.5), when it was renamed UCP1.

UCP1 causes heat production in BAT by acting as a proton leak. It has been demonstrated that norepinephrine induced lipolysis and the increase in the concentration of free fatty acids activates UCP1¹⁸. Once activated UCP1 allows protons and anions to move across the inner mitochondrial membrane, dissipating the electrochemical gradient. This decreases the membrane potential and increases the

respiratory rate¹⁹. This pathway is not coupled to any energy consuming process and bypasses proton transport by the ATPase and thus ADP phosphorylation. Under these conditions the most of the energy from oxidation is released as heat (Figure 1.3). Adrenergic stimulation has also been found to boost UCP1 gene transcription.

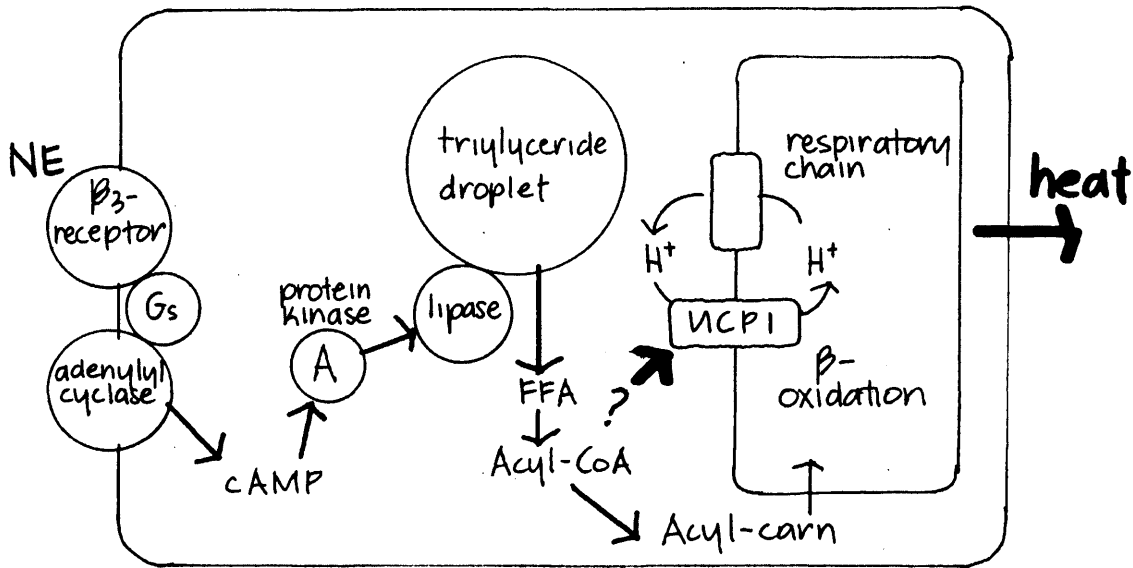


Figure 1.3. Accepted pathway for the stimulation of UCP1 activity by norepinephrine (NE). NE binds to receptors on the surface of brown adipocytes that increase cAMP levels, stimulating lipolysis and the generation of FA that stimulate UCP1 mediated uncoupling and consequent heat production.

The activity of UCP1 has been shown to be inhibited by nucleotides and activated by non-esterified fatty acids²⁰.

Uncoupling by UCP1 is a relevant thermogenic mechanism involved in body temperature regulation in small mammals and rodents. However, the limited expression of BAT in adult humans and other large mammals mean that other mechanisms must be responsible for controlling whole body thermogenesis and energy expenditure.

1.1.5. Other Uncoupling Proteins

As the proton leaks exist in tissues other than BAT, it could be regulated so rather than a constant leak of protons, they could provide a viable, physiological role. This hypothesis led researchers to screen a skeletal muscle library for similar proteins using UCP1 cDNA as a low stringency probe. These experiments concluded in 1997 with the cloning of a second uncoupling protein (UCP2)²¹, which shares a 59% amino acid sequence homology with UCP1²¹. Further cloning experiments led to the discovery of other UCP1 homologues such as UCP3²², UCP4²³ and brain mitochondrial carrier protein I (BMCP-1)²⁴. For the purpose of this study discussion will be focused on UCP2.

Structural modelling studies have indicated that UCP2 conforms to the same triplicate structure that is typical of all inner membrane mitochondrial carriers²⁵. Each of its three domains has been shown to contain the mitochondrial energy transfer site and it has been predicted that each of these contain two transmembraneous helices, linked by a matricial loop between the N- and C- terminus, with cytosolic orientation. A similar model is proposed for UCP1²⁶. Members of the mitochondrial carrier family, which include the UCPs, have been shown to have two transport modes: a substrate-specific carrier activity and a less specific channel activity. Evidence suggests that this character is reflected by UCP1 and 2 by the structural organisation of the two transmembraneous helices that are proposed to form a channel and a gating domain. Studies with UCP1 have suggested that matrix loops that link the transmembrane helices may contribute to the formation of a gating domain that could be a focus for controlling the transport activity of this protein²⁷.

In situ hybridisation has been used to describe UCP2 expression. UCP2mRNA has been found in heart and muscle tissues, in white adipose tissue, the brain, stomach, small intestine, gut, liver, kidney, pancreas and throughout the immune system, in all organs containing macrophages and lymphocytes²¹.

1.1.6. Uncoupling Function of UCP2

The sequence and structural homology between UCP1 and 2 have led to the suggestion that like UCP1, UCP2 uncouples productive respiration. The ubiquitous nature of UCP2 expression led to hypotheses linking this proteins function with whole body temperature regulation and weight regulation. However, the similarities between UCP1 and 2 are not sufficient to determine whether their uncoupling pathways are the same in terms of molecular and regulatory mechanisms, let alone what the physiological function of UCP2 might be. Interestingly, the amino acid sequence of UCP2 lacks two histidine residues that have been argued to be essential for proton transport in UCP1²⁸. Despite the significant homology with UCP1 it is possible that UCP2 does not have an uncoupling function.

Most investigations into the uncoupling function of both UCP1 and 2 have been based on the use of heterologous expression systems. Several groups have used *Saccharomyces cerevisiae* for UCP activity analysis^{21;29}. Expression of UCP1 and UCP2 in this have model appeared to confirm their uncoupling function. However, unlike UCP1, UCP2 uncoupling in isolated mitochondria from *Saccharomyces cerevisiae* did not demonstrate a dependence on fatty acids or inhibition by purine nucleotides³⁰. This result has been taken to mean that uncoupling in UCP2 is different to UCP1. The reduction in mitochondrial membrane potential and increase state 4 respiratory rates that have been reported with UCP2 expression in yeasts²¹ indicate that uncoupling is occurring²⁹. However, it is possible this uncoupling is not intrinsic to activity of UCP2, but occurs as a result of impaired mitochondrial integrity due to over expression of UCP2 in the membrane.

Some studies have reported that UCP2 expression in yeast reduces fully uncoupled respiration rates in isolated mitochondria^{30;31}. This can affect the estimated value of respiratory control that is calculated as the ratio of the fully uncoupled rate to state 4 respiration. There is no reason why uncoupling resulting from UCP2 expression should affect fully uncoupled respiration rates and in these cases decreased respiratory control should not be seen as confirmation of uncoupling activity. A decrease in respiratory control may well indicate a dysfunction of the respiratory chain rather than confirm uncoupling by UCP2 expression.

Another criticism of the experiments with transfected yeast models has been that none have measured the expression levels of the UCP homologues and that in some cases the presence and function of the protein have been inferred by the uncoupling phenotype. It is possible that uncoupling may be the result of a general disruption of mitochondrial physiology rather than the activity of a specific protein. Recent experiments on UCP1 expression in yeast demonstrated that low level mitochondrial expression of this protein led to GDP sensitive uncoupling. However, at higher levels of expression uncoupling became GDP insensitive, suggesting that uncoupling could be an artefact in yeast mitochondria³².

The third argument against the validity of the use of yeast expression systems to report uncoupling by UCP is that amount of protein expressed in these systems do not reflect the native level of UCP in mammalian mitochondria. Proteins are generally far over expressed in transfected models and it is possible that this renders observation of uncoupling activity, physiologically irrelevant³³. The level of UCP2 and UCP3 protein expression in mammalian mitochondria is extremely low.

These arguments could be levied at the some of the conclusions drawn from similar transfection studies of uncoupling with UCP1. However, uncoupling in yeast cells transfected with UCP1 has been reported as GDP sensitive at physiologically relevant levels and UCP1 uncoupling has already been well characterised when isolated from its native tissue³⁴⁻³⁶. It has not been possible to isolate UCP2 due to its low tissue content. Therefore studies have relied on transfection systems such as *Saccharomyces cerevisiae* or *Escherichia coli*. Recent experiments have suggested that UCP2 expression in yeast differs from UCP1. It has been reported that it is expressed in a deranged form in *Saccharomyces cerevisiae* and it is possible that it is an unsuitable host for UCP2 expression³⁷.

1.1.7. Ubiquinone and UCP function.

Initial experiments with *Escherichia coli* were unable to demonstrate proton transport activity from any UCP expressed *E.coli* inclusion bodies³⁸. Rather than

disregard the uncoupling hypothesis, Echtay *et al* continued their enquiries into why expression in inclusion bodies failed to support UCP uncoupling³⁸. Experiments began with UCP1 because a greater body of evidence for uncoupling existed for this member of the uncoupling family^{13;17}. By screening lipophilized mitochondria extracts for their ability to activate proton transport in liposomes including UCP1 and submitting active fractions to silica gel column chromatography, a lipid soluble co-factor was discovered that was essential to uncoupling activity³⁸. Analysis of its absorption spectra identified this compound as ubiquinone₁₀ (UQ₁₀), (commonly known as coenzyme Q). Addition of pure UQ₁₀ to the inclusion bodies was shown to cause a stimulation of proton transport that could be inhibited by purine nucleotides. Ubiquinone has also been reconstituted from native UCP1 and a structural requirement has been reported with respect to the length of its hydrophobic side chain; activation of proton transport decreased with a shorter isoprenoid chain. It has been shown, by using ubiquinone in conjunction with fatty acids, that nucleotide sensitive proton transport rates can be matched to those found in native UCP1. This confirms that UCP1 uncoupling can be reproduced in *E.coli* inclusion vesicles and that ubiquinone is an obligatory co factor for this function³⁸.

Later experiments confirmed that both UCP 2 and 3, when reconstituted under the same conditions for UCP1 activation, could exhibit nucleotide sensitive proton transport activity and were functionally dependent on ubiquinone³⁷. Like UCP1, Uncoupling with UCP2 and 3 has a functional requirement for the hydrophobic side chain. Optimal proton transport rates have been achieved with isoprenoid lengths of between 10 and 13 units³⁷. It is possible that this indicates that ubiquinone has to be embedded deeply in the membrane in order to interact with UCP. UCP3 has been demonstrated to accept shorter chain lengths for activation which may suggest that the quinone docking site is less deeply embedded³⁷.

The requirement for fatty acids (FA) that accompanies the cofactor role of ubiquinone for uncoupling suggests that they may associate directly for this function. Both compounds are bound to the phospholipids of the inner mitochondrial membrane, whereas the hydrophilic carboxyl group of FA would bind to the phospholipid head groups of the membrane, the quinone group of ubiquinone would easily penetrate into the hydrophobic layer. It is possible that by forming a hydrogen bond between the

quinone oxo group and the FA carboxyl group, ubiquinone may allow the entry of undissociated FA (FAH) into the hydrophilic membrane and through the proton transport route of its associated UCP. It is possible that ubiquinone has a catalytic role and takes the proton from FAH and passes it into a proton acceptor group of UCP³⁷ (Figure 1.4.).

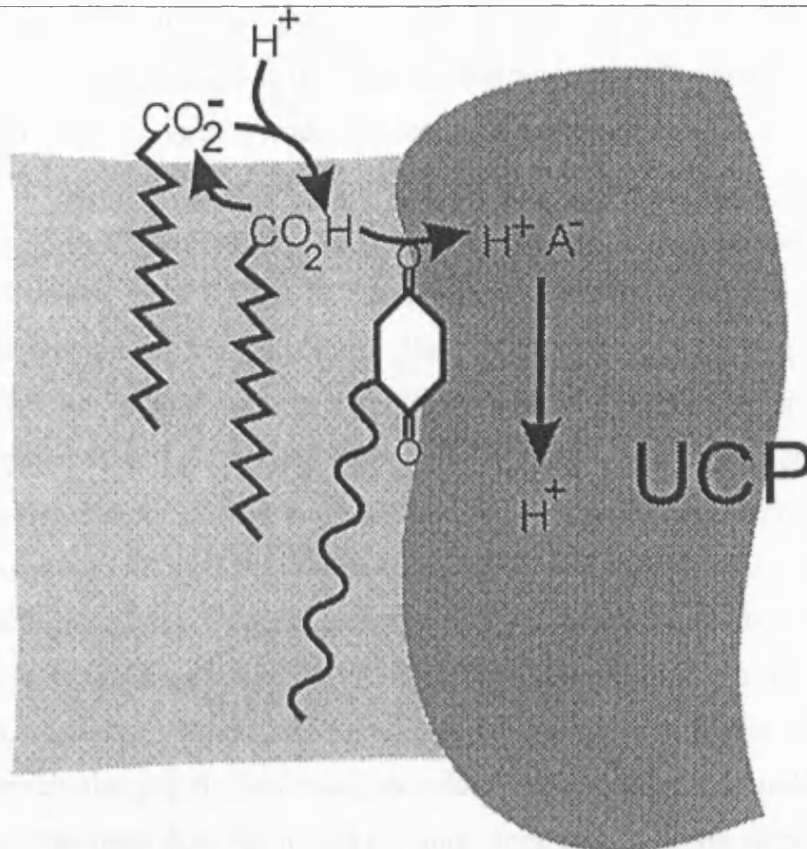


Figure 1.4. Possible mechanism for role of Ubiquinone as an essential co-factor for UCP uncoupling. Undissociated Fatty Acid (FAH) forms a hydrogen bond with the quinone oxo group bound to UCP. This complex eases the delivery of FA carboxyl to UCP, where it donates H^+ to an acceptor group. The FA^- diffuses back to the surface where it obtains another H^+ ³⁸

1.1.8. Physiological nature of Uncoupling proteins.

The structural similarities reported for the UCP proteins that included the conservation of domains for binding nucleotides and for proton transport led to the suggestion that these proteins shared a common function³⁹. The finding that liposomes expressing UCP2 and-3 can demonstrate regulated proton transport supports this initial

hypothesis and would seem to justify the extension of the term uncoupling from UCP1, to UCP2 and 3.

Several physiological roles for UCP2 and 3 have been proposed based on their supposed uncoupling function and expression pattern. Genetic studies have suggested they might be linked to hyperinsulinism or to resting metabolic rate and hence the control of body weight²¹ and the wide spread expression of UCP2 have led to suggestions of a role for UCP2 in diet induced thermogenesis, fever and possibly in the regulation of reactive oxygen species production⁴⁰.

Most of these studies into the physiological role of UCP2 and 3 have been based on the variations of mRNA levels for these proteins⁴¹. Although this is a valid procedure for recognising the factors that affect UCPs at the transcription level, it is not a precise indication of UCP activity or function. The level of UCP2 mRNA expression in the liver and reports that LPS and TNF α induce UCP2 expression in hepatocytes led to the suggestion that UCP2 may have a role in fever response and thermogenesis^{42;43}. However, investigations into the level of UCP2 protein expression have thrown doubt on this hypothesis. Using a highly sensitive polyclonal antibody for UCP2, a large disparity has been demonstrated between UCP2 mRNA and UCP2 protein expression. UCP2 mRNA has been found in many organs in which it is expressed at different levels. However, the protein has only been detected in a limited number of organs. UCP2 protein has been detected in spleen, lung, stomach and white adipose tissue, yet none has been detected in the heart, skeletal muscle or importantly the liver. Even in the organs where UCP2 expression is at its highest, the lung and spleen, the amount of UCP2 protein is 2 orders of magnitude lower than that of UCP1 in BAT mitochondria. Reports indicate that the level of native protein expression is too low to suggest that UCP2 can trigger thermogenesis by strong mitochondrial uncoupling³³. An analysis of UCP2 protein expression in several organs after LPS exposure has reported an increase in expression in both lung and stomach tissues⁴¹. The kinetics of the induction of UCP2 protein after LPS injection were shown to be consistent with a primary immune response leading to oxidative burst in the lung⁴¹. It is possible that UCP2 does not have a function under basal conditions, but is activated when the level of intracellular ROS is too high. In this way its function could be to protect certain tissues from oxidative stress that could be provoked by infection, pollution or allergy.

1.1.9. Studies in UCP2 Knock-out mice ^(-/-).

One way to determine a proteins' function within an organism is to remove it and then study the effects on the organism's physiology. Late in 2000, Arsenijevic *et al* generated UCP2 deficient mice by homologous recombination in stem cells⁴⁴. These mice developed normally, but had no UCP2 expression, confirmed by western blot analysis of mitochondria and northern blot analysis of tissue mRNA. It was found that UCP2 ablation had no effect on cold induced thermogenesis or on body weight regulation.

The responses of UCP2 ^(-/-) mice to cold exposure and a high fat diet did not differ from that of wild type mice, suggesting that UCP2 does not play a major role in energy balance. The extensive distribution of UCP2 mRNA within tissues of the immune system in wild type mice led investigators to explore the immunological phenotype of this knock out model. UCP2 ^(-/-) mice were infected with *Toxoplasma gondii*, an intracellular parasite that infects the brains of normal mice causing death.

All wild type mice in this experiment died between 28-50 days after infection with *Toxoplasma gondii*, yet the UCP2 ^(-/-) mice were completely resistant even 80 days after infection. *In vitro* studies on their isolated macrophages demonstrated that the pathogen was eliminated more efficiently in the absence of UCP2 as compared to isolates from wildtype mice⁴⁴. Somehow the macrophages of the mutant mice had increased toxoplasmacidal and bactericidal activity, a very surprising finding. It is well known that stimulated macrophages produce ROS that have powerful toxoplasmicidal effects and that mitochondria are the main source of these ROS⁴⁵. Further studies demonstrated a higher rate of ROS production in UCP2^(-/-) macrophages compared to control macrophages⁴⁴. It seems that disruption of UCP2 alters macrophage activity in the presence of a pathogen by affecting their level of ROS.

It is therefore possible that UCP2 might be of importance to mitochondrial ROS production and that an alteration in mitochondrial membrane potential could be reflected in mitochondrial superoxide generation. An increase in mitochondrial membrane potential would slow the transport of electrons through the respiratory chain, increasing the amount of time for interaction between electrons and molecular oxygen

facilitating ROS formation. As a respiratory uncoupler, UCP2 may act to vent the membrane potential thus decreasing ROS generation. It has been proposed that mild uncoupling of respiration by UCP2 regulates ROS by modulating protein leakage through the inner mitochondrial membrane⁴⁴. However, it is also possible that in the absence of UCP2, there is an increase in NADPH concentration, the substrate for NADPH oxidase to generate superoxide.

1.1.10. UCP2 uncoupling in macrophages

Isolated macrophages challenged with endotoxin demonstrated a decrease in UCP2 mRNA that was associated with an increase in ROS⁴⁴. Thus, it seemed that increases in UCP2 could be active in the limitation of ROS and an act as antioxidant defence. Decreases in UCP2 expression could be used as a mechanism whereby macrophages could increase their bactericidal power by increases in ROS production. Increases in UCP2 may be a tissue specific response to prevent excessive oxidative stress in response to infection, food restriction or even exercise. In addition, previous studies that indicated increases in UCP2 mRNA expression in different tissues could reflect macrophage infiltration in that tissues rather than UCP2 expression in the native cells of that tissue.

1.1.11. Activation of UCP induced uncoupling

If uncoupling proteins are involved in regulating the level of ROS, the next question is how this response is initiated. Retinoic acid has been shown to strongly increase proton transport by UCP1 in brown adipose tissue mitochondria and in yeast mitochondria expressing UCP1⁴⁶. Given the similarities between UCP1 and 2 it is possible that UCP2 may also be sensitive to retinoic acid. Experiments using the yeast expression system for UCP2 suggest that UCP2 uncoupling activity can be influenced by retinoic acid, but only across a certain pH range³⁰. It has been argued that yeasts are not a suitable expression system for studying UCP2³³. Strong evidence for retinoid activation of UCP2 has been provided by a study of the respiratory rates of thymocytes from wildtype and UCP2^(-/-) mice. Retinoids have been shown to increase the

respiratory rate in thymocytes of normal mice but not in those isolated from UCP2^{-/-} animals⁴⁷.

Ubiquinone has been identified as a regulatory cofactor for uncoupling in UCP1, UCP2 and UCP3 in liposomes^{37,38} (See section 1.2.5.). In the search for an *in vivo* regulator further studies have examined the effect of ubiquinone in isolated mitochondria. Ubiquinone has been found to increase proton transport in mitochondria isolated from rat kidney but not liver. This increase was dependent on the presence of fatty acids and inhibited by purine nucleotides. The addition of superoxide dismutase completely abolished the activation of proton transport thus it was proposed that ubiquinone might be mediating uncoupling through the production of superoxide⁴⁸. To test this hypothesis xanthine plus xanthine oxidase, an exogenous system that generates superoxide, was added to isolated mitochondria. Proton conductance increased in mitochondria expressing UCPs suggesting the ubiquinone did indeed act in these mitochondria through the production of superoxide. Once again this increase was fully inhibited by superoxide dismutase and by purine nucleotides⁴⁸. The effect of superoxide has also been reported to require fatty acids. It has been demonstrated that the addition of bovine serum albumin (BSA), an agent that binds fatty acids, abolishes the increase in proton conductance and that reactivation only occurs when the effects of BSA are countered by Palmitic acid. Superoxide induced, nucleotide sensitive and fatty acid dependent proton conductance has only been reported in isolated mitochondria that express UCPs. Given this and that the conditions for stimulated uncoupling by superoxide mimic those required for uncoupling in UCP expressing liposomes, superoxide seems a likely candidate for an activator of UCP activity.

Two models have been proposed for the mechanism by which superoxide may activate proton transport. The first suggests that superoxide directly activates UCPs by an allosteric interaction that induces proton transport by the mechanisms previously proposed for UCP1⁴⁹. The second suggests that superoxide anions in the matrix are exported to the intermembrane space by the UCPs and once here they undergo rapid dismutation due to the more acidic pH or by antioxidant defences. It has been proposed that the resulting hydroperoxyl radical would diffuse back into the matrix and the superoxide anions would then be exported by UCP¹⁰. If this model were correct then

uncoupling would only become evident when the matrix was flooded with exogenous superoxide.

Both models indicate that UCPs could decrease ROS production by mild uncoupling and that this could be a feedback response to the overproduction of ROS by the electron transport chain. A recent study has provided evidence to support the first model and has suggested that UCP2 is activated by superoxide from the matrix side of the mitochondrial inner membrane. Following the same methodology of previous experiments⁴⁸, studies with isolated mitochondria were performed in the presence of high concentrations of superoxide that was generated using xanthine plus xanthine oxide⁵⁰. This group first established that exogenous superoxide anions could actually reach the mitochondrial matrix by measuring the activity of aconitase, a matrix enzyme which is highly sensitive to superoxide. Compared to controls, aconitase activity was significantly reduced in isolated mitochondria with xanthine plus xanthine oxide. This clearly demonstrated that exogenous superoxide anions could reach the mitochondrial matrix. This matrix exogenous superoxide was then targeted by covalently linking the antioxidants ubiquinone and tocopherol to a lipophilic cation that could penetrate the lipid bilayers and thus accumulate in the mitochondria when a membrane potential was present⁵⁰. The superoxide induced uncoupling demonstrated in the presence of xanthine plus xanthine oxide was shown to be completely inhibited by these targeted antioxidants. Non targeted antioxidants had no effect suggesting that uncoupling could only be prevented by destroying the matrix superoxide.

The role of matrix superoxide as an activator of uncoupling by UCP2 has been investigated by increasing the level of superoxide specifically within the mitochondrial matrix. The moiety of ubiquinone cycles between oxidised and reduced form by exchanging electrons with the respiratory chain^{51,52}. Under reducing conditions the ubiquinone can accept electrons from the respiratory chain and can itself become a source of superoxide. By titrating isolated mitochondria containing matrix targeted ubiquinone with cyanide (an inhibitor of complex IV), it was possible to produce a gradual increase in superoxide as it was generated by the progressively reduced matrix ubiquinone. This was shown to induce GDP sensitive uncoupling. It has been proposed that this increase in uncoupling occurred through the interaction between matrix

superoxide and UCP2 and not by futile cycling of superoxide through the extra mitochondrial space.

It is not possible to extend these findings to whole cells or organisms, because the studies were performed in isolated mitochondria in the presence of high concentrations of superoxide. However, these studies' results could explain the increased production of matrix ROS reported in mitochondria of UCP2 knockout mice and add to the increasing body of evidence that UCP2 is not involved in thermogenesis, but that it functions as a regulator of ROS.

1.2. Discussion

Despite extensive research, the true function of UCP2 remains elusive. It was initially suggested that UCP2 catalyzed mitochondrial proton conductance²⁰. Investigations into the function of UCP2 in isolated mitochondria have proved difficult due to the low level of native UCP2 protein expression.

Abundant expression of UCP2 protein has been achieved in *E.coli* inclusion bodies and, when reconstituted in phospholipid vesicles, demonstrated to have proton transport activity. These studies have identified ubiquinone as an essential cofactor of *in vitro* uncoupling by UCP1, 2 and 3 and shown that these proteins do share the essentially the same functional characteristics³⁷. Although recombinant expression and reconstitution experiments allow the potential biochemical activities of these proteins to be described they can not suggest which are physiologically relevant.

Evidence from UCP2 knockout studies have indicated that its uncoupling activity does not contribute to the basal proton conductance of mitochondria, but that its function is to regulate the level of ROS in certain cells, such as macrophages⁴⁴.

Different claims have been made for the regulation of UCP2 by ubiquinone, fatty acids, nucleotides¹⁸ and lately, by retinoids³⁰ and superoxide⁴⁸. The reported direct effect of superoxides on UCP2 activation fits well with the observation that UCP2 expression occurs under conditions of oxidative stress. UCP2 activity is influenced by retinoids

only within thymocytes⁴⁷ and the effect of UCP2 gene knock out is only evident in certain cells⁴⁴. This evidence suggests that UCP2 functionality may be limited to specific cell types, in particular macrophages, thymocytes and β -cells.

Evidence to date indicates that although UCP2 has similar bioenergetic characteristics to UCP1 its physiological function is not thermogenesis, but regulation of ROS. UCP1 was the first uncoupling protein to be discovered, however in terms of evolution is younger than UCP2. It has been speculated that UCP1s' thermogenic role in mammals evolved from a more general function of protection against cold induced ROS production. This function for UCP2 can explain the association of this protein with cells of the immune system, the observation of nucleotide sensitive ROS production in cells expressing UCP2 and could be the reason that UCP2^{-/-} mice are resistant to endoparasite infection.

1.3. Aims

The aim of this study was to examine the expression of UCP2 protein and its possible function during infection, using endotoxaemic suckling rat pups as a model for neonatal sepsis. The whole body response to endotoxaemia was examined by indirect calorimetry and the effects of endotoxaemia on UCP2 protein expression were assessed by western blotting. The role of UCP2 mediated uncoupling in specific cells was then investigated using an *in vitro* assay of macrophage induced ROS production. Our findings support the hypothesis that UCP2 has a role protecting specific cells against ROS.

2. Whole body energy metabolism of endotoxic suckling rat pups.

2. Whole body energy metabolism of endotoxic suckling rat pups.

2.1 Introduction.

Sepsis is a major cause of morbidity and mortality in neonates. Its physiological manifestations are diverse and mediated by complex cellular and biochemical events. Sepsis has an impact on the metabolic control of mammals and can elicit a range of thermoregulatory responses⁵³. Clinical signs of neonatal sepsis include hypo- or hyperthermia¹.

A locus for the metabolic responses driven by sepsis could be proton flux across the inner mitochondrial membrane. It is known that futile cycling of protons through the proton pumps that drive ATP consumption can modify metabolic efficiency and in some cases have been proved to drive heat production¹⁵. UCP1 has been identified as the molecular key for this process in brown adipose tissue (See Chapter 1). The high level of mRNA expression reported in various tissues for UCP2 has led to the suggestion that this protein may be involved in whole body thermoregulation. As lipopolysaccharide injection increases UCP2 mRNA expression in liver and in other tissues, an effect on whole body energy metabolism could be mediated via UCP2.

Studies suggest that in adults the metabolic response to sepsis consists of a short, initial, hypometabolic phase that is followed by a more prolonged hypermetabolic response⁵⁴. Neonates have a reduced immune function and their metabolic response to sepsis has not been clearly defined. Infants with sepsis frequently present with hypothermia^{1;55}, but it is not known whether transient hypometabolism occurs that may contribute to the observed condition. Studies with children have reported that their hypermetabolic response to sepsis may be short lived or non-existent^{1;56}.

The aim of the study was to investigate respiratory gas exchange and body temperature in suckling endotoxaemic rats to determine the effects of endotoxaemia in this model. Any changes in whole body energy metabolism can then be related to changes in UCP2 expression (see chapter 4).

2.2. Methods

Animals

Single litters of 11-13 day old Wistar rat pups were split into two groups of five and allowed to suckle freely with the mother until the start of the experiment. The experiment commenced with each rat pup being given a single intraperitoneal injection of either 0.9% saline (control group C) or saline plus 300 µg/kg lipopolysaccharide (LPS, *E.coli* 0.55:B5, Sigma, Poole, Dorset, U.K) (endotoxic group E) at 0.024ml/g body weight. Weight and rectal temperatures were measured hourly throughout the time course of the experiment. Rectal temperature was measured with a digital probe and hypothermia was defined as rectal temperature less than 32°C.

Endotoxaemia score

A scoring system was adapted from a system created for adult rats was used to assess the degree of sepsis in each rat pup ⁷

<i>Mobility</i>	
0	The rat pups will not allow themselves to be supine
2	The rat pups can be turned supine for a few seconds
4	The rat pups can be turned supine for more than 5 seconds
6	The rat pups will not turn back over when turned supine
<i>Power</i>	
0	The rat pups can dangle from a finger for more than 5 seconds
1	The rat pups can dangle from a finger for less than 5 seconds
2	The rat pups cannot dangle from a finger
<i>Shivering</i>	
0	No shivering
1	Shivering

Figure 2.1. Sepsis scoring table. The score of shivering is additional. If the total score is 8 for mobility and power then shivering is not counted. i.e. maximum score of 8 (Very ill); minimum score of 0 (no signs of illness).

Indirect Calorimetry

Measurement of respiratory gas exchange was performed using an indirect calorimeter (Oxymax, Columbus Instruments, Columbus, Ohio). The set up consisted of a sealed perspex chamber in which the flow rate could be adjusted; this was connected to an infra-red CO₂ analyser and an electrochemical O₂ sensor. The rate of airflow through the chamber was between 0.3-0.5 litres per minute, and this gave a difference in O₂ between the inflow and outflow from the chamber of approximately – 0.3%. The O₂ and CO₂ sensors were set to zero using oxygen free N₂ and then calibrated using a mixture of 20.5% O₂, 0.5% CO₂ and 79.0% N₂ (BOC, Special Gases, Guildford, Surrey).

The rat pups were placed in the calorimeter chamber in groups of five and assessed for a period of 30 minutes at a time. The temperature of the chamber was monitored throughout indirect calorimetry assessment. After this period, the rats were returned to their mother and allowed to suckle freely for a minimum of 30 minutes, before the next round of assessment. Data were collected every minute and averaged over each 30 minute period; O₂ consumed (VO₂) and CO₂ produced (VCO₂) were expressed in ml/kg/min. Respiratory quotient was calculated as VCO₂/VO₂

Statistical evaluation

Results were normally distributed and are expressed as mean ± SEM. VO₂ and endotoxaemia score were compared by ANOVA with Tukey's Multiple Comparison post-hoc test, or by paired t-tests where animals from the same litter were compared. Incidence of hypothermia was compared between groups by Fisher's exact test. Prism 3.02 and Instat 3.05 (Graphpad software, San Diego, California, USA) were used for statistical comparisons.

2.3. Results

2.3.1. Temperature and endotoxaemia

Cage temperature remained at 23.9 ± 0.1 °C throughout the study. The rectal temperature of LPS injected groups dropped at 90 minutes post injection and remained lower than the control group throughout the experiment (Figure 2.2.).

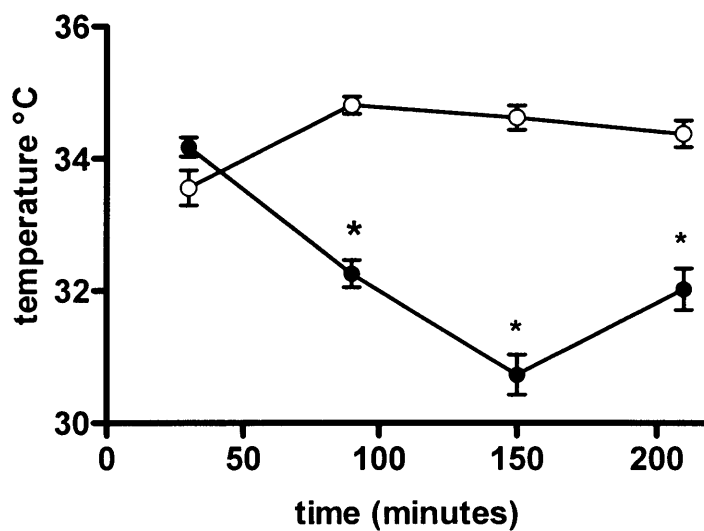


Figure 2.2. Effect of Endotoxaemia on rectal temperature: Rectal temperatures were measured hourly with a digital probe. Hypothermia was defined as temperature below 32°C. Empty circles = measurements from control rat pups (Mean±SEM, n=45) Filled circles = measurements from endotoxic rat pups (Mean±SEM, n=49). Data that is significantly different from control is marked with an asterisk $p < 0.005$. Ambient cage temperature remained at 24 °C±0.12 (Mean±SEM)

2.3.2. Oxygen Consumption.

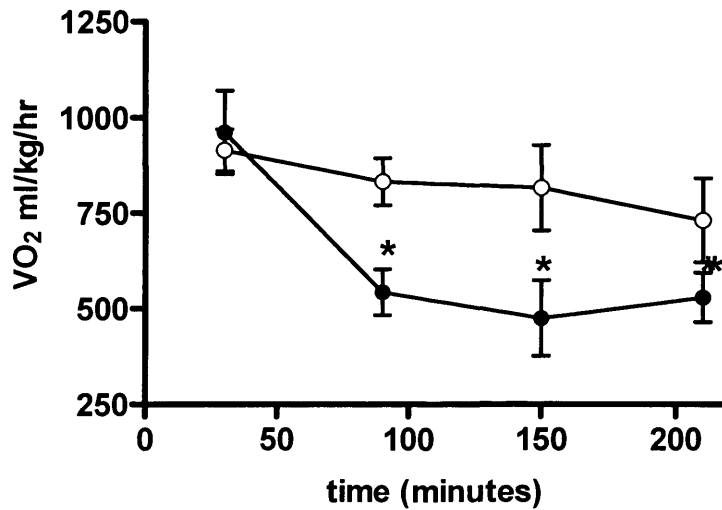


Figure 2.3. Oxygen Consumption. Values for oxygen consumption are given as mean±SEM. Empty circles = measurements from control rat pup. Filled circles = measurements from endotoxic rat pups. $p < 0.005$ $n=8$ paired t-test There was a significant difference between control and septic groups as marked by asterisks.

Oxygen consumption was at 1062 ± 43 ml/kg/min for all rats before injection. This dropped slowly during the course of the experiment with the control group reaching 725 ± 110 ml/kg/min at 210 minutes. Oxygen consumption dropped even lower in endotoxic rats, resulting in a large significant difference in VO_2 between control and endotoxic groups (Figure 2.3).

2.3.3. Correlation between VO₂ and body temperature

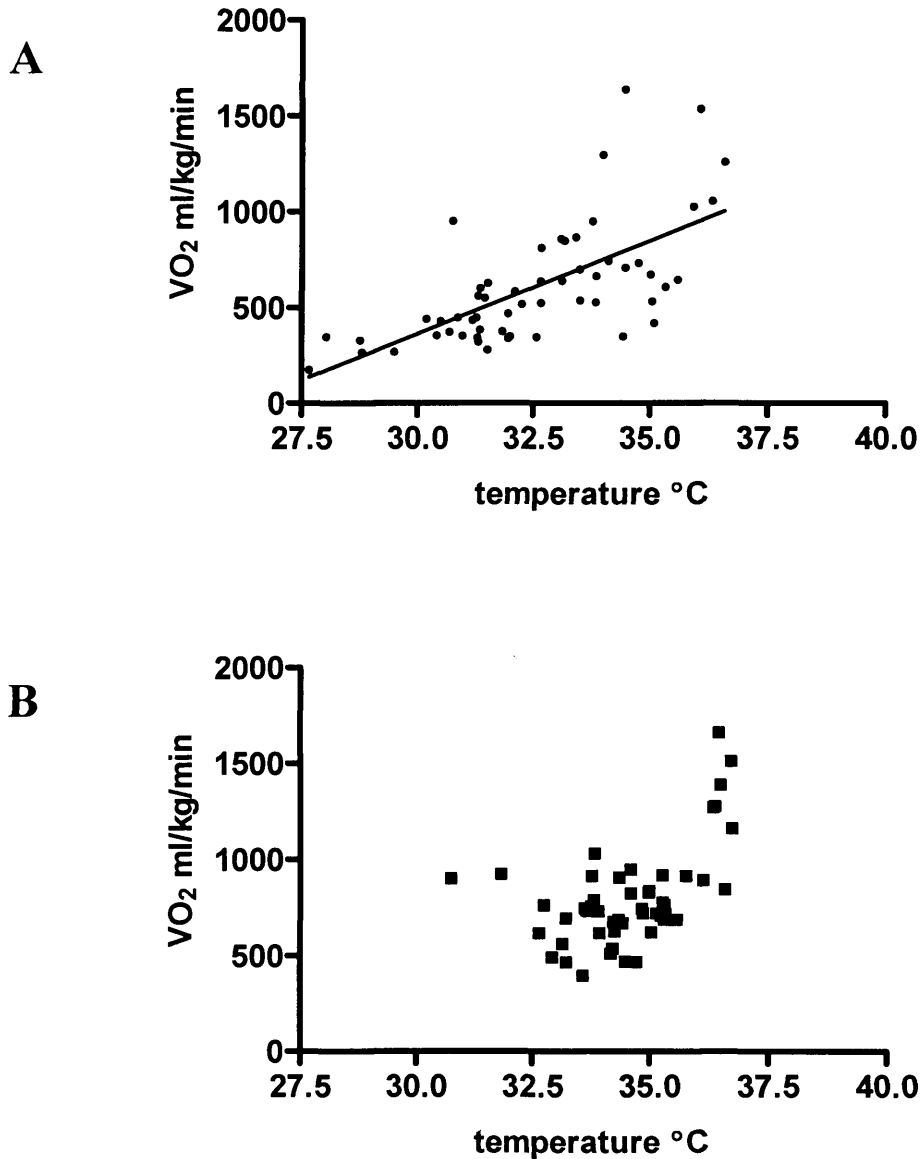


Figure 2.4. Temperature and oxygen consumption. Values for temperature are given as an average for each group of rats analysed at a specific time point. Values for oxygen consumption represent that of the whole group. (A) displays the results from endotoxic rat pups, (B) displays that from controls.

There was a strong positive correlation between VO₂ and rectal temperature in the endotoxic animals (fig.2.3) ($p < 0.001$, $R^2 = 0.43$). The range of rectal temperatures measured in the control groups was insufficient to evaluate whether there was a relationship between temperature and VO₂

2.3.4. Endotoxaemia and respiratory quotient.

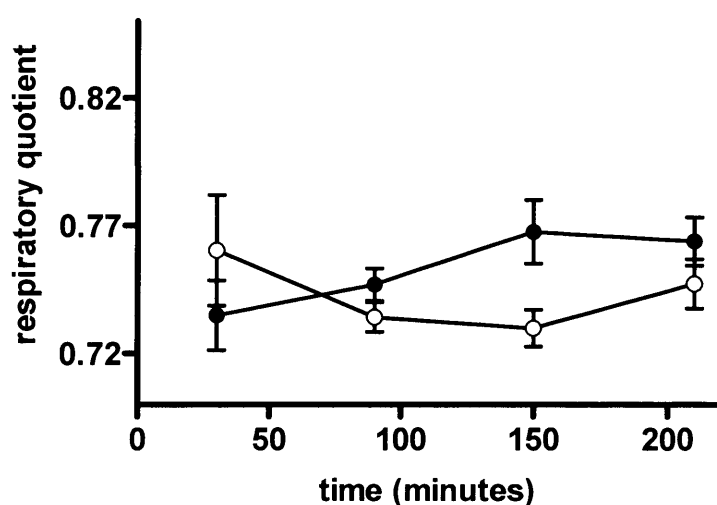


Figure 2.5. Respiratory Quotient. Each value for respiratory quotients represents an average for the five rats in the chamber at each time. Empty circles = measurements from control rat pups. Filled circles = measurements from endotoxic rat pups. A significant difference in values between control and endotoxic groups did not occur until after 150 minutes ($p=0.05$ at this time point). Values expressed as Mean \pm SEM.

The respiratory quotient (RQ) reflects the balance of its substrate oxidation. For net fat oxidation this is expected to be 0.71 and is set at 1.00 for net carbohydrate oxidation, lipogenesis can result in RQs of greater than 1. Respiratory quotients for both control and endotoxic groups remained between 0.71 and 0.78 suggesting a predominance of fat oxidation throughout the duration of the experiment, that is expected for rats of the age (Figure 2.5). Endotoxic rats did show a slight increase in RQ when compared to controls at 150 and 210 minutes. This could reflect a minor inhibition of fat oxidation and/or a shift to carbohydrate oxidation.

2.3.5. Endotoxaemia Score

Only data from rat pups that demonstrated a physiological response to the LPS injection were used in the final analysis and these rats showed an increase in endotoxaemia score over time. Most rats had a response to LPS, a lack of response was most probably due to miss-injection of the endotoxin

2.3.6. Carbon dioxide production and energy expenditure

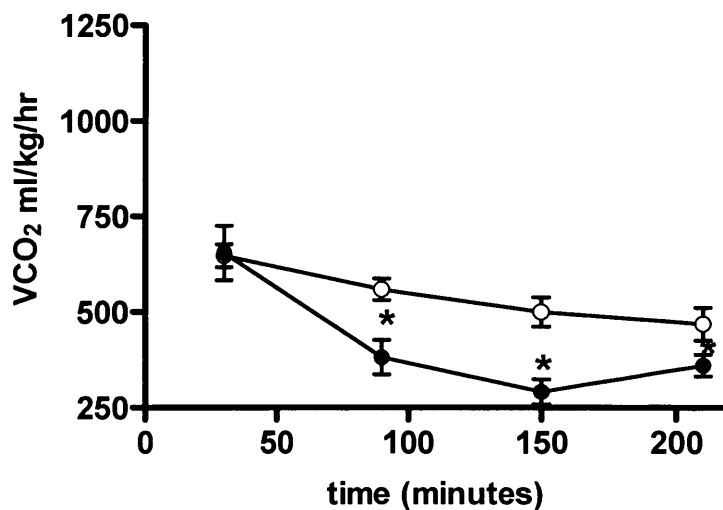


Figure 2.6. Carbon dioxide production. Values for carbon dioxide production are given as mean±SEM. Empty circles = measurements from control rat pup⁵. Filled circles = measurements from endotoxic rat pups. $p < 0.05$ $n = 8$ paired t-test There was a significant difference between control and septic groups as marked by asterisks.

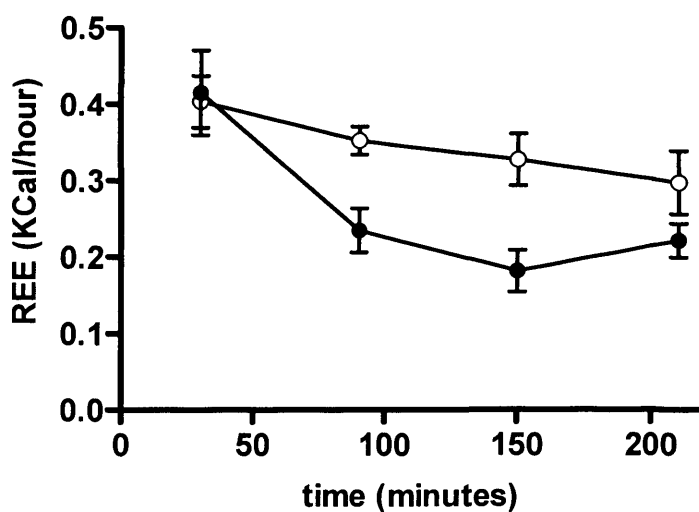


Figure 2.7. Heat production. Values for heat production are given as mean \pm SEM. Empty circles = measurements from control rat pup. Filled circles = measurements from endotoxic rat pups. n=8. Heat = calorific value \times VO_2 . Calorific value = $3.815 + 1.232 \times \text{RQ}$ (Manufacturers recommendations).

As the RQ remained relatively unchanged throughout the course of the experiment the fact that the changes in both VCO_2 and heat production mirrored by those in VO_2 was to be expected. As VO_2 is the major contributor to energy expenditure, the graph of energy expenditure over time is similar to that of VO_2 .

2.4. Discussion

Cardiac mitochondrial function and hepatocyte oxidative metabolism has been shown to be inhibited in ex vivo studies on tissues isolated from this suckling rat model of peritoneal sepsis⁷. Here we have shown that this is accompanied by hypometabolism, which may contribute to the hypothermia observed in these rats.

The oxygen consumption of saline injected animals also dropped during the course of the experiment. It is probable that this is due to the repeated handling and measurement of rectal temperatures of the control animals. VO_2 and temperature were both significantly lower in endotoxic rats as compared to control group.

The low rectal temperature ($\sim 34^\circ\text{C}$) of the suckling rats is in keeping with the findings of other studies of rats at this age⁵⁷. The observed effects of endotoxin on VO_2 and temperature are in agreement with those of DeRijk *et al*⁵⁸ in adult rats. Although other authors have shown increases in both VO_2 and body temperature in adult rat endotoxaemia, these responses vary with both dose and serotype of endotoxin⁵⁹. Studies in infants and children have not demonstrated a hypometabolic phase of sepsis¹. It is possible that this occurs early in sepsis and consequently has not been observed in clinical studies

The respiratory quotient of these rats was low at around 0.75. Similar RQs have been found by many authors⁵⁷ and reflects the reliance of suckling rats on fatty acids as an oxidative fuel. Respiratory quotients have not been corrected for urinary nitrogen output so this figure does include a component of protein oxidation. As mixed protein oxidation has a RQ of 0.835, protein oxidation does not seem to be high in either groups.

Rats at this age feed almost continually. In order to avoid starvation the rat pups were put back with their dams for 30 minutes every hour throughout the experiment. All rat pup stomachs were found to be distended with milk at sacrifice and laparotomy supporting lack of starvation of both the control and endotoxaemic groups. The slight shift in RQ of endotoxaemic rats at later time points could reflect a minor shift in the balance of substrate oxidation towards carbohydrate oxidation.

The cage temperature remained at around 23°C throughout all the experiments, below the range of thermoneutrality for rats of this age. To maintain body temperature rats respond by facultative thermogenesis and by behavioural adaptations such as huddling. Uncontrolled heat loss in these animals was minimised by allowing the rats to suckle with their dams and by measuring five rats together in the indirect calorimetry chamber. The causes of hypothermia in the endotoxic animals could be due to increased vasodilation, decreasing huddling behaviour and increasing heat losses. However, the strong correlation between rectal temperatures and VO_2 suggest that thermogenesis itself is involved in the mechanism of hypothermia in the animals.

Inhibition of the proton leak across the inner mitochondrial membrane could be a factor contributing to hypometabolism in this model and it is possible that UCP2 is involved in this response to sepsis. Under basal conditions the proton leak represents up to 20-40% of tissue VO_2 in rodents¹⁰. The magnitude of temperature decline and drop in VO_2 caused by endotoxaemia appears too large to be accounted for by the proton leak alone and it likely that other factors are involved. Cytokines, prostaglandins, leukotrienes and the vagus nerve have all been implicated in reduced thermogenesis observed in endotoxaemia but the physiological basis is still uncertain^{58;60;61}.

It is clear that endotoxaemia induces hypometabolism and hypothermia in neonatal rats. However, other workers have suggested an increase in UCP2 expression in endotoxaemia, which would be predicted to lead to an increase rather than a decrease in energy expenditure. It was therefore decided to determine how these whole body changes in resting energy metabolism related to changes in UCP2 expression.

3. Development of a method for analysis of UCP2 protein levels in tissues.

3. Development of a method for analysis of UCP2 protein levels in tissues.

3.1 Introduction

Most studies of UCP2 expression rely on Northern Blotting; this technique is based on the detection of mRNA message for the UCP2 protein. Northern Blot analysis has identified UCP2 mRNA in skeletal muscle, lung, heart, placenta, kidney tissue and throughout the immune system²¹. Reports have indicated that expression of this protein occurs in response to mediators of the immune system such as TNF α and under conditions of enhanced fatty acid oxidation^{43;62;63}. Tissue specific expression has been demonstrated with UCP2 up-regulation occurring in the liver during hepatic steatosis and in skeletal muscle upon TNF α administration. Induction of UCP2 expression has also been described during sepsis²⁵, although this may reflect macrophage infiltration into the tissues of these organs. However, mRNA expression is not always indicative of protein expression, therefore conclusions about a proteins function drawn ^{from} mRNA data alone can be flawed. The aim of the work described in this study was to develop a method to determine UCP2 protein expression in a neonatal model of sepsis in order to clarify the relationship between UCP2 protein and whole body metabolism.

In neonatal animal models, sepsis has been associated with a significant decrease in core body temperature and a reduction of the proton leak in hepatocytes⁷. If UCP2 protein expression is up-regulated during sepsis then this is at odds with its supposed role in thermogenesis.

Protein expression is commonly studied by Western blotting, a powerful technique that can separate a protein by means of its molecular weight and detect it by antibody recognition. Good results rely on successfully separating a sample by mass, (SDS-PAGE) and then detecting the protein specifically in an immunoassay step.

This chapter describes the development of a protocol for UCP2 western blotting. As a positive control for UCP2 was not available in initial experiments, SDS-PAGE separations were optimised using SCHAD, a protein of similar molecular weight. Only once a control for UCP2 was obtained was it possible to optimise the

protocol to detect *in vivo* levels of UCP2 protein expression. With this done we went on to identify the pattern of UCP2 expression in rat pups and decide in which tissues this expression would be studied to determine the effects of sepsis. Finally I present the rationale and methods for normalising the level of expression between samples.

3.2. Methods

3.2.1. Animals

Animals from the indirect calorimetry experiments were used as the source of all materials for these experiments. 11-13 day old rat pups were weighed and their rectal temperature were taken before receiving either intraperitoneal saline or Endotoxin, 300µg/g Lipopolysaccharide (LPS; E.coli 055:B5, Sigma, Poole, Dorset, U.K). The rat pups were placed with mother and monitored for a 2hr or 6hr time period, weighing at hourly intervals to assess whether dehydration was occurring. The pups were then blind assessed for signs of sepsis using a scoring system adapted for rat pups⁷ from a system for adult rats⁶⁴ (see chapter 2). Rats that had been injected with LPS and did not become endotoxic were culled and not analysed.

3.2.2. Sample Preparation

Tissues were quickly removed, finely chopped and washed ice cold Medium B (2mM Hepes, 250mM Sucrose, 0.1mM EGTA, pH 7.4 (plus 1% BSA to bind lipids)) and homogenised at a tissue weight to medium volume of approximately 1:2 using a hand held glass homogeniser. Homogenate was kept on ice before isolating mitochondria or stored at -20 °C.

3.2.3. Mitochondria

Methods from paper by Eaton *et al*, 1994⁶⁵. The homogenate was centrifuged at 1047 x g at 4°C for 10 minutes (Sorral Super T-21, SL50T rotor). After this the supernatant was retained and the pellet was re-suspended in Medium B, and re-centrifuged at 1047 x g at 4°C for 10 minutes and the supernatant was retained. The supernatants were combined and then centrifuged at 11621 x g at 4°C for 10 minutes. This mitochondrial pellet was retained, re-suspended in medium B and centrifuged again at 11621 x g at 4°C for 10 minutes. Finally the pellet was washed in medium B by spinning at 11621 x g at 4°C for 10 minutes. This pellet was re-suspended in 300µl of medium B (without BSA) containing Protease inhibitors including a broad spectrum of serine, cysteine and metalloproteases and calpains diluted in accordance with

manufacturers' directions (Complete-mini Protease Inhibitors, Roche). The sample was stored at -20°C .

3.2.4. Mitochondrial Membranes

Mitochondria obtained as above were re-suspended in 20-mM potassium phosphate buffer pH 7.2 containing 0.3 mM KCl and Phenylmethylsulphonylfluoride PMSF (0.1mg/ml) and sonicated on ice with a probe sonicator. Sonication was carried out 8 times for 15 seconds at $10\mu\text{M}$ amplitude, with 15 second cooling periods in between. The sample was then centrifuged at $111500 \times g$ (Sorral Super T-21, SL50T rotor) for 40 minutes, the supernatant was discarded and pellet re-suspended in phosphate/KCL/PMSF buffer. The centrifugation and re-suspension process was repeated twice and the final pellet was re-suspended in a minimum volume of the same buffer containing protease inhibitors and stored frozen at -20°C . Methods adapted from Ghadiminejad *et al*, 1990⁶⁶.

3.2.5. Standard Gel electrophoresis

Samples were heated at 95°C for 5 minutes with loading buffer ($3\mu\text{g}$ Bromophenol Blue, 0.031g Dithiothreitol (DTT), 4% SDS, 25% glycerol, 0.25 M Tris /HCL, ph 6.8, Made up in distilled water to a volume of 20ml and stored in 1 ml aliquots at -20°C), (1/1 v/v), and loaded onto a 12 x 12cm, 12% SDS-polyacrylamide gel. Samples were run at 20V, increasing to 100V, over 5 hours in running buffer (14.85g glycine, 3.78g Tris base in 1 litre of distilled water) with a constant current of 30mA per gel. The separated proteins were then transferred, by electroblotting, to a membrane (HybondTM- C Extra Amersham Pharmacia,) using a Hoefer electrophoretic transfer cell for 2 hours at 100V in running buffer containing 20% methanol, chilled by passing cold water round a water junket.

Total protein content could now be visualised by silver staining using the methods described.

3.2.5.1 Silver Staining⁶⁷

The gel was placed in 200ml of fixing reagent (40% Ethanol/ 10% Acetic acid) for 10 minutes, rinsed in 200ml of distilled water for 10 minutes and placed in 100ml fix/sensitising solution (0.05% Glutaldehyde, 0.0037% Formaldehyde, 40% Ethanol) for 5 minutes. It was then rinsed in 200ml 40% Ethanol for 20 minutes, followed by 200ml of distilled water for a further 20 minutes, before being placed in sensitising reagent (0.2% sodium thiosulphate) for 1 minute. The gel was then rinsed with two, 1 minute washes with 200ml distilled water and placed in 100ml 0.1% silver nitrate solution for 20 minutes. The gel was then rinsed for 1 minute with 200ml of distilled water and then placed in 100ml of developing solution (5.0g of sodium carbonate dissolved in 200ml of distilled water containing 40µl of formaldehyde). This solution was replaced with fresh developing solution after approximately 1 minute and the gel was developed until the required degree of staining was obtained (approximately 15 minutes). The reaction was stopped in 5% Acetic acid for 5 minutes. Wet gels were stored in 0.03% sodium carbonate and sealed in plastic.

3.2.6 Standard Western Blotting

After protein transfer, the membrane was blocked for 1 hour at room temperature in block buffer (2.42 Tris base, 8g sodium chloride, 3.8ml 1M hydrochloric acid and 500 µl Tween-20 dissolved in 1 litre distilled water containing, 5% Marvel™ non fat dried milk protein). The membrane was then exposed overnight at 4°C to a primary antibody diluted to an appropriate concentration in block buffer, washed several times for 10 minute periods with wash buffer (2.42g Tris base, 8g sodium chloride, 3.8ml 1M hydrochloric acid and 5ml Tween-20 diluted to 1 litre in distilled water) and incubated for 1 hour at room temperature with an appropriate alkaline peroxidase-conjugated secondary antibody diluted to the stated concentration in block buffer. The membrane was then washed several times with wash buffer before the appropriate detection step.

3.2.7. Detection

Detection was by either diaminobenzidine (DAB) (Novocastra Laboratories Ltd) or ECL+ (Amersham Pharmacia) substrate and performed according to the manufacturers instructions described below.

3.2.7.1. DAB.

One DAB tablet was dissolved in 10ml of TBS, pH 7.6 (2.42g Tris base, 8g sodium chloride and 3.8ml 1M hydrochloric acid diluted to 1 litre in distilled water). In a separate tube 0.2ml hydrogen peroxide (30% w/v) was added to 5.8ml distilled water. 0.2ml of this diluted hydrogen peroxide solution was added to the dissolved DAB solution. The solution was mixed well and then applied directly to the pre-wetted membrane. Bound peroxidase gave rise to an insoluble brown staining which got progressively stronger over time. To obtain the maximum signal to noise ratio the reaction was observed carefully and stopped at an appropriate time 5-10 minutes after exposure, by washing thoroughly with distilled water.

3.2.7.2 Chemiluminescence detection.

Detection solutions A and B were mixed in a 40:1 ratio. The final volume of detection reagent required was 0.1ml/cm² of membrane. Any excess buffer from the final washing step was drained from the membrane and it was placed protein side up on a sheet of Saran Wrap™. The mixed detection solution was applied to the membrane and it was incubated at room temperature for 5 minutes. The membrane was drained of excess detection solution and placed protein side down onto a fresh piece of Saran Wrap and carefully wrapped up, gently smoothing out any air bubbles. The wrapped membrane was then placed protein side up in an X-ray film cassette. A sheet of autoradiography film (Biomax MR, Kodak) was placed onto the membrane and the film was exposed for a designated period of time (1 - 20 minutes)

3.2.8. *Western blotting adaptations*

3.2.8.1 *SCHAD*

For SCHAD Western blotting, electrophoresis and blotting was performed as described (3.2.5, 3.2.6). The membrane was exposed, first to an anti-SCHAD antibody for 1 hour at room temperature at concentration of 1:1000 in blocking buffer. After the washing step the membrane was then exposed to the secondary antibody for 1 hour at room temperature at a concentration of 1:1,000 (and 1:20,000 after optimisation) in block buffer before the detection step with DAB or ECL+

3.2.8.2 *UCP2*

Electrophoresis was performed as before (3.2.5). However, SDS was not used in the transfer buffer. The Primary antibody, either Santa Cruz (Santa Cruz Biotechnology, Inc. Affinity-purified goat polyclonal antibody raised against a 34 amino acid peptide mapping at the amino terminus of uncoupling protein 2 of human origin) or Calbiochem (Affinity purified rabbit polyclonal antibody raised to an epitope representing amino acids 144-157 of mouse UCP2) was incubated overnight at 4°C in the stated concentrations diluted in block buffer (optimised method used 1:1000) The membrane was then washed several times and then incubated for 1 hour at room temperature with an alkaline peroxidase conjugated polyclonal anti rabbit antibody (Calbiochem) at a 1:2500 concentration in block buffer. The membrane was washed again before the detection step with ECL+ or DAB substrate.

3.2.8.3. *Citrate Synthase*

Electrophoresis and blotting was performed as in the standard protocol described. Polyclonal antibody raised to porcine citrate synthase (Immune Systems Ltd.) was applied to the membrane at the described concentrations for 1 hour at room temperature. The membrane wash washed with wash buffer and then incubated with an alkaline peroxidase conjugated monoclonal anti mouse antibody at the stated concentrations for 1 hour at room temperature. The membrane was then washed several times with wash buffer before the detection step with ECL+ (Amersham Pharmacia)

3.2.9. *Dot Blots*

Dot blots are a quick and effective method of determining the optimum antibody dilutions for a Western blot.

One dot blot was prepared for each combination of antibody concentrations tested. They were prepared by spotting a suitable amount of protein directly onto the membrane pre wetted according to the manufacturer's recommendations. The dot blots were air-dried and then re wetted before blocking for 1 hour with block buffer at room temperature. The blots were then washed in wash buffer for five, x five minute periods, changing the buffer each time. The blots were then incubated individually with the designated concentration of primary antibody diluted in block buffer for 1 hour at room temperature. The blots were washed in wash buffer as before and then incubated individually with the designated concentration of secondary antibody for 1 hour at room temperature. The blots were washed again and finally incubated in ECL+ detection reagents and exposed to Biomax MR Kodak film according to the manufacturer's instructions. The results were then assessed for the strongest true positive and lowest false positive and background reactivity.

3.3 Results

3.3.1. Gel Composition

Gel Electrophoresis is a method by which a sample can be separated into its protein components based on their molecular weight. The primary objective was to determine the composition of gel that would resolve within a molecular weight range comparable to that of UCP2.

As at this stage no UCP2 control was available, protein standards of comparable molecular weight to UCP2 were run with other standards of varying molecular weight on a 10% acrylamide gel and silver stained (See methods section 3.2.6.1) (Figure 3.1)

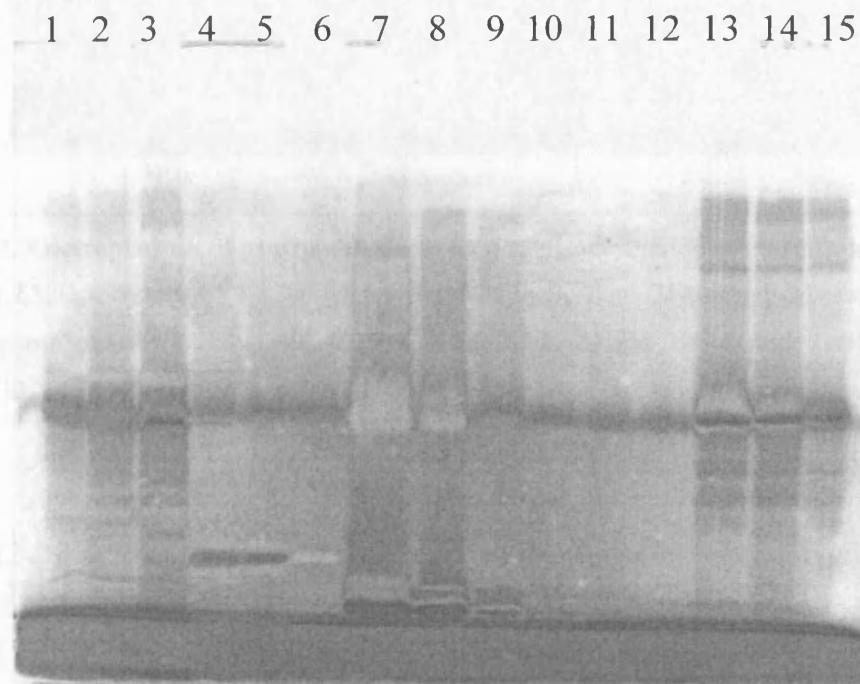


Figure 3.1. Electrophoresis of standard proteins on a 10% acrylamide gel. Standards included; Cytochrome C reductase 1, 2 and 3 at 50, 10 and 5 μ l, Creatine phosphokinase (43kDa) 4,5,6, Short chain 3-hydroxyl- acyl-CoA dehydrogenase (33kDa) 7,8,9 Cytochrome c (12kDa) 10,11,12, and Bovine serum albumin (BSA) (68kDa) 13,14,15 at levels of 1,5 and 10 μ l respectively.

The molecular mass of UCP2 is 32kDa, close to that of SCHAD. SCHAD ran far too close to the solvent front so it was decided to use a 12 % acrylamide gel instead.

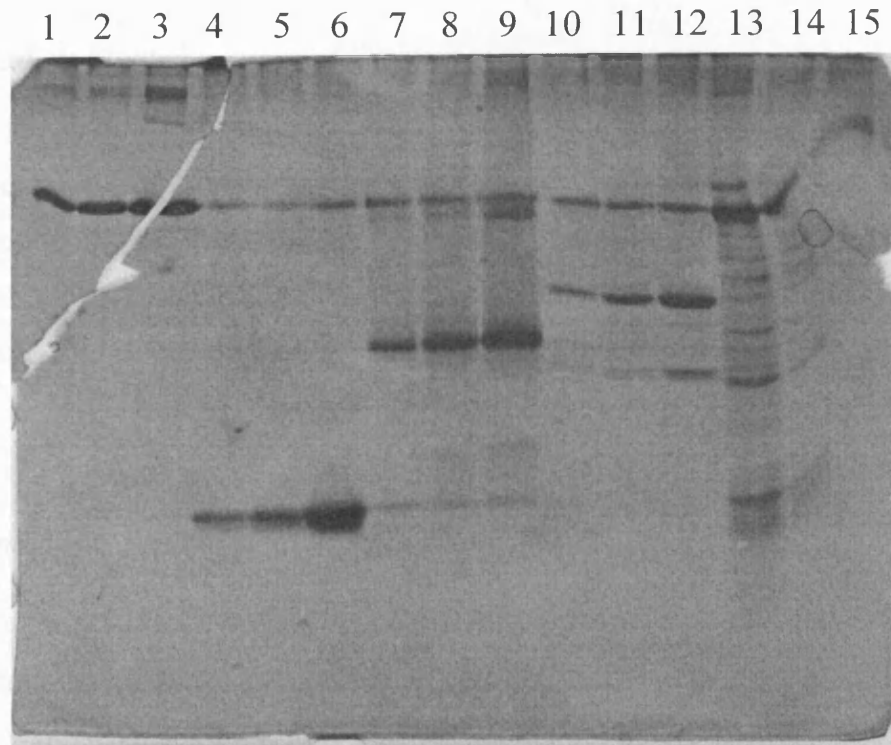


Figure 3.2. Electrophoresis of protein standards on a 12 % acrylamide gel. Standards included: BSA (68kDa) 1,2,3, Cytochrome C (12kDa) 4,5,6, short chain hydroxacyl-CoA dehydrogenase (33kDa) 7,8,9, Creatine phosphokinase (43kDa) 10,11,12, at levels of 1, 5, and 10 μ l respectively. Cytochrome reductase 13, 14 15 was applied at 50, 10 and 5 μ l.

12 % acrylamide gels were found to be suitable for resolving proteins of comparable molecular weights to UCP2. UCP2 is a membrane bound protein and isolation and identification from mitochondrial preparations based on molecular weight alone would prove difficult. The next stage was to attempt to identify UCP2 by immunoblotting the mitochondrial proteins separated on the gel. UCP2 protein standards are not commercially available and optimising the western blot system proved difficult without a protein standard.

UCP2 expression was initially reported to be constitutively expressed in liver mitochondria. It was thought that preparations of this kind might be useful as a native, high titre, sample.

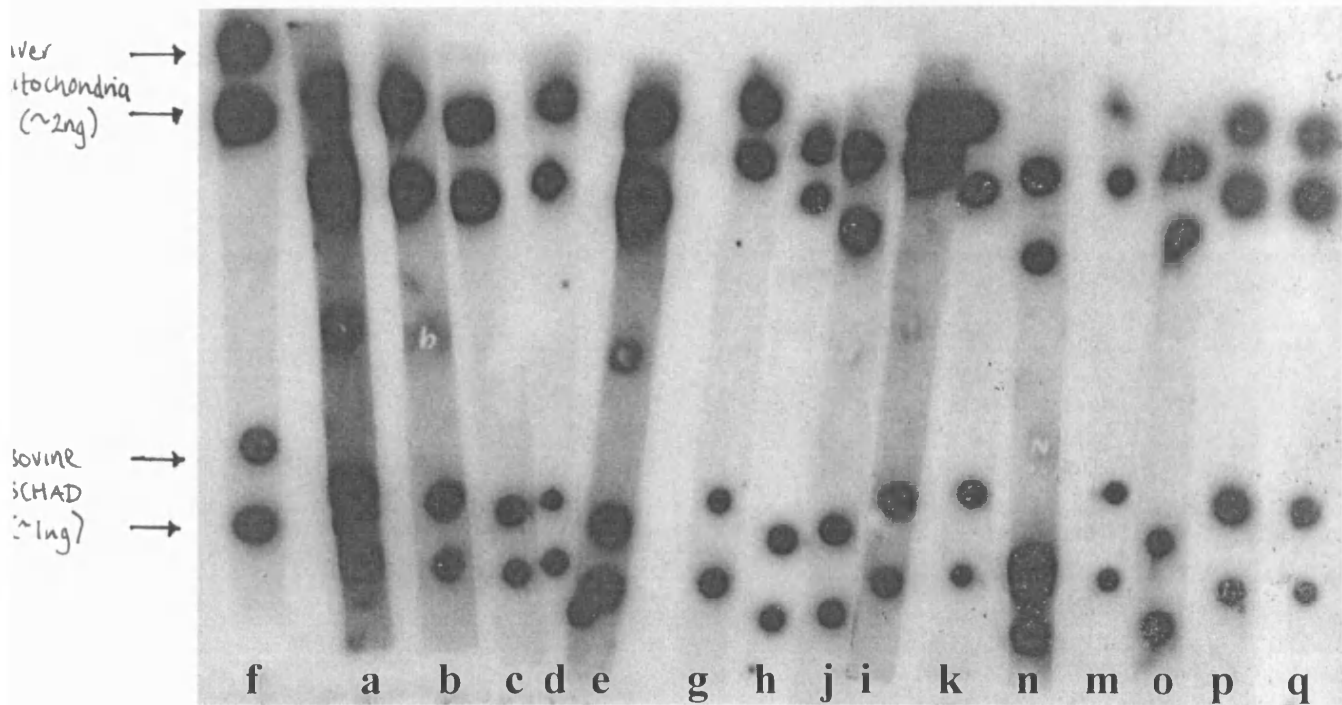
3.3.2. Western Blotting

As no UCP2 protein control was available the Western blotting system was initially optimised for SCHAD. SCHAD is a stable mitochondrial protein with a similar molecular weight to UCP2, in dual blots for UCP2 and SCHAD it was to provide an internal control for the relative amount of mitochondrial protein loaded in each sample.

3.3.3. Optimising western blotting for SCHAD

Protein standards, mitochondrial samples and bovine and porcine SCHAD controls were separated on a 12% polyacrylamide gel before blotting as described in section 3.2.8.2. Buffer solutions, antibody concentration and incubation periods were all optimised by a series of dot blot experiments and the detection limit of DAB and ECL+ were described by serial titration of the SCHAD controls and sample preparations. Silver staining the gel after the transfer procedure confirmed good transfer of protein from the gel to the membrane

3.3.4. Antibody Concentration (Dot blot)



		<i>SCHAD</i> Antibody Concentration			
		1/400	1/1000	1/1500	1/2000
HRPα Goat IgG Antibody concentration	1/2500	A	E	i	n
	1/5000	B	F	j	o
	1/10000	C	G	k	p
	1/20000	D	H	m	q

Figure 3.3. Results of a Dot blot assay. Control and positive native samples were applied to strips of membrane and then incubated with differing concentrations of primary and secondary antibodies. The antibody concentrations that gave the clearest positive results with ECL detection were chosen for future western blot incubation.

Strip h gave the best result, both in clarity and in minimal amount of primary antibody (Figure 3.3). These concentrations were adopted for all future SCHAD western blotting experiments

3.3.5. Determining Detection limits

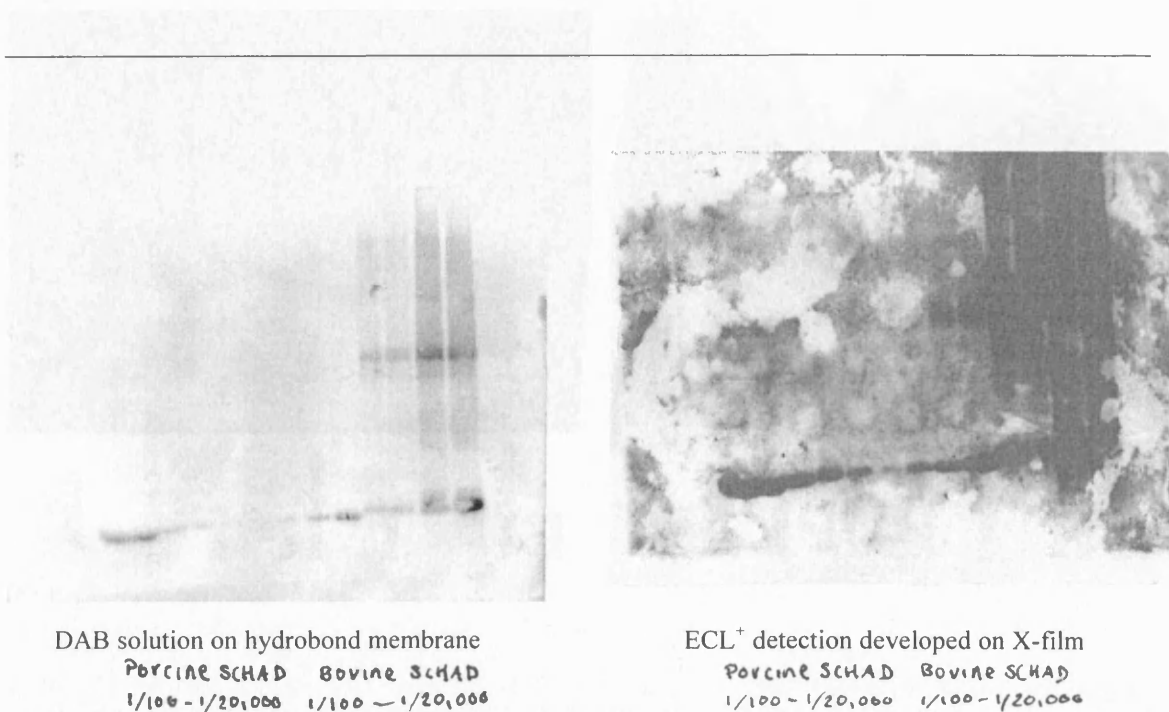


Figure 3.4. Determining the detection limits of SCHAD western blotting. Porcine and bovine SCHAD control were run on a gel at dilutions of 1/100-1/20,000

To determine the detection limit of the ECL and DAB substrate systems, bovine and porcine controls were loaded onto gels at serial dilutions from 1:1000 to 1: 20,000. The DAB substrate system indicated a positive result by a dark grey precipitate directly on the membrane, whereas ECL induced fluorescence of positives had to be developed in the darkroom on MR Kodak film. Dab substrate detection limit was at a 1/1000 dilution whereas ECL s' detection limit was at 1/^{20,000}~~100,000~~ (Figure.3.4)

As UCP2 is expressed at low levels, it is important to obtain maximum sensitivity. The DAB substrate system was a simple procedure but did not have the sensitivity, or the flexibility to study a range of exposure times of the ECL+ system. Future studies concentrated on ECL+ detection

3.3.6. Comparing standard and optimised SCHAD western blotting

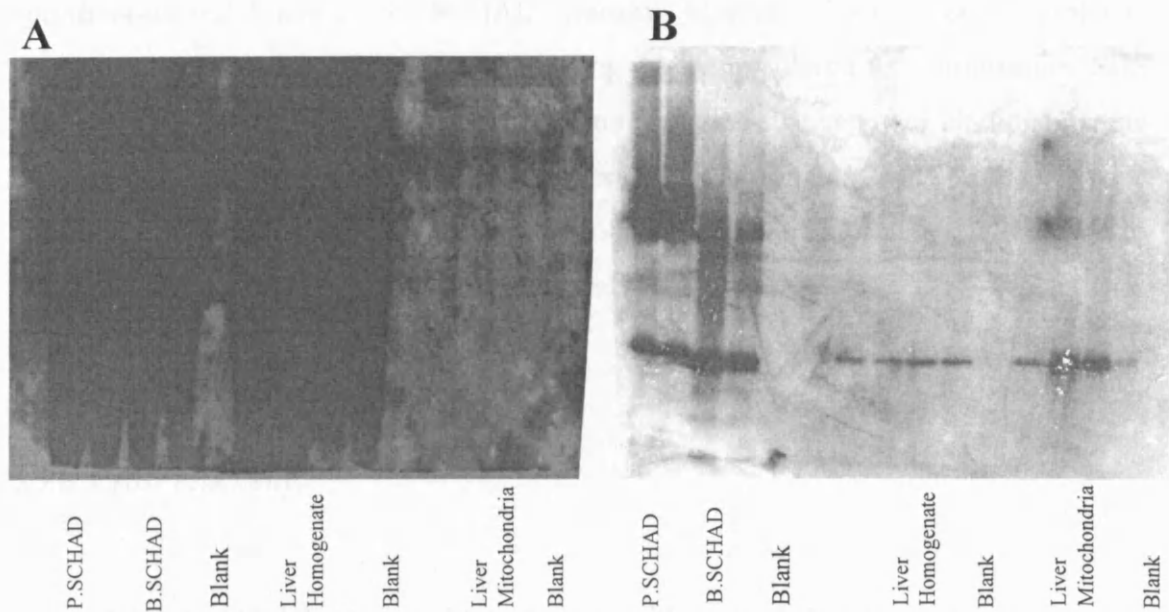


Figure 3.5. Before (A) and After (B) SCHAD Western Blot Optimisation: Porcine and bovine controls were loaded at 1:5000 dilution, liver homogenate at ~30 ng and liver mitochondria were loaded at ~5ng and ~10ng. Samples for both (A) and (B) were from the same stock solutions kept at -20°C

To investigate the overall effect of the optimisation process dual blots of control and laboratory prepared samples were prepared and developed using the standard and optimised procedure. The improvement made by adjusted the standard procedure was clear (Figure 3.5).

3.3.7. *Optimising Western Blotting for UCP2*

Initial western blots for UCP2 in liver homogenate were carried out using the specification established for SCHAD western blotting. These were completely unsuccessful. Each step of the western blotting was reconsidered for optimisation. SDS was removed ~~from~~^{from} the transfer buffer as it can reduce the stringency of binding of some proteins (as advised by Stuart, JA), other blocking agents and protocols were considered, washing time was extended and chessboard dot blot assays were used to determine optimal antibody concentrations and incubation periods.

3.3.8. *Cross reactivity.*

Blots had high background interference with multiple banding patterns and gave false positive results to purified SCHAD controls. The cross reactivity of the primary antibody (Santa Cruz) was confirmed by further dot blot assays (Figure 3.6). It is interesting to note the dark ring around the perimeter of the liver homogenate blot. UCP2 protein is reportedly expressed in Kupffer cells in the liver⁶³. Dot blotting onto the membrane could by some chromatographic effect, separate the kupffer fraction of the liver homogenate. The cross reactivity to SCHAD protein would question the reliability of any UCP2 western blotting data obtained with this antibody. However, an alternative explanation could be due to the presence of UCP2 in purified SCHAD. This is thought to be unlikely due to the low amount of UCP2 in heart tissue, the source of purified SCHAD.

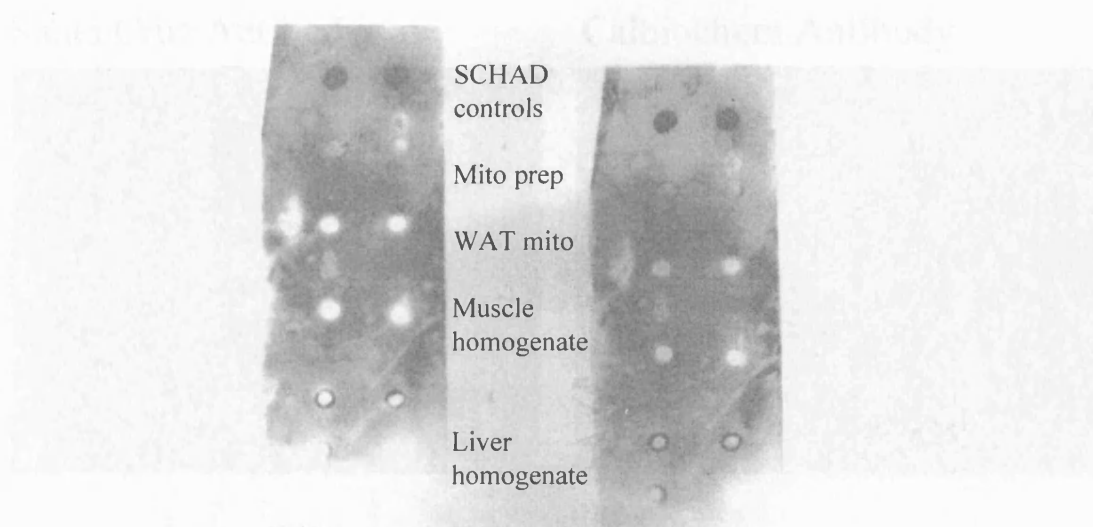
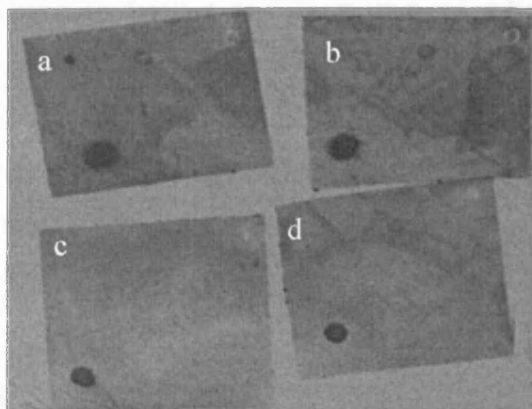


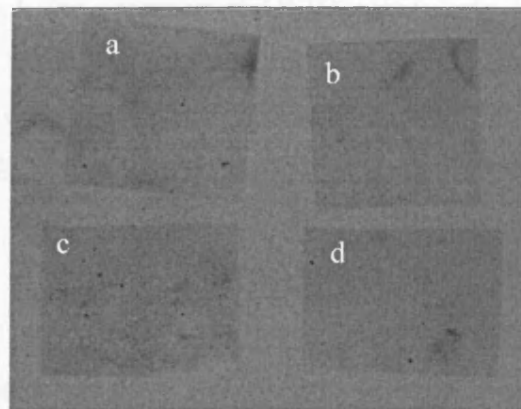
Figure 3.6. Cross reactivity of UCP2 antibody. Dot blot for UCP2 (antibody concentrations 1°Ab 1:500, 2°Ab 1:1000). Samples include SCHAD controls Mitochondrial preparations from Liver and White Adipose Tissue (WAT) homogenate and homogenate from muscle and liver tissue. Dark image on film indicates positive reaction. SCHAD control reacts strongly to ECL+ reagent when incubated with UCP2 antibody.

The specificity of the Santa Cruz antibody was compared to a UCP2 antibody from Calbiochem. Dot blots probed with the Calbiochem antibody, unlike Santa Cruz probed blots, did not give positive reactions to either SCHAD or liver homogenate (Figure 3.7). Further investigations with the Santa Cruz antibody were abandoned in favour of the Calbiochem Antibody.

Santa Cruz Antibody



Calbiochem Antibody



		UCP2 Antibody Concentration	
		1/1000	1/2500
HRPα rabbit IgG Antibody concentration	1/2500	A	B
	1/10000	C	D

Figure 3.7. Comparing Santa Cruz and Calbiochem UCP2 Antibody. 3 μ l aliquots of liver homogenate, liver mitochondria and porcine SCHAD control were applied to each piece of membrane. After allowing drying the membranes were probed with the stated concentration of primary and secondary antibody. Blots were developed on Film using ECL+ detection system.

The lack of a proper control for UCP2 protein was a significant problem to optimising the system. In an attempt to obtain high UCP2 titre samples mitochondrial preparations were fractionated to isolate the supposed UCP2 rich inner membrane (method section 3.2.4.). These blots were unclear, the liver mitochondria did not seem to provide a source of high concentration UCP2 protein. Western blots of these samples for UCP2 did not give rise to distinct bands at a position comparable to 32Kda and Maldi-tof analysis of the silver stain band at this position established by molecular weight markers were not successful in identifying UCP2 protein.

Although initially, UCP2 was described as being present in hepatocytes⁶², whilst this work was being undertaken other studies determined that the apparent UCP2 expression in hepatocytes is due to low level expression in Kupffer cells⁶³. It is likely there are many other be proteins or fragments other than UCP2 within a mitochondrial membrane fraction at 32Kda, that would mask the presence of UCP2 particularly if UCP2 protein is expressed at the low levels described by Stuart *et al* ³³. It was not possible to optimise the system for UCP2 western blotting until a control (UCP2 protein raised by heterologous expression in *E.coli*) was made available (kind gift Jeff Stuart, University of Cambridge)

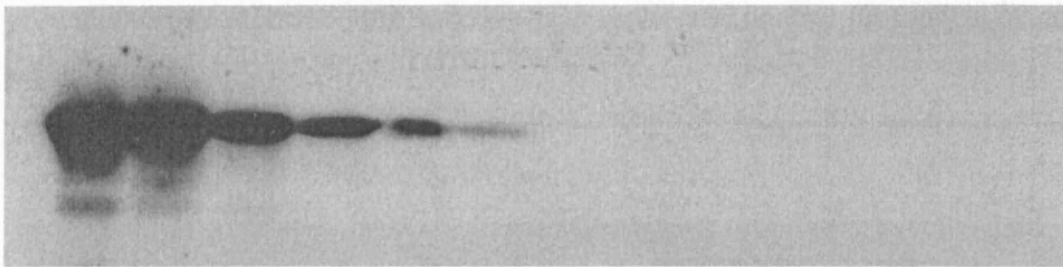


Figure 3.8. Titration of UCP2 Control. UCP2 control loaded onto gel at concentrations of 1/500, 2ng, 1ng, 0.5ng, 0.25ng, 0.167ng, 0.125ng, 1/1000, 1/2000, 1/4000, 1/6000, 1/8000. Western blotting with in house method (Antibody concentration: 1°Ab, 1:1000, 2°Ab, 1:2500) film exposed for 5 min.

Once a control for UCP2 had been obtained it was possible to optimise the western blotting procedure and establish the expression pattern for this protein in our model (see Figure 3.8 for an optimised western blot of different dilutions of the UCP2 control).

3.3.9. Sample Choice

UCP2 western blotting was applied to a wide range of mitochondrial samples from rat pups (see Figure 3.9). The clearest positive results were obtained with those samples prepared from lung and spleen. Other tissues, including the liver did show some faint reactivity towards the UCP2 antibody. However studies with UCP2 knockout mice suggested that this reactivity was likely to be due to a lack of antibody specificity rather than the presence of UCP2 protein⁴⁴.

Further studies with UCP2 concentrated on determining the level of UCP2 protein expression in the lung and spleen in septic and control rat models of neonatal sepsis.

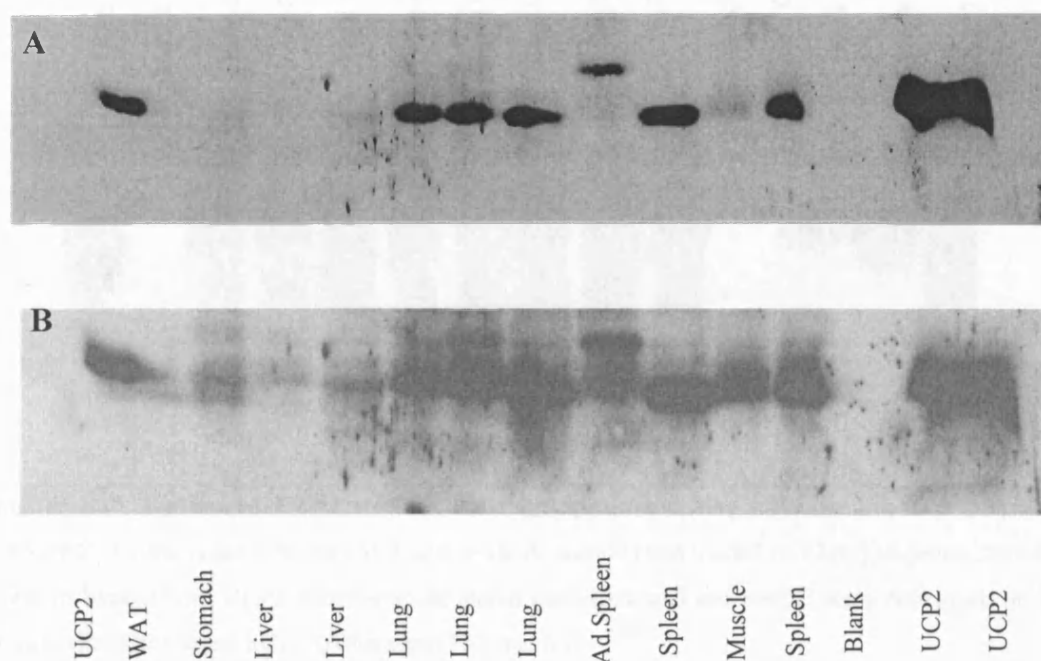


Figure 3.9. UCP2 western blot sample range. Mitochondrial preparations from each tissue were loaded at (~30ng, 12.5µl volume) and tested for UCP2 reactivity. Tissues were taken from 11-13 day old rats unless stated Ad. (adult) Western blotting was performed following the in house protocol. Films were exposed for 5mins (A) and 20 mins (B)

Mitochondrial preparations of the lung and spleen tissue harvested from our control and endotoxic rat pups were subject to UCP2 western blot analysis. Lung and spleen samples were run on dual gels and the respective UCP2 band densities were analysed pair-wise, control vs. endotoxaemia.

Using the described protocol for UCP2 western blotting we obtained reasonable blots with low background and a clear band in a position comparing well to the molecular weight of UCP2 and to the UCP2 standard (see Figure 3.10).

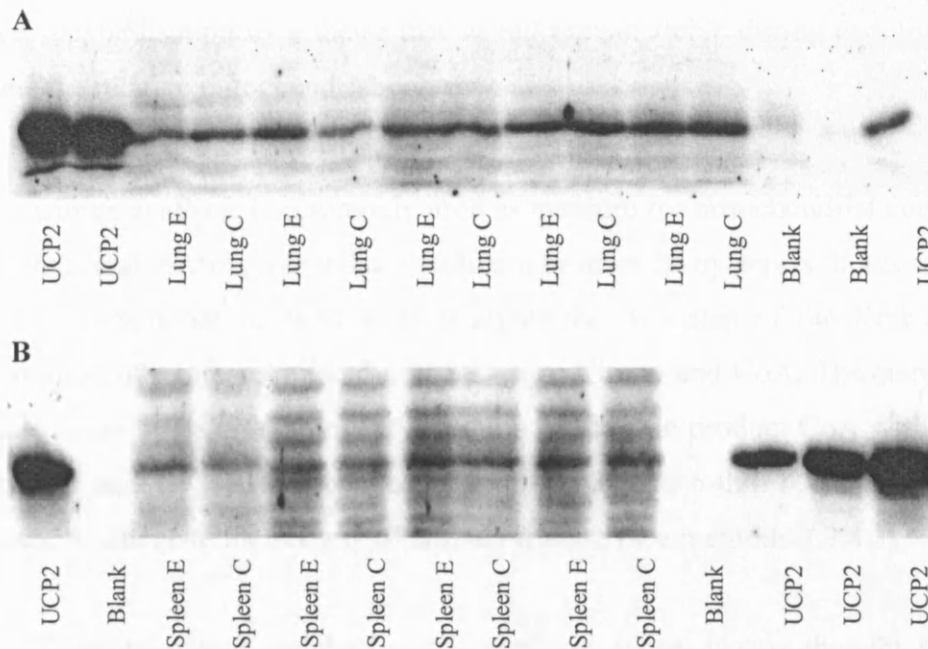


Figure 3.10. Optimised UCP2 western blotting. Spleen and lung mitochondria were prepared from endotoxic (E) and control rat pups (C) (see methods section) and loaded in 12.5 μ l aliquots. Samples were western blotted with UCP2 controls at the stated concentrations and results were developed on Biomax MR Kodak films using ECL+ (Amersham Pharmacia).

From these western blots we could compare the levels of UCP2 protein expression between samples by comparing their band densities using a densitometry programme (Scion image, Beta version 4.0.2). Running respective sets of control and endotoxic samples together on the same gel and then analysing them pair-wise eliminated gel to gel differences. This did not eliminate differences that could exist in

the relative levels of mitochondrial protein between samples. For this other controls were needed.

3.3.10. Controls

When analysing protein expression of a mitochondrial protein it is not enough to normalise just for total protein content. Two samples may have the same total protein content but this does not mean they have the same amount of mitochondrial protein, even when the samples have been prepared in the same way. UCP2 is localised to the inner mitochondria membrane. Comparative analyses of control and endotoxic samples needed standardisation by a factor that would remain stable during endotoxaemia and indicate the relative mitochondrial content.

Citrate synthase is commonly used as measure for mitochondrial content as it is a mitochondrial matrix protein that should not be affected by sepsis. It has an important role in mitochondrial function as it catalyses the first step of the Krebs cycle, the condensation of oxaloacetate and acetyl CoA to Citrate and CoA. The standard citrate synthase assay relies on a secondary reaction of the side product CoA with dithio-1,4-nitrobenzoic acid (DTNB). The coloured product, 2-nitro-5-thio benzoic acid (NTB) is then used to calculate the activity of citrate synthase (see methods 3.2.8.3).

Together with a standard citrate synthase assay, it was thought it would be useful to develop a citrate synthase western blot. As citrate synthase has a molecular weight of ~ 52kDa it was thought possible to measure expression levels of citrate synthase on the same blot as UCP2, therefore providing an on gel standard for the level of mitochondrial protein.

It was envisaged that mitochondrial samples, plus appropriate controls for UCP2 and citrate synthase, could be run following the in house protocol for UCP2 western blotting. Once separated by electrophoresis and transferred, the membrane would then be divided into UCP2 and Citrate synthase reactive sections that could be probed with the appropriate antibody.

Unfortunately, the only commercially available antibodies for citrate synthase was raised against pig heart citrate synthase and did not cross react with rat citrate synthase (see Figure 3.11).

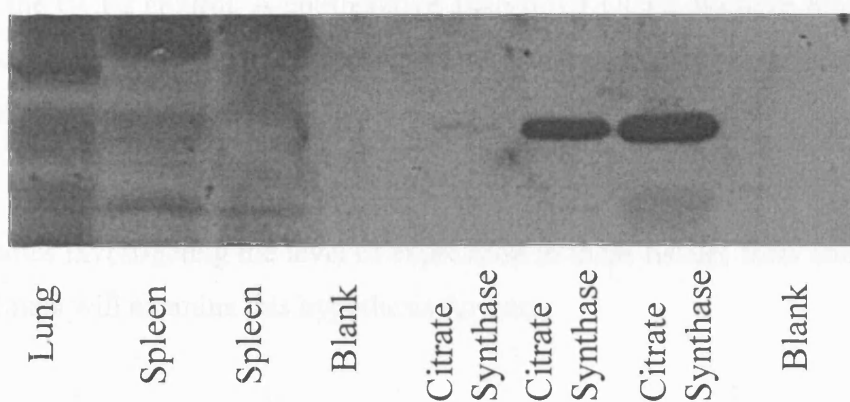


Figure 3.11. Western Blotting for Citrate Synthase. Spleen and Lung mitochondria were loaded as for UCP2 blotting and run with porcine heart Citrate synthase controls (at 5, 10 and 20 μ g). After electrophoresis and transfer, the resulting membrane was probed with Citrate synthase Antibody (Immune Systems Ltd).

Mitochondrial samples were standardised simply based on the activity of their citrate synthase activity.

3.4 Discussion

This study demonstrated that it was possible to use Western blotting to study the expression of UCP2 protein in neonatal rat pups. UCP2 mRNA is reported as being extensively expressed in the liver but this does not seem to be translated into protein expression. Western blots of liver mitochondria gave rise to indistinct bands relative to the UCP2 control. It has been suggested that this low level reactivity is likely to be due to lack of antibody specificity rather than the presence of UCP2 protein⁴⁴. Mitochondrial samples from the lung and spleen both gave rise to distinct bands relative to the UCP2 control. A comparative analysis of UCP2 Western blotting, using control and UCP2 knockout mice support these findings and suggest that UCP2 may have a role in the immune response.

Studies investigating the level of expression in these tissues from endotoxic and control animals will examine this hypothesis further.

4. UCP2 Western blotting

4. UCP2 western blotting

4.1 Introduction

Our investigations with UCP2 western blotting in neonatal rat tissue (chapter 3) revealed that a high level expression of UCP2 did not reside in liver tissues as had been previously thought. However, there was high expression in tissues that have significant populations of immune cells, such as the lung and spleen. This evidence is supported by other western blot investigations of UCP2 expression in adult rats and knock out studies of UCP2 in mice, implicating a role for this protein in the regulation of immune function^{44;68}.

The uncoupling action of UCP2 is reported to be functionally dependent on the presence of an obligatory co-factor, ubiquinone³⁷. The primary role of this compound in eukaryotes is to transfer electrons between redox components of the electron transport chain and therefore create a proton gradient across the inner mitochondrial membrane. Evidence suggests that ubiquinone in mitochondria may be involved in ROS production. Its distribution is not limited to mitochondria and in its reduced form, ubiquinol, it has been shown to act as an antioxidant against lipid peroxidation⁶⁹. Therefore, in tissues in which UCP2 expression occurs, such as spleen and lung, UCP2 expression could be co-regulated with levels of ubiquinone. This situation is complicated further by recruitment and movement of macrophages, which strongly express UCP2.

Mitochondria were prepared from lung and spleen from control and endotoxic rat pups and analysed for UCP2 expression and ubiquinone levels by western blotting and HPLC respectively. Once normalised for mitochondrial content by citrate synthase activity, a clearer picture of the relationship of UCP2 and ubiquinone, with endotoxaemia could be established. Our results suggest that UCP2 may be involved with macrophage mediated attenuation of ROS as part of the immune response.

4.2 Methods

4.2.1. Animals

Animals from the indirect calorimetry experiments (Chapter 2) were used as the source for all the materials for these experiments..

4.2.2. Mitochondrial Preparation

Mitochondria were prepared as described previously (section 3.3.2.) from control and endotoxic rat pup lung and spleen tissue collected 2 or 6 hours after LPS or saline injection. The tissues from each batch of rat pups were pooled so that each mitochondrial preparation was from 4-6 rat pups. Samples were then stored at -20°C until analysis (within 6 weeks of sample generation).

4.2.3. UCP2 Western Blotting

Proteins were separated by electrophoresis and electro-blotted as described previously (Chapter 3). The primary antibody, UCP2 (Calbiochem) was incubated at a 1:2500 dilution overnight at 4°C. Bound peroxidase conjugated antibody was revealed with an enhanced chemiluminescence reagents kit (ECL+, Amersham-Pharmacia Biotech) and the results were recorded on Biomax MR Kodak film by a 5 minute exposure to the phosphorescing membrane. Films were scanned and the signal was quantified using a densitometry programme (Scion image software Beta version 4.0.2). For statistical analysis, control and endotoxic samples were compared on the same blot only.

4.2.4. HPLC analysis of ubiquinone

To 100µl of each mitochondrial sample, 900µl of MilliQ water was added. To these samples were added 1ml methanol, 25µl co-enzyme Q₈ (internal standard) and 3.9ml *n*-hexane. The solution was thoroughly mixed by a bench vortex and left to settle. Once the layers had separated, the upper (hexane) layer was removed and retained in a clean tube. The bottom layer was re-extracted twice with 4 ml hexane and the extracts were combined and blown to dryness under nitrogen. Samples were re-dissolved in 400µl ethanol/methanol (1:1) and analysed by HPLC on a Hypersil 50DS 250mm x 4.6mm C₁₈ column (Hypersil, Runcorn, Chesire) using a gradient of 60 to 86% ethanol (containing 50mM NaClO₄) against methanol containing 50 mM NaClO₄ over 20 minutes. Quantification was on the basis of the absorption of oxidised coenzyme Q at 275nm with reference to the internal standard; recovery was 63 ± 5 % (mean±SEM).

4.2.5. Citrate synthase Assay

965µl Tris HCL (pH 8.0), 10µl, 5µM acetyl CoA, 10µl 10mM DTNB (Sigma), 10µl Triton-X (Sigma) and 10µl of each mitochondria sample(1:100 diluted in double distilled H₂O) were combined in a cuvette, placed in a spectrophotometer and allowed to run to baseline at 37.5°C, 412nm absorption. Once a stable baseline was obtained, 5µl of 50mM sodium oxaloacetate pH 8.0 (freshly prepared) was added and the sample measured continuously for 5 minutes. Once recording had finished appropriate graphical co-ordinates were set to calculate the rate of 2-nitro-5thio benzoic acid (NTB) formation from DTNB and thus the activity of citrate synthase.

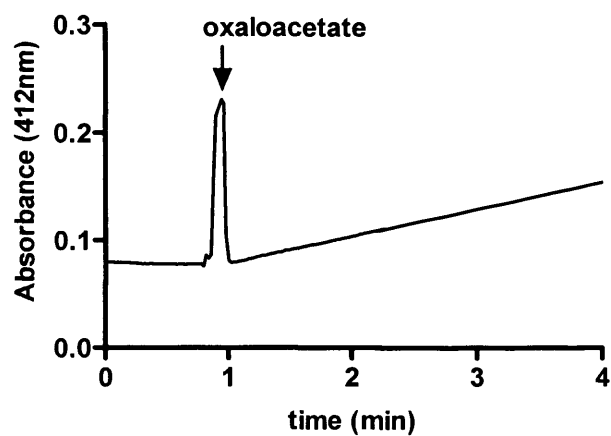


Figure 4.1. Citrate synthase assay trace. Addition of oxaloacetate permits the formation of CoA from Acetyl-CoA. Citrate synthase present in the mitochondrial sample then catalyses formation of the coloured NTB from DTNB and CoA.

4.2.6. Protein Assay

Protein levels were quantified using the Folin-Ciocalteu reagent method as described by Peterson *et al*

Solutions;

- (i) Copper-tartrate-carbonate (CTC). 0.1% copper sulphate (pentahydrate), 0.2% potassium tartrate, 10% sodium carbonate.
- (ii) 10% Sodium dodecyl sulfate (SDS)
- (iii) 0.8 N Sodium hydroxide

Reagent A: Solutions i, ii and iii diluted in distilled water at a 1:1:1:1 ratio.

Reagent B: Folin-Ciocalteu phenol reagent (Fisher Scientific (2N)) diluted at a 1:5 ratio with distilled water.

A ten step dilution series of a 200 μ g/ml stock of bovine serum albumin (BSA) was prepared in distilled water to give a range of 2-20 μ g in 4.5ml cuvettes. Three step dilutions were prepared from each sample using 5, 10 and 20 μ l of a 1:100 dilution of the sample made up to a total volume of 1ml in distilled water in 4.5 ml cuvettes. 1 ml of Reagent A was added to each prepared cuvette. These were then mixed thoroughly and allowed to stand at room temperature. After 10 minutes, 0.5ml of reagent B was added and thoroughly mixed in each cuvette. Samples were left for another 30 minutes at room temperature. Absorbance was read at 720nm. Total protein content was calculated using linear regression of the BSA standard curve (range 0-20 μ g) (see figure 4.2). Unknowns were calculated by interpolation on this standard curve for each sample. Standards were always analysed with each set of samples.

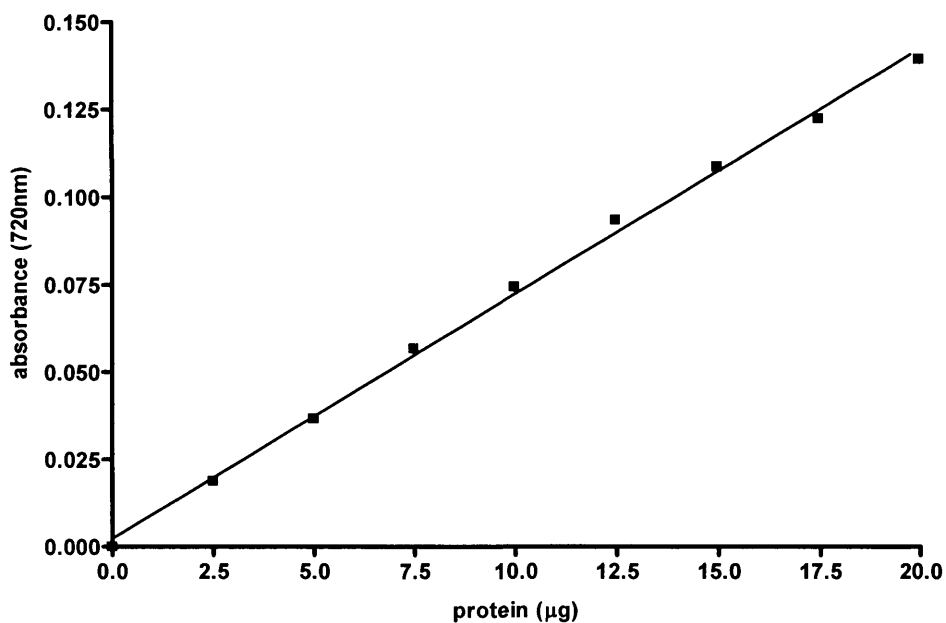


Figure 4.2 Protein assay trace. Chart displays a standard curve for BSA, from which the values for approximate protein content of each sample could be calculated.

4.3 Results

4.3.1 Normalisation of data

SDS PAGE electrophoresis and electroblotting are complicated multi-step procedures. A slight difference at any stage can have an impact on the final result. To minimise gel-to-gel differences, each step was carefully optimised and in each experiment all procedures were carried out to the set standards. To ensure gel to gel differences did not affect results, samples were only compared on the same blot, i.e. date matched control and endotoxic samples were run together and compared against one another.

Using the described protocol, the difference in the level of UCP2 protein between samples could be detected as a difference in band density. It was important that this difference was ~~qualified~~^{quantified} by normalising for total mitochondrial content. Band density was normalised to citrate synthase, a commonly used measure for mitochondrial content. The level of this mitochondrial matrix protein is thought not to be affected by sepsis, to ensure that this was the case we compared the level of citrate synthase, normalised for total protein content, between the control and endotoxic samples for each type of mitochondrial preparation.

There are many factors that can alter the level of citrate synthase and total protein content in an individual mitochondrial preparation. However, it is reasonable to assume that by following the same protocol, the range of values for each type of preparation will be normally distributed within a certain range. There was no significant difference in the value for the level of citrate synthase activity per mg/~~ml~~ of total protein between control and septic samples from each type of mitochondrial preparation (Figure 4.3). This suggests that citrate synthase levels were not affected by endotoxaemia and that it was a suitable control for mitochondrial protein content.

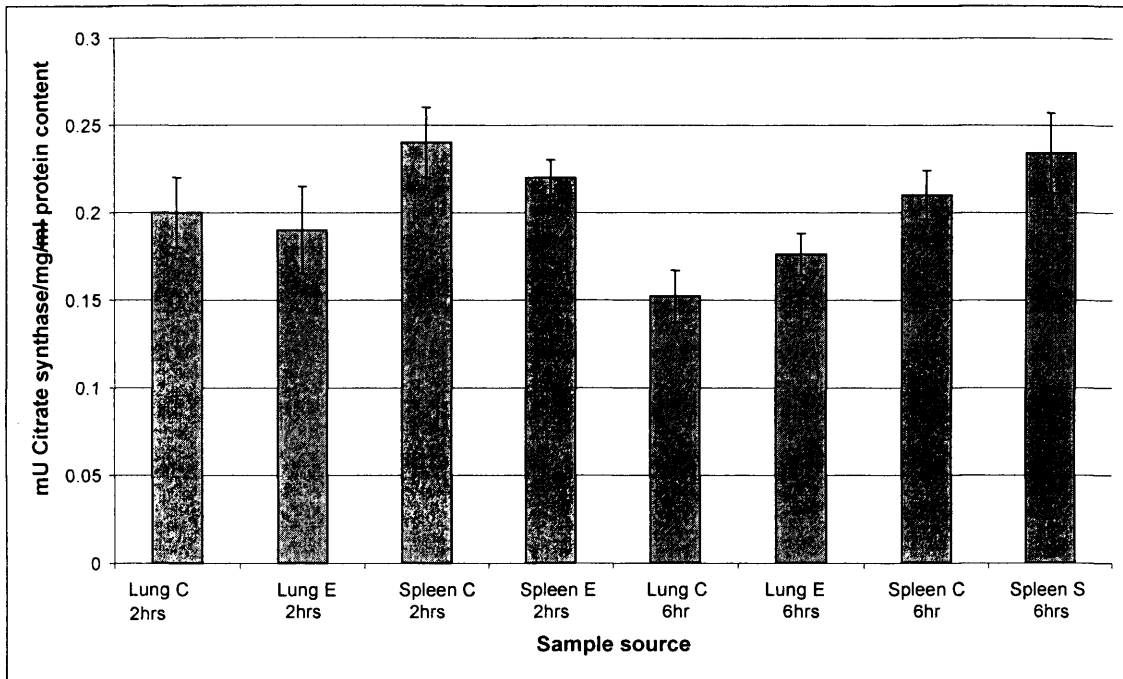


Figure 4.3. Comparing the level of citrate synthase activity per mg of the total protein content between mitochondria isolated from endotoxic and control rat pups. There was no significant difference in this value between control and septic samples from each type of mitochondrial preparation. For samples from rat pups culled 2 hours after LPS or saline injection n=16. For samples from rat pups culled 6 hours after LPS or saline injection n=10. Results expressed as mean \pm SEM

4.3.2. UCP2 Western Blotting

Results are presented as mean \pm SEM for each type of mitochondrial preparation. Although this gives us an idea of the comparative expression of UCP2 between different types of mitochondrial preparations it does not take into account the effect that gel-to-gel differences may have on the results. This is likely to be great as densitometry is very dependent on the film background and precise exposures etc. Control and endotoxic samples from the same litter of rats were run together on the same gel and these results were analysed by paired t-test to identify the significance of any differences between sample types and decrease variation due to gel to gel differences.

When comparing mitochondrial samples from rat pups culled 2 hours after injection (Figure 4.2 A) we found a significant difference in Band density / mU citrate synthase between samples from control and endotoxic rat pups. UCP2 protein expression was increased in mitochondrial preparations from lung tissue during endotoxaemia (p value <0.05). There was no significant difference in UCP2 expression between control and endotoxic spleen samples (p value >0.05)

Similarly, results of mitochondrial preparations from rat pups culled 6 hours after LPS or saline injection (Figure 4.4 B), suggest that UCP2 expression in spleen mitochondria is unaffected by endotoxaemia. Although there had been an increase in UCP2 expression at 2 hours in lung caused by endotoxaemia, this difference was no longer significant at 6 hours (p value >0.05). Unfortunately levels of UCP2 expression cannot be compared between 2 and 6 hours as the samples were run on different gels.

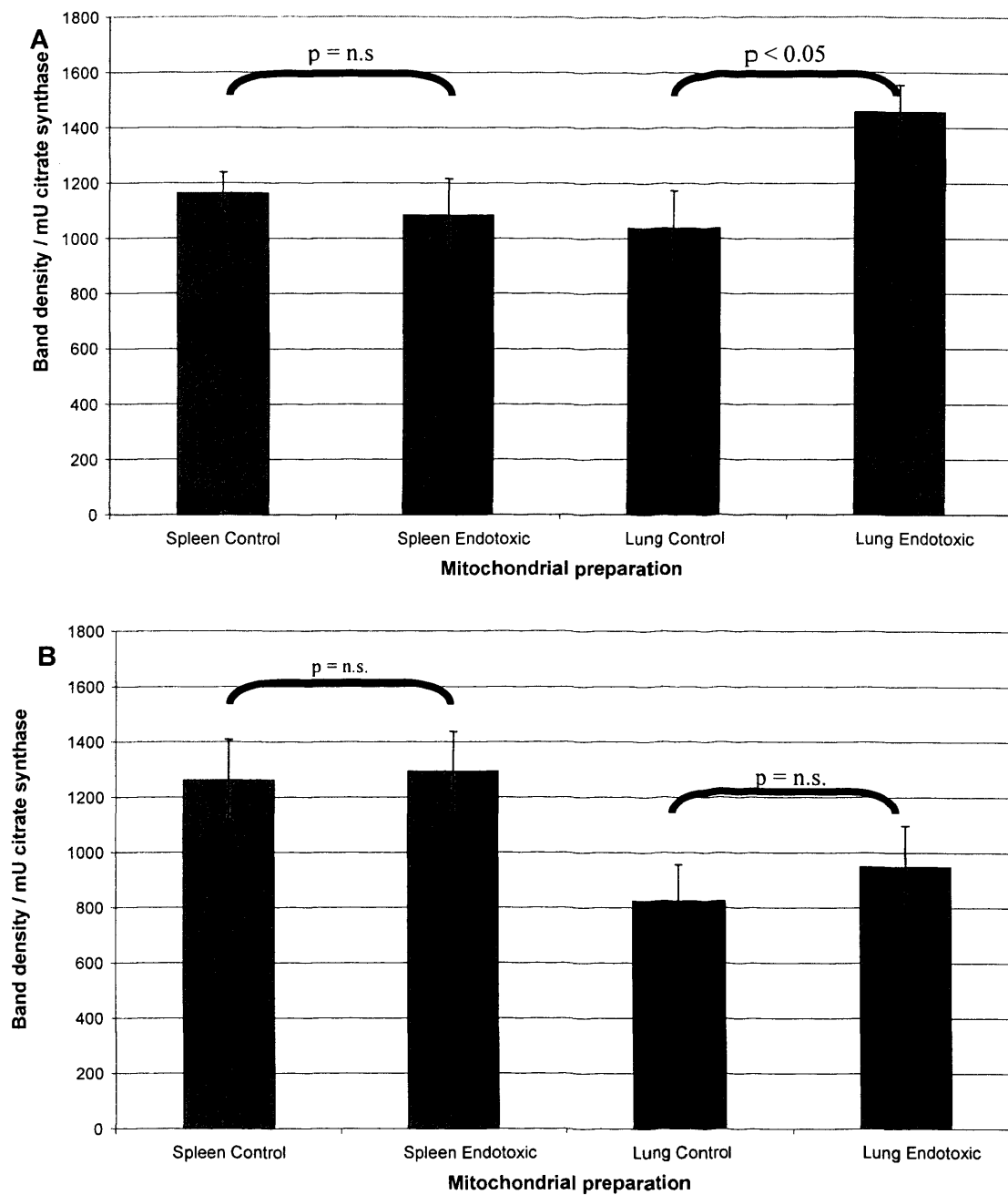


Figure 4.4. UCP2 protein expressed in lung and spleen mitochondria from control and endotoxic rat pups. The level of UCP2 protein was qualified by band density and normalised for total mitochondrial protein content by the activity of citrate synthase. Results are displayed as mean \pm SEM for each type of mitochondrial preparation. (A) displays the results of mitochondrial preparations from rat pups culled 2 hours after LPS and saline injection (n=16). (B) displays results of mitochondrial preparations from rat pups culled 6 hours after LPS and saline injection (n=10). Results are displayed as mean \pm SEM.

4.3.3. Ubiquinone

It has been suggested that ubiquinone is an essential co-factor for the activity of UCP2³⁷. To investigate this relationship further, we studied the amount of ubiquinone that existed within each mitochondrial preparation.

Ubiquinone can exist in a number of forms, each of these are classified based on the number of isoprenoid units in their hydrophobic side chain. The commonest forms of ubiquinone that exist in the mammalian body have 9 or 10 isoprenoid units and are known as Ubiquinone 9 and 10 (UQ₉ and UQ₁₀). Rats have UQ₉ predominantly, whereas in humans UQ₁₀ predominates. We analysed each of mitochondrial samples for these isoforms by HPLC. The results were normalised for total mitochondrial content by citrate synthase activity and are presented as mean ± SEM for each type of mitochondrial preparation. (Figure 4.5 and 4.6)

Comparing the sample means of each type of mitochondrial preparation from rat pups culled 2 hours after LPS and saline injection, suggests that there were no significant differences between control and endotoxic mitochondria for either UQ₉ or UQ₁₀.

The sample means of mitochondrial preparations isolated from rat pups culled 6 hours after LPS and saline injection indicate that sepsis caused a decrease in the level of UQ₁₀ in lung and spleen mitochondria and in UQ₉ in lung mitochondria. There was also a slight increase in the level of UQ₁₀ of spleen mitochondria when compared to control. However, the only significant difference found between paired samples was the level of UQ₉ in mitochondrial preparations isolated from control and endotoxic rat pups

When compared to samples prepared from spleen tissue, those from lung tissues seem to have a higher level of UQ₉. The difference in UQ₉/UQ₁₀ ratio between these samples may reflect the functional differences between lung and spleen tissue.

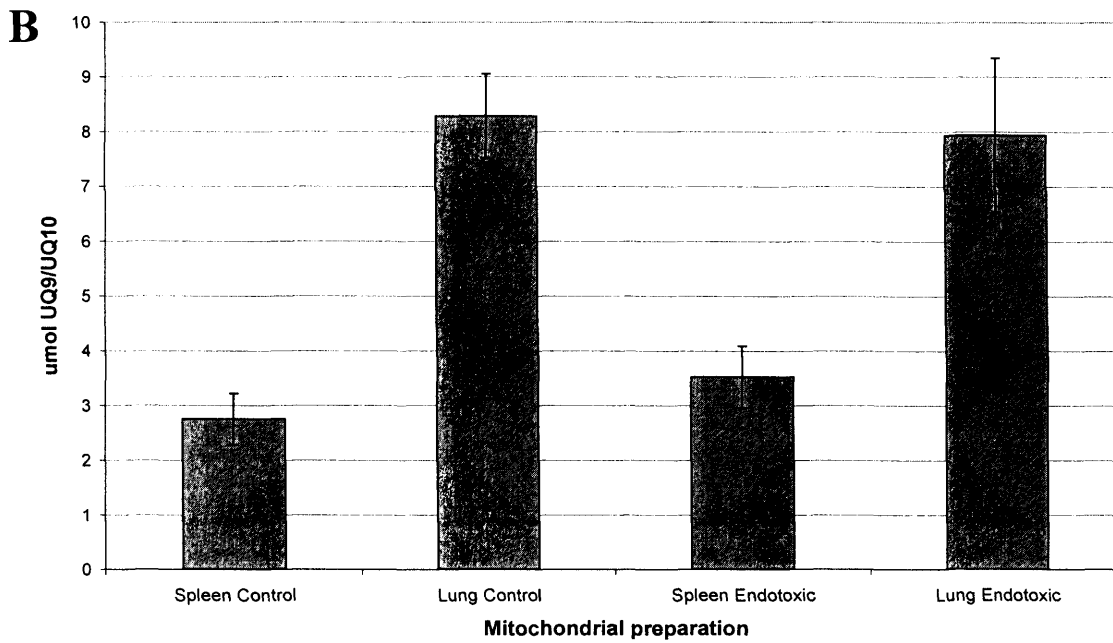
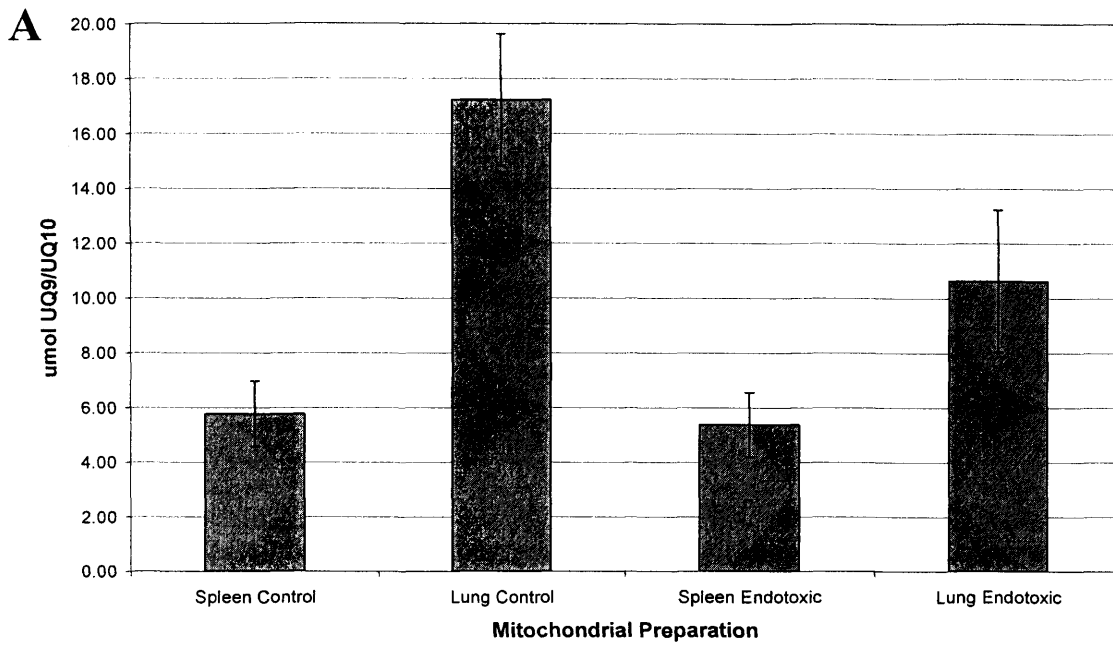


Figure 4.5. Comparing the UQ₉/UQ₁₀ ratio between lung and spleen samples. Values are expressed as mean±SEM. Chart **B** presents the results after a 2hr exposure to LPS and Chart **A** presents that after a 6hr exposure.

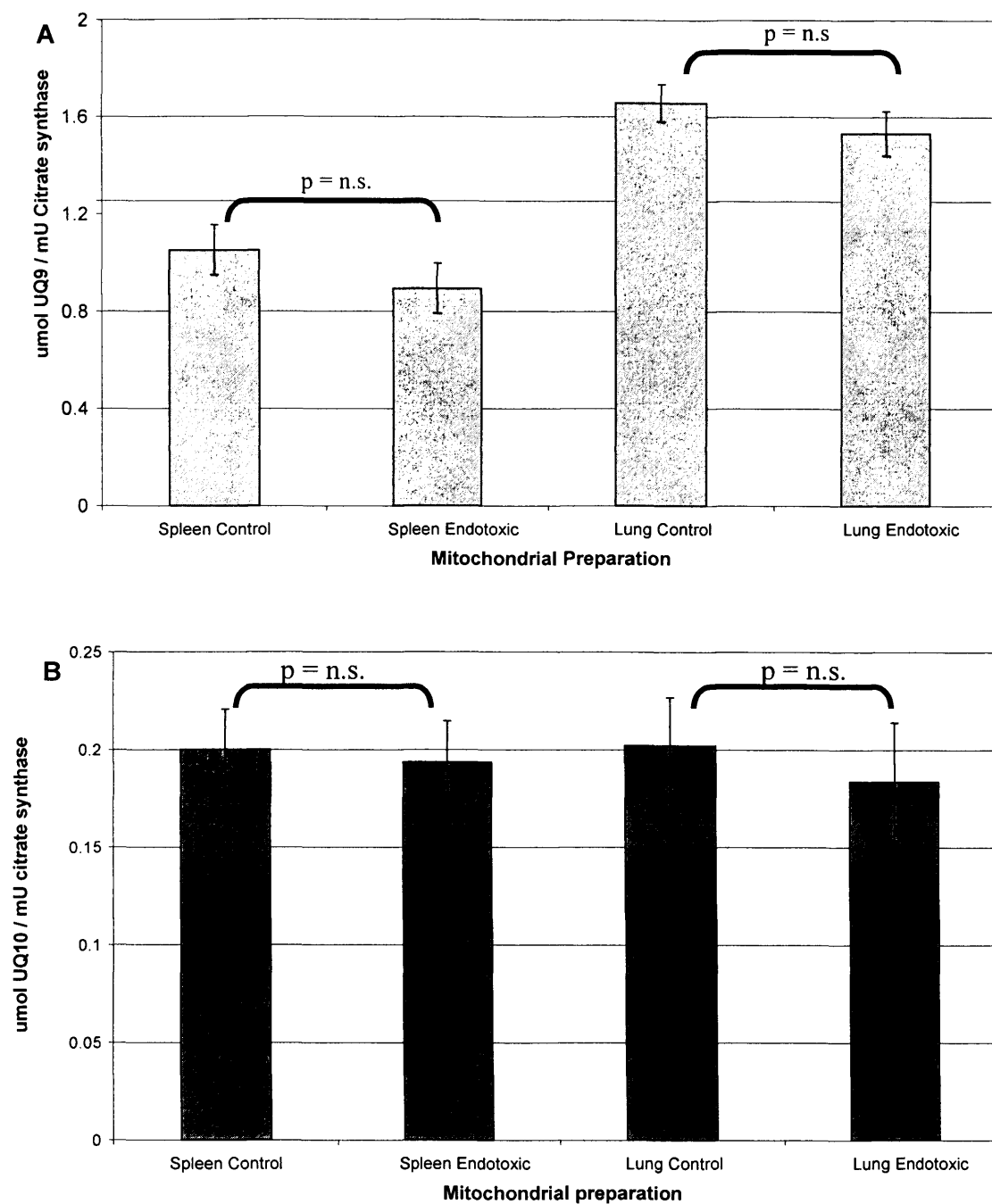


Figure 4.6. Comparing the levels of UQ₉ and UQ₁₀ between control and endotoxic mitochondrial preparations from lung and spleen tissue after a 2hr exposure to LPS. The ubiquinone content of each mitochondrial preparation was assessed by HPLC and then normalised for total mitochondrial content by citrate synthase activity. The relative level of UQ₉ and UQ₁₀ are presented in chart A and B respectively. Results for each type of mitochondrial preparation are displayed as average \pm SEM. (n=16)

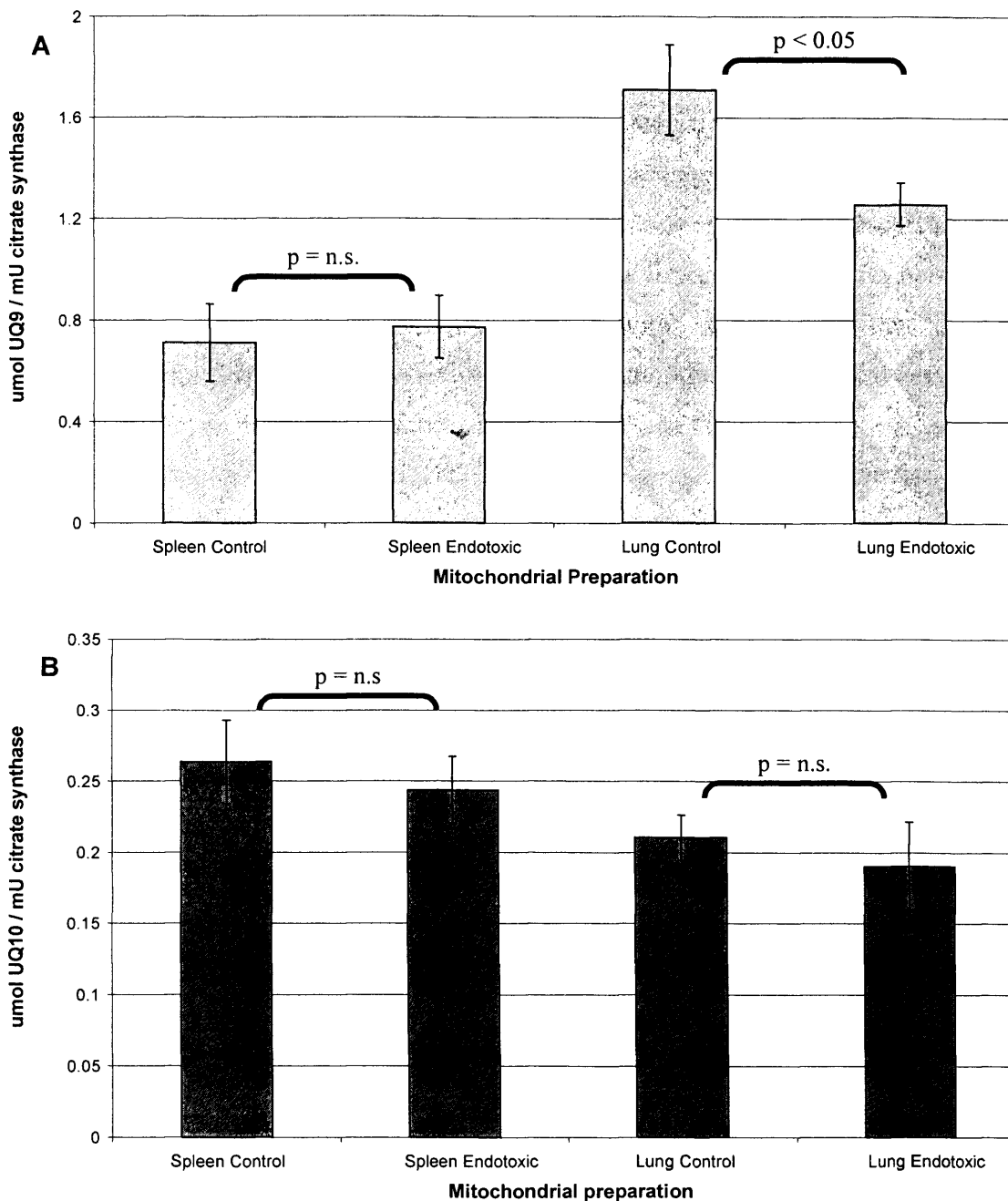


Figure 4.7. Levels of UQ₉ and UQ₁₀ in control and endotoxic mitochondrial preparations from lung and spleen tissue after a 6hr exposure to LPS. The ubiquinone content of each mitochondrial preparation was assessed by HPLC and then normalised for total mitochondrial protein content by citrate synthase activity. The relative level of UQ₉ and UQ₁₀ are presented in (A) and (B) respectively. Results for each type of mitochondrial preparation are displayed as average \pm SEM. (n=10)

4.4 Discussion

LPS-induced expression of UCP2 protein in specific organs has been described previously⁶⁸. UCP2 protein expression was shown to increase 12 fold in lung mitochondria 14 hours after LPS injection when compared to controls. No change in UCP2 expression was reported in stomach, liver, duodenum, kidney, heart, muscle or spleen of the LPS injected adult mice⁶⁸. The results from our study with neonatal rats are similar, although the magnitude of the change is much smaller. The only statistically significant difference between control and endotoxic samples was found in preparations from lung mitochondria. In samples taken from rat pups culled 2 hours after LPS and saline injection UCP2 protein expression was increased in lung mitochondrial preparations from endotoxic rats when compared to control. UCP2 protein expression was unaffected by LPS in mitochondrial preparations from the spleen. It is interesting that this effect of LPS on UCP2 expression in lung mitochondria occurs so early after LPS injection and that it seems to be diminished 6 hours after LPS injection, although it is possible that more samples should have been analysed. It would also have been interesting to observe later time points in the suckling rats, although mortality is significant at 6 hours.

A previous western blotting study found that significant differences in the level of UCP2 protein expression between control and septic samples were not evident until 10 hours after LPS injection⁶⁸. It was suggested that the kinetics of the induction of UCP2 protein after LPS injection were consistent with a primary immune response leading to oxidative burst in lung. LPS has been reported to activate macrophage receptors that stimulate the production of proinflammatory cytokines, eventually leading to an increase in intracellular ROS⁷⁰. It has been proposed that increased intracellular ROS causes an upregulation of the translation of the large pool of UCP2 mRNA already present in lung mitochondria. The lung is constantly exposed to toxic compounds and pathogens. An induction of UCP2 protein expression by LPS exposure in the lung fits well with the hypothesis that UCP2 might function to protect an organism from oxidative stress. However, there are considerable difficulties in comparing studies made using different models of endotoxaemia.

It is unlikely that our results reflect an LPS stimulated *de novo* synthesis of UCP2 protein, 2 hours after LPS exposure; it is more probable that they reflect early macrophage infiltration into the lung. UCP2 protein expression has been shown in macrophages and several studies suggest that UCP2 function may be more limited to specific cells types such as thymocytes⁴⁷ and macrophages⁶⁸. In the early stage of sepsis, macrophages are recruited to lung to help fight infection in this sensitive tissue. It is possible that a proportion of mitochondria isolated from septic lung tissue originated from these infiltrating macrophages and it is their UCP2 expression that is reflected in our results for this tissue. The results from samples isolated from rat pups culled 6 hours after LPS and saline injection suggest that this effect is diminished at later stages of sepsis. Further studies could be made to examine macrophage and neutrophil infiltration histologically or by marker enzyme measurement and to compare this with UCP2 expression.

The amount of UQ₉ was diminished in mitochondrial preparations from endotoxic lung tissue when compared to control from rat pups culled 6 hours after LPS and saline injection. The lack of impact of sepsis on UQ₁₀ expression and the temporal separation of the effect of sepsis on UQ₉ and UCP2 protein expression questions the reported functional relationship between UCP2 and ubiquinone. It could be argued that if such a relationship existed then an increase in UCP2 protein expression should be met by a concurrent increase in ubiquinone. Studies examining the relationship between UCP2 and ubiquinone in *E.coli* inclusion bodies have suggested that 1-2 nmols of UQ₁₀ (or a UQ₁₀ molar ratio of 80:1 UCP2 dimer) were sufficient to activate UCP2³⁷. Given the reported low level of UCP2 native protein expression³³, the levels of UQ₁₀ reported in our study should be more than enough to support UCP2 activity. Any change in the amount of UQ₁₀ needed to support UCP2 function during sepsis would be masked by pool of UQ₁₀ already present in the mitochondria.

The length of the hydrophobic isoprenoid side chain in ubiquinone has been shown to be important for the activation of UCP2. A minimum chain length of 10-13 C atoms has been described for UCP2 activation in UCP2 expressing inclusion bodies from *E.coli*³⁷. This and the suggested low level of Ubiquinone required for UCP2 activation indicate that the decrease in UQ₉ from septic samples compared to controls from rat pups culled 6 hours after LPS and saline injection found in our experiments

were not a result of its relationship with UCP2. Other studies have suggested that antioxidant damage increases the catabolism of UQ₉ in a range of tissues^{71,72,73,74}. It is possible that the oxidative stress of endotoxaemia causes an increased consumption of UQ₉ and that this accounts for the decrease in lung mitochondria from rats culled 6 hours after LPS injection.

Little is known about the subtle differences in the function of UQ₉ and UQ₁₀ in different tissues. It is interesting to note that the UQ₉/UQ₁₀ ratio is markedly different between spleen and lung. This would suggest that there are some differences in function.

5. Reactive Oxygen Species Production in Macrophages

5. Reactive Oxygen Species Production in Macrophages

5.1 Background

Phagocytes play an important role in the host defence against microorganisms. In response to stimuli they assert microbicidal effects, producing proteolytic enzymes and reactive oxygen metabolites. This occurs via a co-ordinated sequence of biochemical events, known as the oxidative burst. The sequence is marked by a rapid uptake of oxygen molecules that are then reduced to superoxide anion. The reaction is catalyzed by NAD(P)H oxidase, using NADPH or NADH as the electron donor⁷⁵. The oxygen free radical is subsequently converted to hydrogen peroxide by spontaneous or enzyme mediated dismutation (catalysed by superoxide dismutase).

The UCP2 knockout mouse has implicated UCP2 in the regulation of reactive oxygen species (ROS) in macrophages during the oxidative burst⁶⁸. Mice lacking UCP2 were resistant to *Toxoplasma gondi* infection and their macrophages were found to contain higher levels of ROS than wild type mice. Earlier studies have suggested that the activity of UCP2 is functionally dependant on ubiquinone³⁷ and may be stimulated by the by retinoids^{30;47}. We have attempted to study the level of ROS production in human macrophages in order to determine whether ubiquinone or retinoids affect ROS production.

Many methods exist for monitoring oxidative burst in macrophages. Some groups have measured the level of oxygen consumption utilising hexose monophosphate shunt activity or chemiluminescence⁷⁶, whereas others looked at the formation of redox products and protein iodination using tetrazolium dye reduction⁷⁷. Reactive oxygen species can be measured directly.

A simple rapid assay for measuring ROS generation from macrophage populations using membrane permeate 2',7'-dichlorofluorescein diacetate (DCFH-DA) has been described⁷⁸. The non-fluorescent substrate, DCFH-DA, diffuses easily through the plasma membranes of macrophages and is trapped within the cells upon hydrolysis to non fluorescent 2',7' dichlorofluorescein (DCFH). Intracellular oxidation by ROS converts this compound into the green fluorochrome, 2',7' dichlorofluorescein

(DCF) (Figure 5.1). Measuring the fluorescence from macrophage populations incubated with DCFH-DA can give an accurate indication of the level of ROS evolution. Unlike many other studies on oxidative burst in phagocytes⁷⁹, this method does not rely on flow cytometry, but measures the fluorescence from cells incubated with DCFH-DA directly.

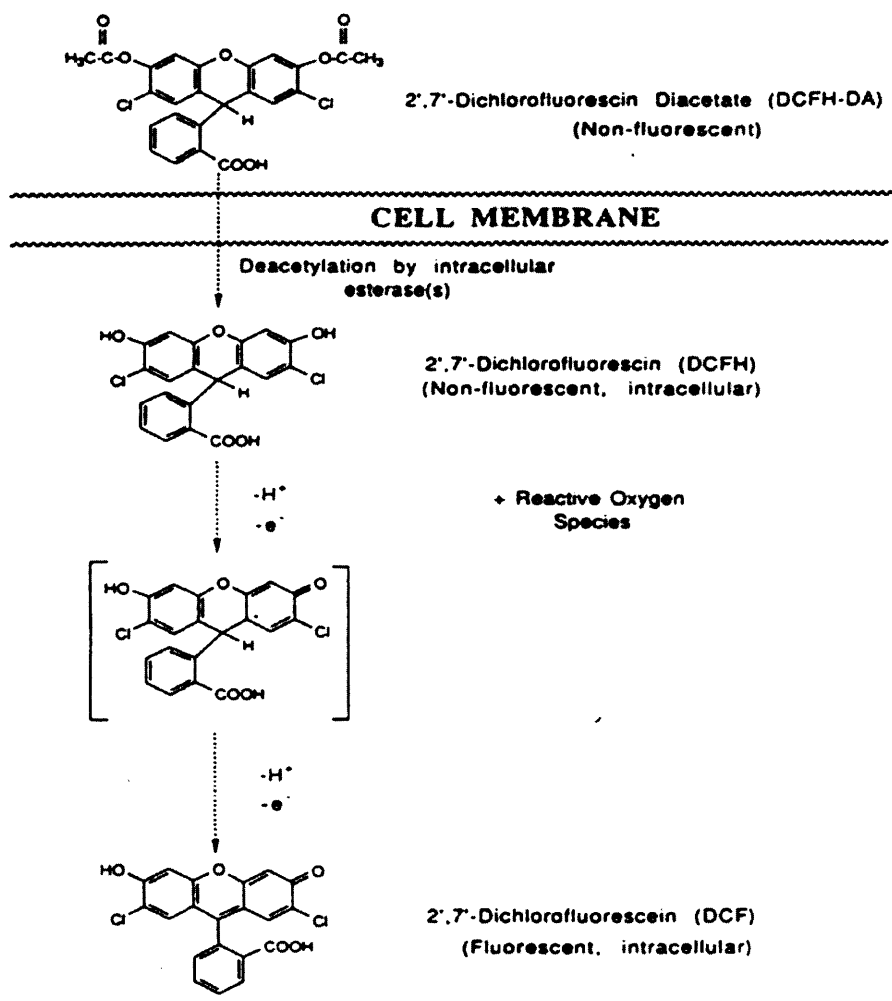


Figure 5.1 Diagram showing the conversion of 2',7'-dichlorofluorescein diacetate to fluorescent 2',7'-Dichlorofluorescein by intracellular ROS.

The results from this study were also compared to a microplate assay of macrophage ROS production based on tetrazolium dye reduction.

5.2. Methods

5.2.1. Isolation of monocytes/macrophages from peripheral whole blood.

20ml of blood from healthy adult volunteers was collected in heparinized tubes and mixed 1:1 with phosphate buffered saline (PBS). 20 ml of this mixture was then carefully layered onto 10 ml of Lymphoprep in 50 ml falcon tubes. The tubes were then placed a centrifuge set at 15°C, and was centrifuged for 30 mins, at 2000rpm, in a swing out rotor with the brake off. This process allowed the white mononuclear cell layer to be isolated in a distinct band at the sample/medium interface. The mononuclear cells from each of the tubes were removed using 2ml plastic pipettes and pooled into a single tube. These cells were then washed twice with 20ml of PBS by spinning at 1200rpm for 10 minutes. After this stage the cells were re-suspended in 10ml Hanks Balanced Salt Solution (HBSS) and counted using a haemocytometer (see section 5.2 below). The cell count was then used to determine an appropriate level of dilution that would result in an approximate cell density of 2.5×10^5 /ml. Control aliquots were diluted in HBSS. Aliquots used to assess the effects of particular compounds on reactive oxygen species production were diluted in HBSS with the appropriate concentration of the compound.

5.2.2. Monocyte viability count

After each incubation period the viability of the macrophages was assessed. 50µl of each sample was removed and placed into a 1ml eppendorf tube to which was added 50 µl of 1% typhan blue solution and 100µl of HBSS. This mixture was vortexed briefly before being transferred to a haemocytometer and covered carefully with a glass cover slip. The samples were analysed under light microscopy and live cell count and percentage viability were recorded. Viable macrophages were identified by morphology as shiny, bright white cells. Dead cells appeared blue due to the uptake of trypan blue.

5.2.3. Standard curve for 2,7-dichlorofluorescein.

Appropriate amounts of DCF were diluted in methanol to give a range of solutions from 0.1-1.0nM DCF. The solutions were placed in fluorescence cuvettes and triplicate measures of the fluorescence from each were taken at 504nm emission, 523 excitation spectra⁸⁰, using a Perkin Elmer LS-3 fluorimeter. These results were then used to describe the standard curve for DCF. A standard curve is shown in figure 5.2.

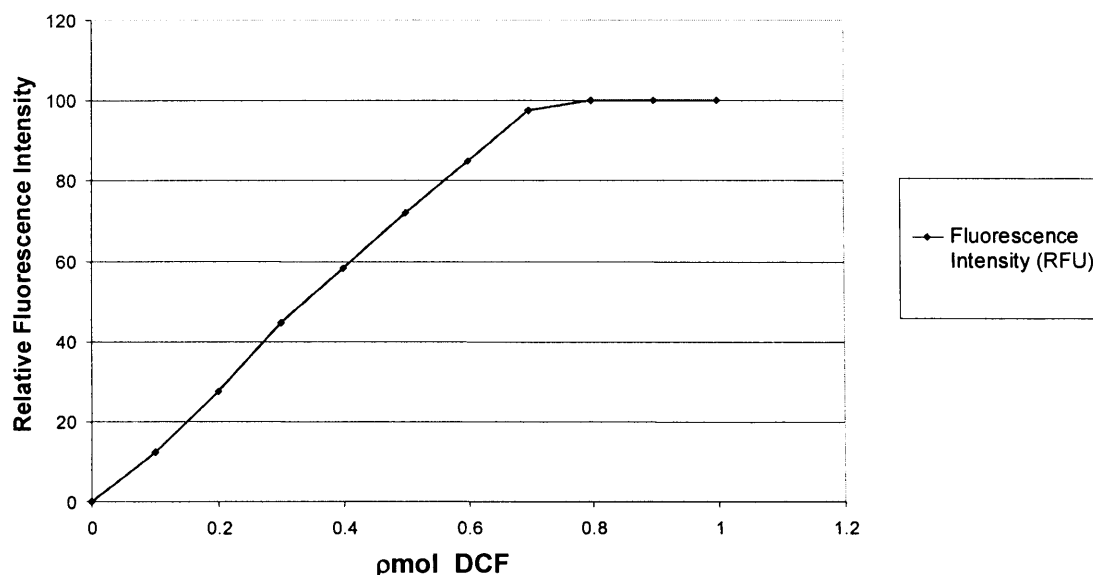


Figure 5.2. Standard Curve DCF. Pmol DCF(Sigma), dissolved methanol. Fluorescence measured at 504nm excitation and 523 emission spectra in Perkin-Elmer LS-3 fluorescence spectrometer at 37 °C. DCF concentration is proportional to absorbance at 504nm emission, 523nm excitation, between the limits of 0.1 and 0.7 pmol DCF.

5.2.4 Cuvette assay for reactive oxygen species production.

450µl aliquots of the macrophage preparation (approximate cell density, 2.5×10^5 /ml) were placed in 20 ml glass scintillation tubes to which was added 50µl of 100µM DCFH-DA. These aliquots were then gassed with 95% O₂, 5% CO₂, fitted with

rubber seals and incubated in the dark at 37°C in a shaking water bath for prescribed incubation periods.

The cuvette assay was used to assess reactive oxygen species production in control populations of macrophages and in those to which various compounds had been added. These compounds were introduced to the macrophages at the primary dilution stage to give final listed concentrations of; Zymosan (125µg/ml), Lipopolysaccharide (LPS; 90µg/ml), (4-[(E)-2-(5,6,7,8-tetrahydro-5,5,8,8-tetramethyl-2-naphthalenyl)-1-propenyl] benzoic acid) (TTNPB, a retinoid analogue. 4µM) Phorbol myristate acetate (PMA; 250 ng/ml), Ubiquinone₁₀ (UQ₁₀; 11.5uM solution).

5.2.5 Non continuous measurement (methanol added).

After the defined incubation period, 2.5ml of ice cold methanol was added to both control and test aliquots and they were vortexed for 2 minutes. The resulting solution from each tube were transferred to fluorescence cuvettes and kept on ice until their fluorescence could be determined as above.

5.2.6. Preparation of ubiquinone multi-lamellar liposomes⁸¹

16 mg of di-myristylphosphatidylcholine (DMPC, Sigma) was dissolved in 1ml of ethanol containing 1mg of ubiquinone₁₀ at a Q₁₀/DMPC ratio of 1:16. This solution was then evaporated under nitrogen, dispersed in degassed PBS buffer pH 7.4, and vortexed and sonicated at 40 °C for 20 minutes. The emulsion was then centrifuged at 100xg for an hour. The resulting supernatant contained the multilamellar liposomes. The concentration of ubiquinone present in the supernatant was examined by HPLC (for methods, see section 4.2.4.)

5.2.7. Microplate Assay.

Isolated macrophages were suspended in PBS (pH7.4) at a concentration of 10^5 cells/ml. 100 μ l of this suspension was added to each well of a microplate and the microplate was incubated for 2 hours at 37°C in a 5% O₂, 95% CO₂ atmosphere. After the initial incubation period 100 μ l of the effector reagent, diluted in PBS to give the final listed amounts of each reagent, were added to each well.

LPS 90 μ g/ml

TTNPB 4 μ M

PMA 250ng/ml

UQ₁₀ 11.5 μ M

Immediately after the addition of the effector reagents, 100 μ l of PBS containing 20mg/ml Nitro-blue-tetrazolium NBT and 5% glucose was added to each microplate well. The Microplate was then incubated for a further 3 hours, in a 5%CO₂, 95% air Atmosphere, at 37°C.

At the end of this incubation period, the supernatants from each well were discarded and the wells were washed 4 times with 70% methanol. Once the wells had dried 100 μ l of 2M potassium hydroxide was added to each, followed by 100 μ l of dimethylsulphoxide. This produces the yellowed colour product. The absorbance of this product was measured at 630nm using an automated plate reader.

To establish whether there were any intrinsic effects of each of the medium additives on formazan levels microplate wells prepared with appropriate concentration of each medium and NBT were incubated without macrophages. The wells were incubated and washed with methanol under the same conditions as the with macrophage assay. Once the potassium hydroxide and dimethylsulphoxide were added absorbance measurements were taken at 630nm and the level of formazan assessed.

5.3. Results.

5.3.1. Macrophage ROS stimulation

Incubation of monocyte preparations with known macrophage stimulators of the oxidative burst, Zymosan and PMA at concentrations greater than 500ng/ml and 250ng/ml respectively, caused a significant increase in fluorescence. This demonstrated it was possible use cuvettes to study the level of ROS production from short term cultures of human macrophages, treated with DCFH-DA. Using cuvettes meant that only one sample could be measured at one time point. To adjust for this in initial experiments, reactions in each incubation media were stopped at specific time intervals with methanol (100%), before fluorescence readings were taken (section 5.2.5)

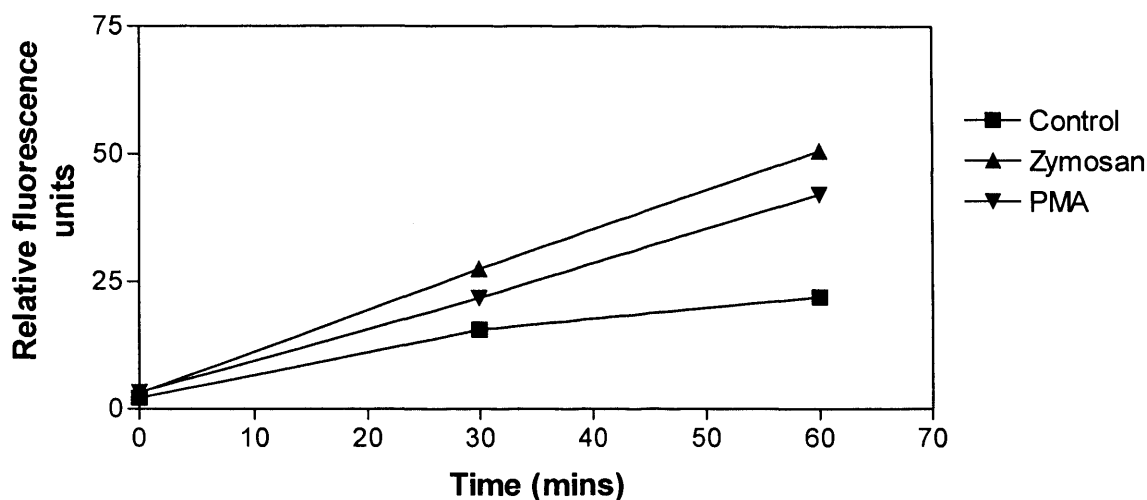


Figure 5.3. ROS production from stimulated and control macrophage suspensions: Macrophage preparations were incubated at 37°C in the dark. The Reaction was stopped at each time point by the addition of 2.5ml methanol (100%). Cell viability 95%, n=3. Values are given as Mean \pm SEM (error bars to small to be visible)

5.3.2. Increasing sample size.

The non-continuous method limited the sample size as stopping the reaction with methanol meant that a new sample was required with each time point. We studied the possibility of implementing a continuous measuring procedure. Samples were measured directly in the fluorimeter without the addition of methanol to the macrophage cultures. An initial experiment demonstrated that it was possible to measure fluorescence directly from the samples. However, the study showed exposure to light from the fluorimeter caused increased levels of fluorescence from the cultures (Figure 5.4.). It was not clear whether this was caused by degradation of DCFH-DA to DCF by exposure to light alone, or whether macrophage ROS production was stimulated.

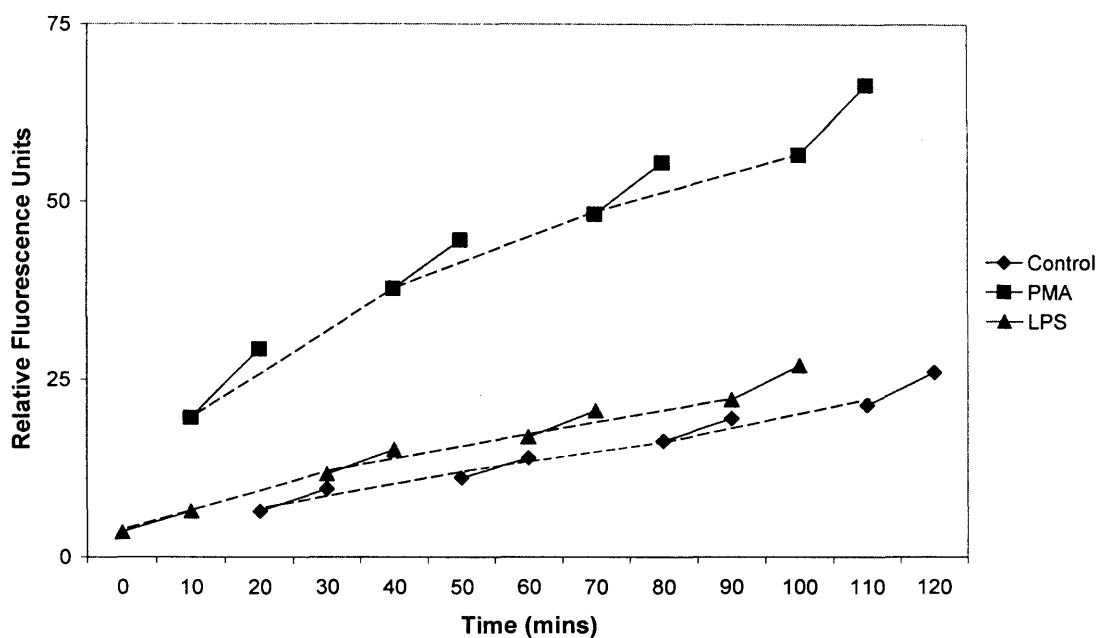


Figure 5.4. ROS production from control and stimulated macrophages, prolonged incubation. Methanol was not added to the culture media. A solid joined line indicates a 10-minute period of continuous measurement that for each sample was restored after 20 minutes. A dotted line indicates the time period in which the sample was not exposed to light from the fluorimeter.

Despite the intrinsic fluorescence caused by the measuring procedure, it is likely that the additional increase from control values in PMA and LPS are due to their effects on macrophage ROS production. To remove the confounding factor presented by prolonged exposure to the fluorimeter, subsequent experiments kept light exposure to a minimum, measuring only at specific time points.

5.3.3 Continuous Measurement

In order to know whether any of the compounds directly caused fluorescence of DCFH-DA, they were incubated with media in the absence of cells and the fluorescence was recorded.

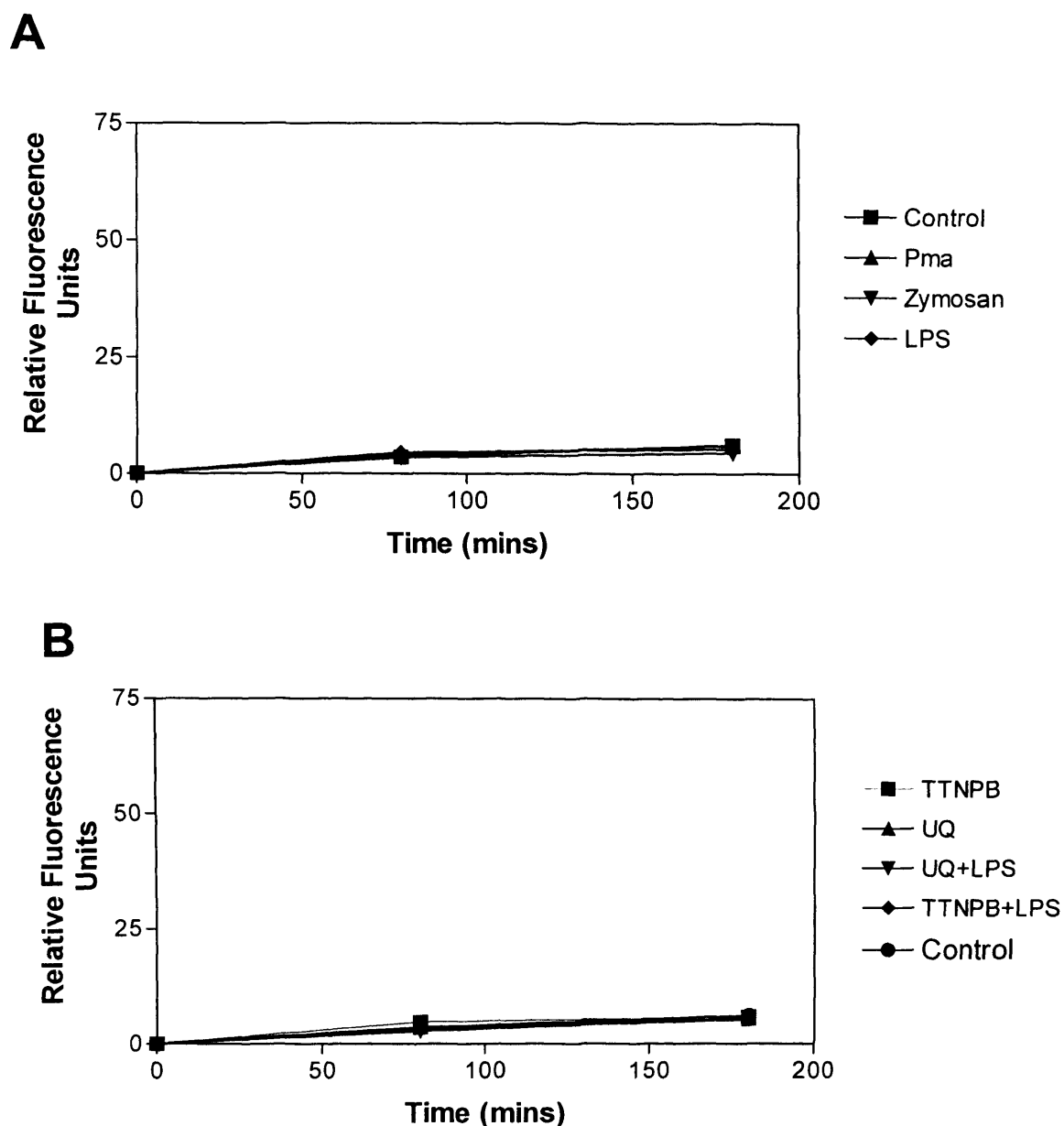


Figure 5.5. Control Assay. Incubation of DCFH-DA with various compounds. Values shown as Mean \pm SEM, n=3.

None of the compounds seemed to have a dramatic effect on DCFH-DA fluorescence that was different from control. However, there was a slow hydrolysis of DCFH-DA solution over time, resulting in a slow increase in fluorescence. Despite this, it was still possible to conclude that changes reported with different DCFH-DA macrophage cultures are based on the compounds different effects on macrophage ROS production.

5.3.4. Exposure to LPS

By keeping the period of light exposure to a minimum, a clearer picture of the effect of LPS on macrophage culture was established

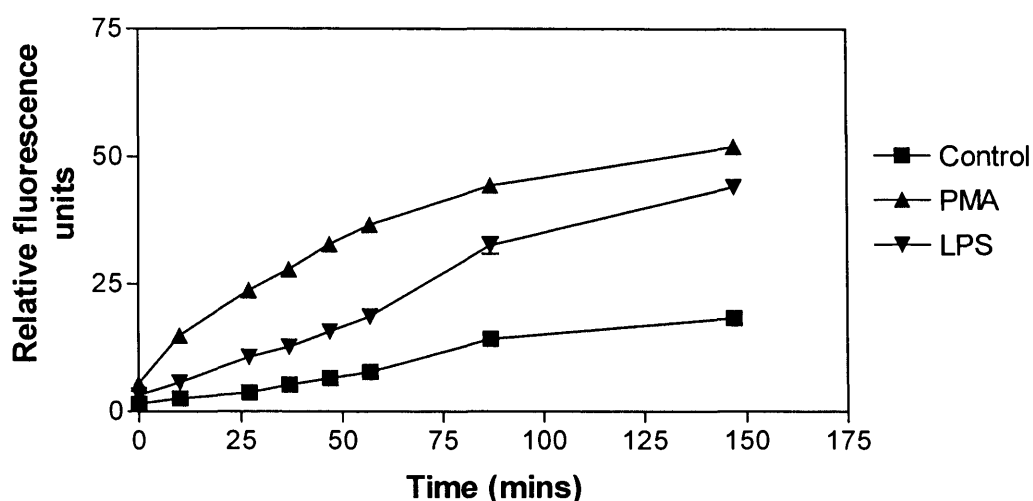


Figure 5.6. ROS production from stimulated and control macrophages, LPS exposure. Samples were incubated in the dark at 37°C and the periods of exposure to light in the fluorimeter were kept to a minimum. Values shown as Mean \pm SEM n=3, Cell Viability 95%

Incubation with LPS caused a smaller increase in ROS than PMA. However, both compounds increased ROS above the control level. The increase in ROS induced by LPS was important as it demonstrates that the oxidative burst response to this initiator of sepsis *in vivo* could be reproduced *in vitro* with macrophages.

5.3.5 TTNPB

UCP2 has a proposed role in regulating ROS production in macrophages by modulating proton leakage and superoxide production at the inner mitochondrial membrane⁴⁴. Studies have demonstrated that retinoid derivatives can enhance uncoupling by UCP1 and 2 in recombinant yeast models³⁰ and stimulate ROS production in thymocytes through UCP2 activation⁴⁷. Both studies cite TTNPB as a strong and specific enhancer of UCP2 activity.

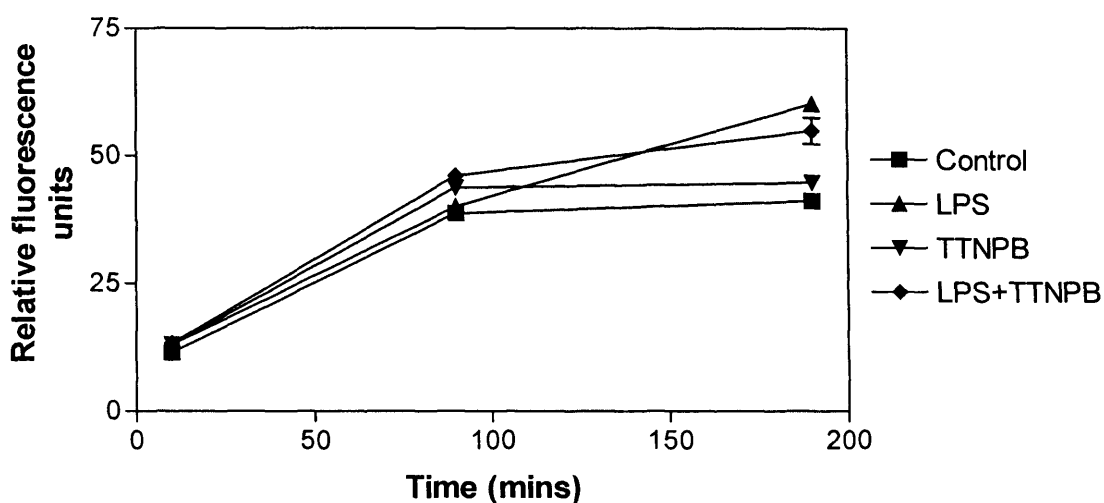


Figure 5.7. Effect of TTNPB on LPS induced ROS production. Values represented as Mean \pm SEM, n=3, Cell viability 95%.

An investigation into the effect of TTNPB incubation with both LPS stimulated and control macrophages showed TTNPB had little effect on ROS production.

5.3.6 Ubiquinone

Ubiquinone is another compound reported to have an effect on UCP2¹⁸ Echta *et al* present ubiquinone as an obligatory co-factor for UCP2's uncoupling function. In a reduced form ubiquinone is a natural quencher of ROS. Ubiquinone's effect on ROS production from macrophages may therefore be two fold. Firstly it may affect UCP2 function and secondly it may directly influence ROS scavenging. However, UQ was added in the oxidised form rather than the reduced form which is directly antioxidant. Ubiquinone is highly hydrophobic and insoluble in aqueous solutions. To ensure macrophages could take up UQ they were incubated with multi-lamellar liposomes of UQ10 prepared in PBS (methods section, 5.2.6.).

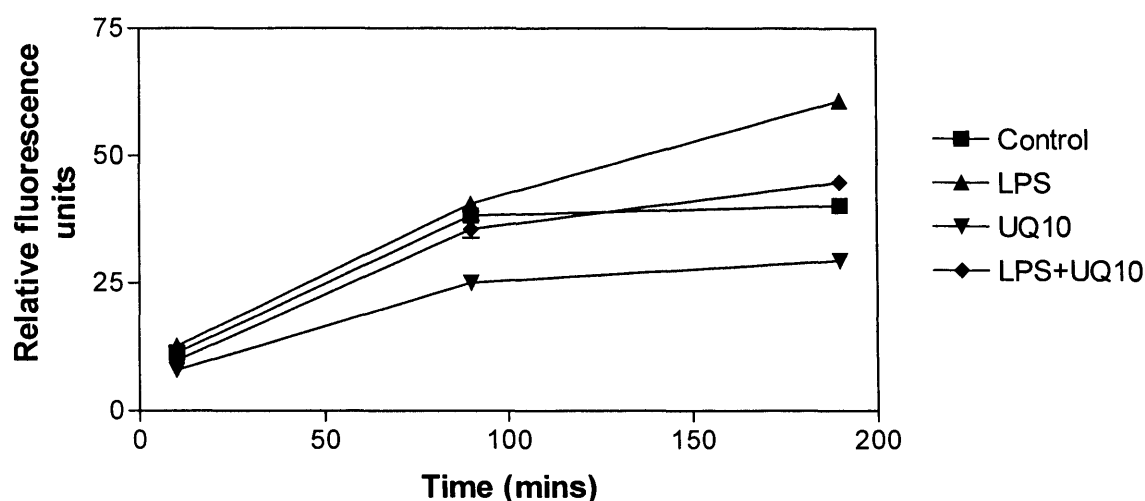


Figure 5.8. Attenuation of ROS macrophage ROS production with UQ₁₀ Values represented as Mean \pm SEM, n=3, Cell Viability 95%.

When incubated with UQ the level of ROS production appeared to be reduced in both control and LPS stimulated macrophages. It is difficult to determine whether this effect is the result of UQ stimulating UCP2 activity or of intrinsic ROS quenching.

5.3.7. Microplate Assay

The results from the DCFH-DA investigation into ROS production were interesting. However, this method was not the most efficient way of accumulating significant data. A micro-plate assay would offer a simple yet effective solution. In the absence of a fluorometric micro-plate reader, a ROS assay using nitro-blue-tetrazolium (NBT) was formulated.

In the presence of redox products, NBT is reduced, precipitating formazan that reacts with KOH and DMSO to form a soluble blue compound that absorbs at 630nm. A high turn over of ROS leads to accumulation of a high concentration of redox products giving a stronger reaction to NBT.

The data obtained from these experiments were subject to statistical analysis by one way ANOVA parametric analysis, using Tukey's multiple comparison test.

5.3.8. Control Assay

To account for any intrinsic effect that any studied compound might have on tetrazolium dye reduction, the microplate assay was set up with the appropriate concentration of each compound and tested in the absence of macrophages.

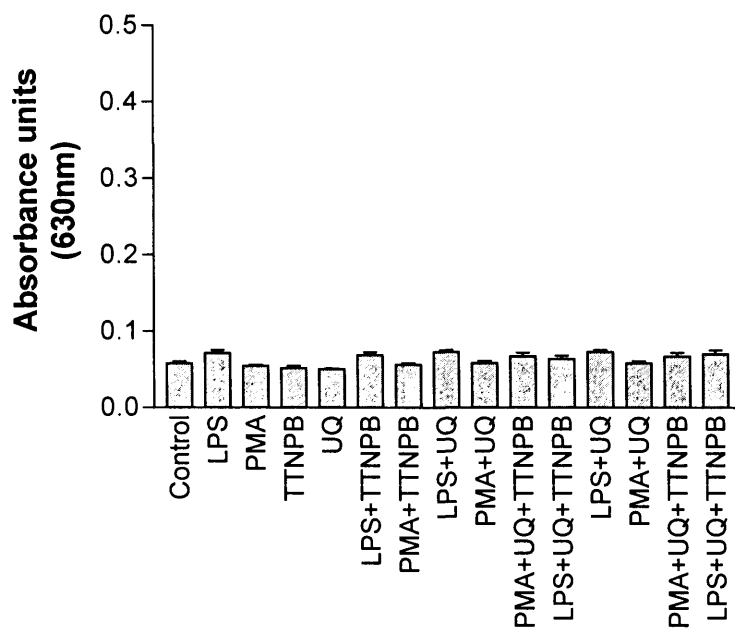


Figure 5.9. Absorbance from media in the absence of cells. Appropriate concentrations of each compound were added to microplate wells and their absorbance was measured in the absence of macrophages. Values represented as mean \pm SEM, n=12.

The level of formazan was about a sixth of that found in the presence of macrophages and there were no significant differences between compounds. Changes in absorbance when compounds were incubated with macrophages are likely to be related to their interaction and their effect on the oxidative burst

5.3.9. Measuring ROS production

Macrophages were incubated in micro wells containing different combinations of LPS, PMA, TTNPB and UQ. After three hours formazan was solubilised using DMSO and KOH and read on a Dynex microplate reader at 630nm. (*Methods Section 8: Microplate assay*)

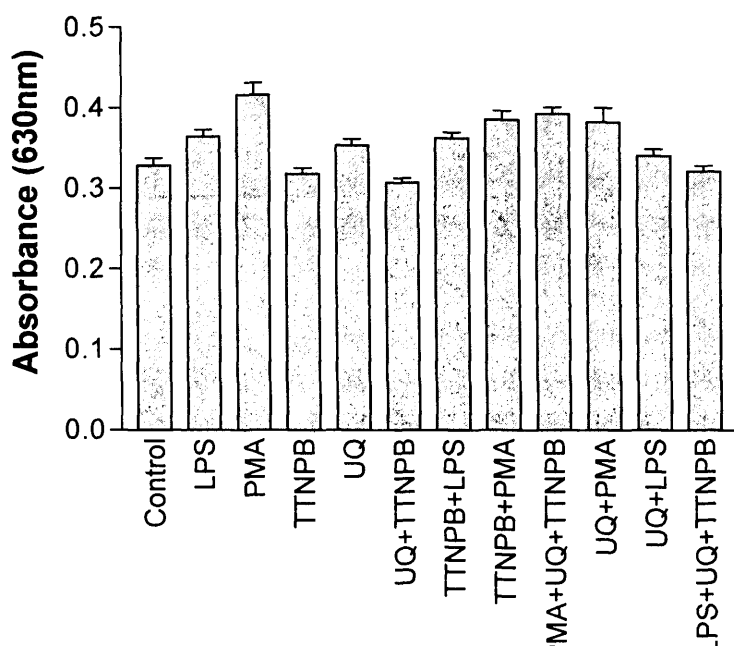


Figure 5.10. ROS production in microplate culture. Macrophages incubated at 37°C for 3 hours with described media. Absorbance read against reagent blank, at 630nm in Dynex plate reader. Values represented as Mean \pm SEM, n=18.

As much data was accumulated from each micro-plate experiment the data was separated into groups and values were presented as the difference from control value.

5.3.10. Incubation with active compounds.

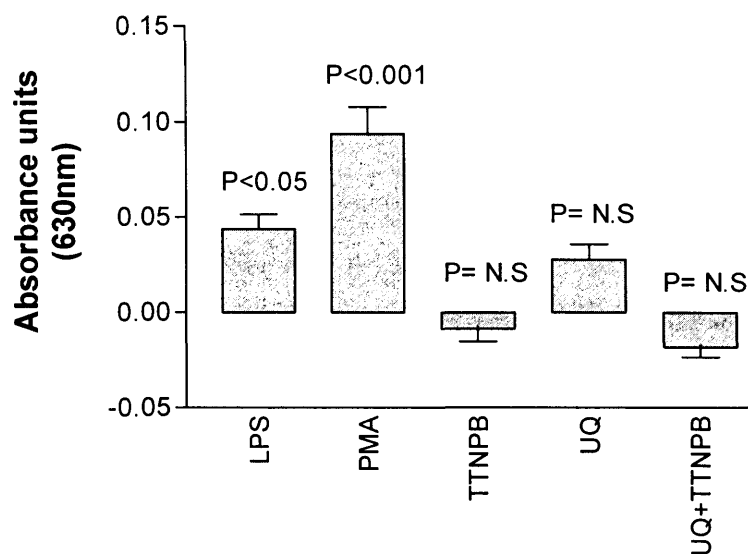


Figure.5.11. Incubation with enhanced media, difference from control. Values represented as absorbance units against control value, Mean \pm SEM, n=18. p values shown are calculated Vs control.

Both LPS and PMA incubation caused a significant increase in absorbance at 630nm as compared to control. This indicates that a higher concentration of formazan was present in these wells. It is likely that this was produced as a direct result of an increase in the level of ROS produced by the PMA and LPS stimulated macrophages. These results compared favourably with that from the DCFH-DA studies suggesting both are viable measures of the oxidative burst response *in vitro*.

The detected decrease in absorbance readings from cultures incubated with TTNPB, as compared to control were not significant in this study.

Incubation with UQ seemed to increase absorbance readings although this was not significant. There is evidence that suggests UQ in mitochondria may be involved in ROS generation and this might explain the slight increase in absorbance readings. Conversely, in its reduced form, UQ acts as an antioxidant both *in vitro* and *in vivo* and

as a reported quencher of ROS and could be expected to reduce formazan levels in this experiment. The increase in absorbance reading was not significant. When UQ was incubated with macrophage free NBT solution it had no significant effect on absorbance levels. This suggests that UQ alone does not potentiate the level of formazan.

Incubating macrophages with a combination of UQ and TTNPB seemingly caused the greatest reduction in absorbance but this was not significant. Incubation with TTNPB alone had indicated that it was acting to stimulate UCP2 uncoupling activity in macrophages. UQ has a reported role as a co-factor for UCP2s' uncoupling function. Although not statistically significant, these results could provide cursory evidence to support the hypothesis that UCP2 has an uncoupling function in macrophages and that it is supported by UQ.

5.3.11. Attenuating ROS production under stimulated conditions.

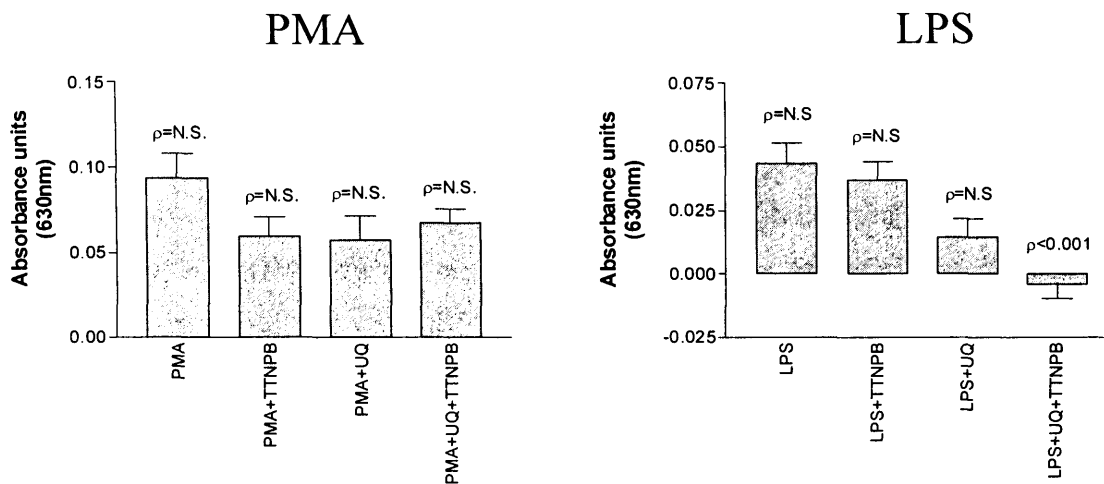


Figure 5.12. Attenuating LPS and PMA induced ROS production. Values represented as absorbance units against control value, Mean \pm SEM, n=18

When co-incubated with known stimulators of ROS, both TTNPB and UQ seemed to attenuate ROS production. A significant reduction was only found with the LPS stimulated samples (LPS vs. LPS+UQ+TTNPB $P < 0.001$). This may reflect differing mechanisms of macrophage stimulation between LPS and PMA.

In both cases UQ caused a reduction in absorbance. This is interesting given that incubation with UQ alone had little effect on the absorbance reading of the micro-plate cultures. Although the results are not statistically significant it is possible to hypothesise that UQ's antioxidant function is only active under the reducing conditions imposed by PMA or LPS co-incubation and does not have an effect under native conditions. Superoxide has been reported to activate UCP2 activity⁴⁸. It is possible that PMA and LPS stimulated ROS production activate UCP2 mediated uncoupling in the mitochondria of these macrophages and that this uncoupling activity is supported by the supplementary UQ₁₀. In this way UQ₁₀ supplementation would only have an effect on ROS production in stimulated macrophage cultures.

It is difficult to make a judgement as to the mechanism by which TTNPB or UQ cause the possible reduction in ROS from stimulated Macrophages. However, the significant reduction in absorbance seen when both UQ and TTNPB are incubated together with LPS stimulated macrophages, suggests that their actions are synergistic. Although this is not seen with PMA stimulated macrophages these results do support the hypothesis that UQ can function with UCP2 to reduce oxidative stress in macrophages. In this way TTNPB would function to stimulate UCP2 uncoupling activity and UQ supplementation would ensure that a sufficient pool of UQ was available to support UCP2s' uncoupling function as an essential co-factor. Increased UCP2 uncoupling would cause a decrease in the mitochondrial membrane potential and a consequent decrease in the production of ROS.

6. Discussion

6. Discussion

Using endotoxaemia in suckling rat pups as a model for neonatal sepsis we have established that the hypothermia observed in this model is accompanied by hypometabolism, as reflected by decreased energy expenditure and oxygen consumption. Previous studies of neonatal sepsis have associated the observed decrease in body temperature with impaired hepatocyte mitochondrial metabolism and suggested that this could be due to inhibition of the proton leak⁷. If the function of UCP2 was to drive heat production by acting as a proton leak then it is possible that changes in body temperature in response to sepsis would be reflected by the level of its expression. The finding of increase UCP2 expression with a decrease in body temperature is at odds with this.

UCP2 mRNA is reported to be ubiquitously expressed in the mammalian body. Its expression in the liver and up-regulation in hepatocytes during sepsis suggested that UCP2 could be involved in the fever response to sepsis^{43,62}. We investigated the expression of UCP2 protein in rat pups by western blotting. The strongest positive reactivity to the UCP2 antibody was from mitochondrial samples isolated from spleen and lung tissue. Western blots of mitochondrial samples from liver tissue gave rise to indistinct bands in relation to UCP2 control, suggesting that a low level of UCP2 protein existed in this tissue. A comparative analysis of UCP2 western blotting from control and UCP2 knock out mice reported that UCP2 expression was robust in spleen, lung, stomach and white adipose tissue. Detection in other preparations such as liver, BAT and brain mitochondria were reported to be non specific as the 32 kDa band detected by UCP2 western blotting of these samples were also present in samples from UCP2^{-/-} mice⁴⁴. It is likely that the low level of reactivity of liver mitochondria to the UCP2 antibody in our study of neonatal rats is due to lack of antibody specificity rather than evidence of UCP2 protein. Another explanation could be that the reactivity to the antibody was due to the presence of kuppfer cells in our liver samples. The pattern of UCP2 protein expression from our study does not support a role for this protein in whole body thermogenesis. This is in agreement with other UCP2 western blotting investigations performed in adult mice, whilst these studies were in progress.

To investigate the relationship between UCP2 protein expression and sepsis, we focused on the expression of UCP2 in lung and spleen mitochondria in control and endotoxic rat pups. UCP2 protein expression normalised for total mitochondrial protein content by citrate synthase was increased in lung mitochondria from rats culled 2 hours after LPS injection. This effect did not seem to be maintained in mitochondrial samples from rats culled 6 hours after LPS injection. The level of UCP2 expression in spleen was unchanged between control and septic samples from rats culled at both 2 and 6 hours after LPS and saline injection.

It would be interesting to study the level of UCP2 expression in rat pups after extended periods of endotoxaemia. A similar study of UCP2 expression in adult mice found that significant induction of UCP2 expression did not occur until 10 hours after exposure to LPS⁶⁸. Future work might determine the temporal expression pattern of UCP2 over a 24 hour period. However it is likely that suckling rat pups will stop feeding during later stages of endotoxaemia and this may affect the results of such a study.

Inhibition of the proton leak across the inner mitochondrial membrane could be a factor contributing to the hypometabolism observed in this model of sepsis. If the expression of UCP2 was related to this observed hypometabolism we might expect to observe a decrease in band density in UCP2 western blots from mitochondria isolated from septic tissues when compared to controls. In our study, the only significant difference in UCP2 protein expression between mitochondria isolated from control and septic rat pups was a short lived increase in endotoxic lung mitochondria. Results from UCP2 western blotting do not suggest UCP2 expression is related to a hypometabolism during neonatal sepsis. Moreover, the magnitude of temperature decline and drop in oxygen consumption recorded by indirect calorimetry of septic rat pups appears too large to be accounted for by the proton leak alone.

An increase in UCP2 protein expression in lung mitochondria during sepsis has been observed by other authors in adult mice⁶⁸. In that study, UCP2 induction was not apparent until 10 hours after exposure to LPS. The kinetics of this induction seemed consistent with a primary immune response leading to oxidative burst in the lung. Our investigation focused on the earlier stages of infection and found UCP2 protein

expression was increased in lung mitochondria from rat pups culled just 2 hours after LPS exposure. The lung has a unique relationship with its environment. It is constantly exposed to microbial challenges to which it must respond to quickly in order to preserve gaseous exchange. One of the early innate immune responses is a recruitment of macrophages to the lung. UCP2 expression has been found in macrophages and it has been suggested that they may regulate their UCP2 expression in response to infection⁴⁷. It is unlikely that the increase in UCP2 protein expression found in lung mitochondria represents an increase in UCP2 synthesis but it could reflect macrophage infiltration into this organ as part of the immune response.

The difference in UCP2 protein expression between control and septic lung mitochondria is not maintained to a significant level in rats culled 6 hours after LPS injection. If the level of UCP2 protein in mitochondrial preparations from the lung did drop between 2 and 6 hours after exposure to LPS it is possible that this could be due to macrophage redistribution away from the lung. Isolated macrophages have been shown to decrease their UCP2 mRNA expression when exposed to LPS⁶⁸ and the apparent drop in UCP2 expression in lung mitochondrial preparations could also be as a result of the macrophages present in this sample decreasing UCP2 expression to increase bacterial killing. To study this further it would be necessary to correlate UCP2 expression with lung content of macrophages.

The uncoupling activity of UCP2 is reported to be functionally dependent on the presence of ubiquinone³⁸. To investigate this relationship further, we examined the level of ubiquinones 9 and 10 (UQ₉ and UQ₁₀) in our mitochondrial preparations. Our results suggest that the level of UQ₉ is decreased in lung mitochondria from septic rats culled 6 hours after LPS injection. Oxidative stress has been reported to cause an increase in UQ₉ and UQ₁₀ levels in the plasma membrane and it is possible that this additional ubiquinone is recruited from the mitochondria⁸². The decrease of UQ₉ observed in septic lung mitochondria could reflect a redistribution of UQ₉ to the plasma membrane as a form of oxidative defence. It has been suggested that conditions of oxidative stress can impair ubiquinone biosynthesis or increase its catabolism⁸³. The decrease in UQ₉ in septic lung mitochondria may simply reflect an increase in its decomposition. Whether it is by increased catabolism or dispersal from the mitochondria it is unlikely that this decrease is related to UCP2 protein expression. It is

reported that the minimum length of the side chain in ubiquinone needed to activate UCP2 is 10 isoprenoid units³⁷. If a relationship did exist between UCP2 protein expression and ubiquinone it is likely that it would be with UQ₁₀. The levels of UQ₁₀ in this study were unchanged between control and septic samples collected from rats culled at 2 and 6 hours after LPS and saline injection. An investigation into the relationship between UCP2 and UQ₁₀ in *E.coli* inclusion bodies has suggested that a UQ₁₀ molar ratio of 80:1 UCP2 dimer is sufficient to activate uncoupling³⁷. Given the low level of Protein expression described for UCP2, the level of UQ₁₀ reported in our study is probably more than sufficient to activate uncoupling. It is likely that any change in the level of UQ₁₀ that might be needed to support UCP2 activity would be masked by the pool of UQ₁₀ already present in these mitochondria. It has not been possible to draw any conclusions about the relationship between UCP2 and ubiquinone by comparing the relative levels of these compounds by western blotting and HPLC analysis. It may be possible to use a linker molecule to determine whether UCP2 and ubiquinone are physically associated in the mitochondrial membrane.

The distribution of UCP2 protein and the changes in its expression revealed by western blotting in our model of neonatal sepsis suggested that UCP2 may have a role in the immune response and may be expressed in macrophages. It was not possible to determine UCP2 protein expression in isolated macrophages using our methodology for western blotting. The blood volume in rat pups was too low to give workable yields of isolated macrophages and western blots of human macrophages had very high background reactivity (results not shown), this was probably due to lack of antibody specificity. Macrophage UCP2 expression has been demonstrated and evidence from the knock out model of UCP2 strongly suggests that UCP2 is involved in regulating macrophage ROS production^{44;68}. The results from our ROS assays in macrophage populations support the hypothesis that UCP2 activity may mediate the generation of ROS.

We demonstrated that it was possible to measure ROS production from populations of isolated human macrophages using both DCFH-DA and tetrazolium dye reduction. Macrophage populations co-incubated with DCFH-DA and LPS had increased fluorescence compared to controls, indicating a higher level of ROS. Similarly treated cultures of macrophages had lower fluorescence when either TTNPB

or UQ was added to the culture media, suggesting that these compounds were attenuating macrophage ROS production. These findings were supported by results from our microplate assay of macrophage ROS production using tetrazolium dye reduction. Here we demonstrated that the PMA and LPS stimulation of ROS production from human macrophages was significant. TTNPB and UQ were both shown to attenuate this response. However, the only statistically significant reduction in stimulated ROS production was found when macrophage populations exposed to LPS were incubated with UQ and TTNPB simultaneously. Ubiquinone is a known quencher of ROS and it is reported that retinoic acids can reduce the oxidative burst in macrophages⁵. It is possible that both these compounds reduce the ROS production of stimulated macrophages by mechanisms independent of UCP2. However the significant decrease in ROS from LPS stimulated macrophages observed when UQ and TTNPB are present together in the culture media suggests that their actions are synergistic. TTNPB has been reported to specifically activate UCP2³⁰ and the activity of UCP2 is reportedly dependant on the presence of UQ³⁸. Given that previous studies have implicated UCP2 in the regulation of macrophage ROS, it seems possible that the focus of TTNPB and UQs' synergy in our experiments could be a relationship with UCP2 activity.

A recent paper by Echtay *et al*⁵⁰ supports the hypothesis that UCP2 function may be related to mediating the level of ROS. They report that superoxide activates mitochondrial proton transport through UCP2 and suggests that activation of UCP2 is from the matrix side of the inner mitochondrial membrane. In this way it is easy to see how UCP2 could function by uncoupling in response to an increase in internal oxidative pressure. The majority of ROS produced during sepsis is generated outside the mitochondria. Echtay *et al* have demonstrated that exogenous superoxide anions can reach the mitochondrial matrix and it will be interesting to see if the results from these experiments can be reproduced in other cell types, particularly in macrophages and other immune specific cells.

A conclusive discussion of UCP2's function and its relationship to the biochemical and physiological response to infection in neonates is beyond the scope of this study. However, the findings we report suggest that UCP2 does not have a role in maintaining body temperature during sepsis, but support other studies that suggest it

UCP2 is involved in protecting the body against the detrimental effects of reactive oxygen species.

Acknowledgements

I would like to thank the Institute of Child Health for providing me with the opportunity to undertake this project and everyone working there who offered me support and guidance. In particular Robin Garret-Cox who worked with me on the indirect Calorimetry experiments and Dr Simon Eaton for his help and advice, especially towards the end of the project.

On a personal note I would also like to thank my family and friends for their support, understanding and patience.

Reference List

1. Turi RA, Petros A, Eaton S. Energy metabolism of infants and children with systemic inflammatory response syndrome and sepsis. *Ann Surg* 2001;233:581-7.
2. Carcillo JA, Cunnion RE. Septic shock. *Crit Care Clin* 1997;13:553-74.
3. Lewis D. Host defence mechanisms against bacteria, fungi, viruses and normal intracellular pathogens. *Fetal and Neonatal Physiology* 1998;1869-919.
4. Anderson MR, Blumer JL. Advances in the therapy for sepsis in children. *Pediatr.Clin.North.Am* 1997;44:179-205.
5. Morel F, Doussiere J, Vignais PV. The superoxide-generating oxidase of phagocytic cells. Physiological, molecular and pathological aspects. *Eur.J Biochem.* 1991;201:523-46.
6. Santos AA, Wilmore DW. The systemic inflammatory response: perspective of human endotoxemia.
7. Markley MA, Pierro A, Eaton S. Hepatocyte mitochondrial metabolism is inhibited in neonatal rat endotoxaemia: effects of glutamine. *Clin.Sci.(Lond)* 2002;102:337-44.
8. Nicholls DG, Snelling R, Rial E. Proton and calcium circuits across the mitochondrial inner membrane. *Biochem.Soc.Trans.* 1984;12:388-90.
9. Nethery D, Callahan LA, Stofan D, Mattera R, DiMarco A, Supinski G. PLA(2) dependence of diaphragm mitochondrial formation of reactive oxygen species. *J Appl.Physiol* 2000;89:72-80.
10. Brand MD, Chien L.F, Ainscow E.K., Rolfe DF, Porter RK. The causes and functions of mitochondrial proton leak. *Biochim.Biophys.Acta* 1994;1187:132-9.

11. Ricquier D, Bouillaud F. The uncoupling protein homologues: UCP1, UCP2, UCP3, StUCP and AtUCP. *Biochem.J* 2000;345 Pt 2:161-79.
12. Taylor DE, Ghio AJ, Piantadosi CA. Reactive oxygen species produced by liver mitochondria of rats in sepsis. *Arch.Biochem.Biophys.* 1995;316:70-6.
13. Heaton GM, Wagenvoort RJ, Kemp A, Jr., Nicholls DG. Brown-adipose-tissue mitochondria: photoaffinity labelling of the regulatory site of energy dissipation. *Eur.J Biochem.* 1978;82:515-21.
14. Perkins MN, Rothwell NJ, Stock MJ, Stone TW. Activation of brown adipose tissue thermogenesis by the ventromedial hypothalamus. *Nature* 1981;289:401-2.
15. Nicholls DG, Locke RM. Thermogenic mechanisms in brown fat. *Physiol Rev.* 1984;64:1-64.
16. Klingenberg M, Winkler E. The reconstituted isolated uncoupling protein is a membrane potential driven H⁺ translocator. *EMBO J* 1985;4:3087-92.
17. Enerback S, Jacobsson A, Simpson EM, Guerra C, Yamashita H, Harper ME *et al.* Mice lacking mitochondrial uncoupling protein are cold-sensitive but not obese. *Nature* 1997;387:90-4.
18. Rial E, Gonzalez-Barroso MM. Physiological regulation of the transport activity in the uncoupling proteins UCP1 and UCP2. *Biochimica et Biophysica Acta-Bioenergetics* 2001;1504:70-81.
19. Nedergaard J, Golozoubova V, Matthias A, Asadi A, Jacobsson A, Cannon B. UCP1: the only protein able to mediate adaptive non-shivering thermogenesis and metabolic inefficiency. *Biochimica et Biophysica Acta-Bioenergetics* 2001;1504:82-106.
20. Stuart JA, Cadenas S, Jekabsons MB, Roussel D, Brand MD. Mitochondrial proton leak and the uncoupling protein 1 homologues. *Biochimica et Biophysica Acta-Bioenergetics* 2001;1504:144-58.

21. Fleury C, Neverova M, Collins S, Raimbault S, Champigny O, Levi-Meyrueis C *et al.* Uncoupling protein-2: a novel gene linked to obesity and hyperinsulinemia. *Nat. Genet.* 1997;15:269-72.
22. Gong DW, He Y, Karasand M, Reitman M. Uncoupling protein 3 is a mediator of thermogenesis regulated by thyroid hormone, β 3-adrenergic agonists and leptin. *J Biol. Chem.* 1997;26:24129-32.
23. Mao W, Yu XX, Zhong W, Li J, Brush SW, Sherwood SH *et al.* UCP4, a novel brain specific mitochondrial protein that reduces membrane potential in mammalian cells. *FEBS Lett.* 1999;443:326-30.
24. Sanchis D, Fleury C, Chomiki M, Goubern M, Huang SG, Neverova M *et al.* BMCP1, a Novel Mitochondrial carrier with high expression in the central nervous system of humans and rodents and respiration uncoupling activity in recombinant yeast. *J Biol. Chem.* 1998;273:34611-5.
25. Fleury C, Sanchis D. The mitochondrial uncoupling protein-2: current status. *Int. J. Biochem. Cell Biol.* 1999;31:1261-78.
26. Miroux B, Frossard V, Raimbault S, Ricquier D, Bouillaud F. The topology of the brown adipose tissue mitochondrial uncoupling protein determined with antibodies against its antigenic sites revealed by a library of fusion proteins. *EMBO J* 1993;12:3739-45.
27. Gonzalez-Barroso MM, Fleury C, Jimenez MA, Sanz JM, Romero A, Bouillaud F *et al.* Structural and functional study of a conserved region in the uncoupling protein UCP1: The three matrix loops are involved in the control of transport. *Journal of Molecular Biology* 1999;292:137-49.
28. Bienengraeber M, Echtay KS, Klingenberg M. H⁺ transport by uncoupling protein (UCP-1) is dependent on a histidine pair, absent in UCP-2 and UCP-3. *Biochemistry* 1998;37:3-8.
29. Gimeno RE, Dembski M, Weng X, Deng N, Shyjan AW, Gimeno CJ *et al.* Cloning and characterization of an uncoupling protein homolog: a

- potential molecular mediator of human thermogenesis. *Diabetes* 1997;46:900-6.
30. Rial E, Gonzalez-Barroso M, Fleury C, Iturrizaga S, Sanchis D, Jimenez-Jimenez J *et al.* Retinoids activate proton transport by the uncoupling proteins UCP1 and UCP2. *Embo Journal* 1999;18:5827-33.
 31. Zhang CY, Hagen T, Mootha VK, Sliker LJ, Lowell BB. Assessment of uncoupling activity of uncoupling protein 3 using a yeast heterologous expression system. *FEBS Lett.* 1999;449:129-34.
 32. Stuart JA, Harper JA, Brindle KM, Jekabsons MB, Brand MD. A mitochondrial uncoupling artifact can be caused by expression of uncoupling protein 1 in yeast. *Biochemical Journal* 2001;356:779-89.
 33. Stuart JA, Harper JA, Brindle KM, Jekabsons MB, Brand MD. Physiological levels of mammalian uncoupling protein 2 do not uncouple yeast mitochondria. *Journal of Biological Chemistry* 2001;276:18633-9.
 34. Lin CS, Klingenberg M. Characteristics of the isolated purine nucleotide binding protein from brown fat mitochondria. *Biochemistry* 1982;21:2950-6.
 35. Nedergaard J, Matthias A, Golozoubova V, Jacobsson A, Cannon B. UCP1: The original uncoupling protein - and perhaps the only one? New perspectives on UCP1, UCP2, and UCP3 in the light of the bioenergetics of the UCP1-ablated mice. *Journal of Bioenergetics and Biomembranes* 1999;31:475-91.
 36. Matthias A, Ohlson KBE, Fredriksson JM, Jacobsson A, Nedergaard J, Cannon B. Thermogenic responses in brown fat cells are fully UCP1-dependent - UCP2 or UCP3 do not substitute for UCP1 in adrenergically or fatty acid-induced thermogenesis. *Journal of Biological Chemistry* 2000;275:25073-81.
 37. Echtay KS, Winkler E, Frischmuth K, Klingenberg M. Uncoupling proteins 2 and 3 are highly active H⁺ transporters and highly nucleotide

- sensitive when activated by coenzyme Q (ubiquinone). *Proceedings of the National Academy of Sciences of the United States of America* 2001;98:1416-21.
38. Echtay KS, Winkler E, Klingenberg M. Coenzyme Q is an obligatory cofactor for uncoupling protein function. *Nature* 2000;408:609-13.
 39. Klingenberg M, Echtay KS, Bienengraeber M, Winkler E, Huang SG. Structure-function relationship in UCP1. *International Journal of Obesity* 1999;23:S24-S29.
 40. Ricquier D. Uncoupling protein-2 (UCP2): molecular and genetic studies. *Int.J.Obes.Relat Metab Disord.* 1999;23 Suppl 6:S38-S42.
 41. Pecqueur C, Alves-Guerra MC, Gelly C, Levi-Meyrueis C, Couplan E, Collins S *et al.* Uncoupling protein 2, in vivo distribution, induction upon oxidative stress, and evidence for translational regulation. *Journal of Biological Chemistry* 2001;276:8705-12.
 42. Faggioni R, Shigenaga J, Moser A, Feingold KR, Grunfeld C. Induction of UCP2 gene expression by LPS: a potential mechanism for increased thermogenesis during infection. *Biochem.Biophys.Res Commun.* 1998;244:75-8.
 43. Cortez-Pinto H, Yang SQ, Lin HZ, Costa S, Hwang CS, Lane MD *et al.* Bacterial lipopolysaccharide induces uncoupling protein-2 expression in hepatocytes by a tumor necrosis factor-alpha-dependent mechanism. *Biochem.Biophys.Res.Commun.* 1998;251:313-9.
 44. Arsenijevic D, Onuma H, Pecqueur C, Raimbault S, Manning BS, Miroux B *et al.* Disruption of the uncoupling protein-2 gene in mice reveals a role in immunity and reactive oxygen species production. *Nat.Genet.* 2000;26:435-9.
 45. Murray HW, Juangbhanich CW, Nathan CF, Cohn ZA. Macrophage oxygen-dependent antimicrobial activity. II. The role of oxygen intermediates. *J Exp.Med.* 1979;150:950-64.

46. Puigserver P, Vazquez F, Bonet MI, Pico C, Palou A. *In Vitro* and *in vivo* induction of brown adipocyte uncoupling protein (thermogenin) by retinoic acid. *Biochem.J* 1996;317:827-33.
47. Krauss S, Zhang CY, Lowell BB. A significant portion of mitochondrial proton leak in intact thymocytes depends on expression of UCP2. *Proceedings of the National Academy of Sciences of the United States of America* 2002;99:118-22.
48. Echtay KS, Roussel D, St Pierre J, Jekabsons MB, Cadenas S, Stuart JA *et al.* Superoxide activates mitochondrial uncoupling proteins. *Nature* 2002;415:96-9.
49. Klingenberg M, Echtay KS. Uncoupling proteins: the issues from a biochemist point of view. *Biochimica et Biophysica Acta-Bioenergetics* 2001;1504:128-43.
50. Echtay K, Murphy MP, Smith RAJ, Talbot DA, Brand MD. Superoxide activates mitochondrial uncoupling protein 2 from matrix side: studies using targeted antioxidants. *Journal of Biological Chemistry* 2002;87:456.
51. Kelso GF, Porteous CM, Coulter CV, Hughes G, Porteous WK, Lederwood EC *et al.* *J Biol.Chem.* 2001;276:4588-96.
52. Smith RAJ, Porteous CM, Coulter CV, Murphy MP. *Eur.J Biochem.* 1999;263:709-16.
53. Jacobi J. Pathophysiology of sepsis. *Am.J Health Syst.Pharm.* 2002;59 Suppl 1:S3-S8.
54. Plank LD, Connolly AB, Hill GL. Sequential Changes in the metabolic response in severely septic patients during the first 23 days after the onset of peritonitis. *Annals of Surgery* 1998;228:146-58.
55. Chwals WI, Lally KP, Wolley MM. Measured energy expenditure in critically ill infants and young children. *J.Surg Res* 1988;44:467-72.

56. Jaskic T, Shew SB, Keshen TH. Do critically ill surgical neonates have increased energy expenditure? *J Pediatr Surg* 2001;36:63-7.
57. Bertin R, Demarco F, Moroux I. Post-natal-development of nonshivering thermogenesis in rats-effectsof rearing temperature. *J Dev physiol* 1993;19:9-15.
58. Derijk RH, Van Kampen M, Van Rooijen N, Berkenbosch F. Hypothermia to endotoxin involves reduced thermogenesis, macrophage- dependent mechanisms, and prostaglandins. *Am.J Physiol* 1994;266:R1-R8.
59. Dogan MD, Ataoglu H, Akarsu ES. Effects of different serotypes of Escherichia coli lipopolysaccharides on body temperature in rats. *Life Sci* 2000;67:2319-29.
60. Paul L, Fraifeld V, Kaplanski J. Evidence supporting involvement of leukotrienes in LPS-induced hypothermia in mice. *Am.J Physiol* 1999;276:R52-R58.
61. Romanovsky AA, Simons CT, Szekely M, Kulchitsky VA. The vagus nerve in the thermoregulatory response to systemic inflammation.
62. Cortez-Pinto H, Zhi LH, Qi YS, Odwin DC, Diehl AM. Lipids up-regulate uncoupling protein 2 expression in rat hepatocytes. *Gastroenterology* 1999;116:1184-93.
63. Larrouy D, Laharrague P, Carrera G, Viguerie-Bascands N, Levi-Meyrueis C, Fleury C *et al*. Kupffer cells are a dominant site of uncoupling protein 2 expression in rat liver. *Biochem.Biophys.Res.Commun.* 1997;235:760-4.
64. Morton DB,Griffiths PH. Guidelines on the recognition of pain, distress and discomfort in experimental animals and an hypothesis for assessment. *Vet.Rec.* 1985;116:431-6.
65. Eaton S. Redox control of beta-oxidation in rat liver mitochondria. *Eur.J Biochem.* 1994;671-81.

66. Ghadiminejad I, Saggerson ED. The relationship of rat liver overt carnitine palmitoyltransferase to the mitochondrial malonyl-CoA binding entity and to the latent palmitoyltransferase. *Biochem.J* 1990;270:787-94.
67. Swain M, Ross NW. A silver stain protocol for protein yielding high resolution and transparent background in sodium dodecyl sulphate polyacrylamide gels. *Electrophoresis* 1995;16:948-51.
68. Pecqueur C, Alves-Guerra MC, Gelly C, Levi-Meyrueis C, Couplan E, Collins S *et al.* Uncoupling protein 2, in vivo distribution, induction upon oxidative stress, and evidence for translational regulation. *Journal of Biological Chemistry* 2001;276:8705-12.
69. Shi H, Noguchi N, Niki E. Dynamics of antioxidant action of ubiquinol: a reappraisal. *Biofactors* 1999;9:141-8.
70. Sanlioglu S, Williams CM, Samavati L, Butler NS, Wang G, McCray PB, Jr. *et al.* Lipopolysaccharide induces Rac1-dependent reactive oxygen species formation and coordinates tumor necrosis factor- α secretion through IKK regulation of NF- κ B. *J Biol.Chem.* 2001;276:30188-98.
71. Littarru GP, Ho L, Folkers K. Deficiency of coenzyme Q₁₀ in human heart disease. *International Journal of Vitamins and Nutrition Research.* 1972;291.
72. Littarru GP, Jones D, Sholler J, Folkers K. Deficiency of Coenzyme Q₁₀ in a succinate CoQ₁₀ enzyme in the dystrophic rabbit on an antioxidant deficient diet. *International Journal of Vitamins and Nutrition Research.* 1972;42:127.
73. Littarru GP, Nakamura R, Lester H, Folkers K, Kuzell WC. Deficiency of coenzyme Q₁₀ in gingival tissue from patients with periodontal disease. *Proceedings of the National Academy of Sciences of the United States of America* 1971;68:2332.
74. Littarru GP, Jones D, Sholler J, Folkers K. Deficiency of Coenzyme Q₁₀ in mice having hereditary muscular dystrophy. *Biochem.Biophys.Res Commun.* 1970;41:1306-14.

75. Babior BM. Superoxide production by phagocytes. Another look at the effect of cytochrome c on oxygen uptake by stimulated neutrophils. *Biochem.Biophys.Res.Commun.* 1979;91:222-6.
76. Allen RC, Stjernholm RL, Steele RH. Evidence for the generation of an electronic excitation state(s) in human polymorphonuclear leukocytes and its participation in bactericidal activity. *Biochem.Biophys.Res.Commun.* 1972;47:679-84.
77. Segal AW. Nitroblue-tetrazolium tests. *Lancet* 1974;2:1248-52.
78. Wan CP, Myung E, Lau BH. An automated micro-fluorometric assay for monitoring oxidative burst activity of phagocytes. *J.Immunol.Methods* 1993;159:131-8.
79. Bass DA, Parce JW, Dechatelet LR, Szejda P, Seeds MC, Thomas M. Flow cytometric studies of oxidative product formation by neutrophils: a graded response to membrane stimulation. *J.Immunol.* 1983;130:1910-7.
80. Molecular Probes inc. Absorption and fluorescence spectra of 5-(+6)-carboxy 2' 7', dichlorofluorescein in pH 9.0 buffer. 2000.
Internet Communication
81. Tomasetti M, Alleva R, Collin AR. In vivo supplementation with coenzyme Q10 enhances the recovery of human lymphocytes from oxidative DNA damage. *The FASEB Journal* 2001.
82. Navarro F, Arroyo A, Martin SF, Bello IR, deCabo R, Burgess jR *et al.* Protective role of ubiquinone in vitamin E and selenium deficient plasma samples. *Biofactors* 1999.
83. Lass A, Kwong L, Sohal RS. Mitochondrial coenzyme Q content and aging. *Biofactors* 1999;9:199-205.